



UNIVERSITY OF THESSALY  
SCHOOL OF ENGINEERING  
DEPARTMENT OF MECHANICAL ENGINEERING

Diploma Thesis

Parameters influencing long-term performance and durability of PEM  
fuel cells.

by

**PLAFADELIS DIMITRIS & GIANNAKOS ALEXANDROS**

Under the supervision of Prof. Panagiotis Tsiakaras

Submitted to fulfill part of the requirements for the acquirement of the Diploma of  
Mechanical Engineer

June 2023, Volos



ΠΑΝΕΠΙΣΤΗΜΙΟ ΘΕΣΣΑΛΙΑΣ

ΠΟΛΥΤΕΧΝΙΚΗ ΣΧΟΛΗ

ΤΜΗΜΑ ΜΗΧΑΝΟΛΟΓΩΝ ΜΗΧΑΝΙΚΩΝ

Διπλωματική Εργασία

Παράμετροι που επηρεάζουν την απόδοση και την αντοχή των Κυψελών  
Καυσίμου Μεμβράνης Ανταλλαγής Πρωτονίων μακροπρόθεσμα.

Υπό

**ΠΑΛΑΦΑΔΕΛΗΣ ΔΗΜΗΤΡΗΣ & ΓΙΑΝΝΑΚΟΣ ΑΛΕΞΑΝΔΡΟΣ**

Επιβλέπων καθηγητής Παναγιώτης Τσιακάρας

Υπεβλήθη για την εκπλήρωση μέρους των απαιτήσεων για την απόκτηση του  
Διπλώματος Μηχανολόγου Μηχανικού

Ιούνιος 2023, Βόλος

© Πλαφαδέλης Δημήτρης & Γιαννακός Αλέξανδρος

Η έγκριση της διπλωματικής εργασίας από το Τμήμα Μηχανολόγων Μηχανικών της Πολυτεχνικής Σχολής του Πανεπιστημίου Θεσσαλίας δεν υποδηλώνει αποδοχή των απόψεων του συγγραφέα (Ν. 5343/32 αρ. 202 παρ.2).

**Approved by the Committee on Final Examination:**

Advisor      Dr. Tsiakaras Panagiotis (Supervisor)  
Professor of Department of Mechanical Engineering  
School of Engineering  
University of Thessaly

Member      Dr. Charalampous Georgios  
Assistant Professor of Department of Mechanical Engineering  
School of Engineering  
University of Thessaly

Member      Dr. Brouzgou Angeliki  
Assistant Professor of Department of Energy Systems  
School of Technological Sciences  
University of Thessaly

## **ΕΥΧΑΡΙΣΤΙΕΣ**

Αυτή η διπλωματική εργασία αποτελεί το τελευταίο στάδιο του ακαδημαϊκού μας κύκλου. Αρχικά, εκτιμούμε ειλικρινά τη βοήθεια και τη στήριξη του καθηγητή και επόπτη μας, κ. Παναγιώτη Τσιακάρα, να πετύχουμε το στόχο μας και να ολοκληρώσουμε την εργασία μας.

Στη συνέχεια, θα θέλαμε να ευχαριστήσουμε τους αγαπητούς γονείς μας, Θωμά Γιαννακό και Βασιλική Γκανούρη και Ιωάννη Πλαφαδέλη και Γεωργία Καψάλη, αλλά και τα υπόλοιπα μέλη της οικογένειας μας για την υπομονή και τη στήριξη τους.

Τέλος, θα θέλαμε να ευχαριστήσουμε θερμά τους φίλους μας που στάθηκαν στο πλευρό μας σε αυτό το πολύχρονο ταξίδι.

## **ACKNOWLEDGEMENTS**

This thesis is the final stage of our academic cycle. Initially, we sincerely appreciate the support and assistance of our professor and supervisor, Mr. Panagiotis Tsiakaras, to achieve our goal and complete this thesis.

Next, we would like to thank our beloved parents Thomas Giannakos and Vasiliki Gkanouri, and Ioannis Plafadelis and Georgia Kapsali, and the rest of the family members for their patience and support.

Finally, we would like to warmly thank our friends who have been standing next to us throughout this journey.

## ABSTRACT

This thesis is concerned with the study of proton exchange membrane fuel cells (PEMFCs), which are fueled with hydrogen. More specifically, the parameters that affect the performance and durability of PEM fuel cells during their long-term operation will be studied.

First, reference is made to the rapid increase in demand for energy needs and that the fossil fuels that meet these needs are diminishing and causing pollution problems in the natural environment. Renewable Energy Sources (R.E.S.) are those that tend to replace fossil fuels.

In the following, the various electrochemical devices for energy storage and production are presented. First, fuel cells are presented, in which their various types, their ability to achieve particularly high yields, and their applications are discussed in detail. This is followed by an analysis of electrolyzers, batteries, capacitor-supercapacitors, and electrochemical sensors in terms of their different types and their operating mechanism.

Then we focus on PEM fuel cells and their operating mechanism. We analyze the advantages, and disadvantages of their various structural components, with particular emphasis on the membrane, the catalytic layer, the gas diffusion layer, and the bipolar plates.

Finally, we continue the analysis of PEM fuel cells, studying the parameters that affect their performance and durability during their long-term operation. The study focuses on the leaching conditions, the structural elements, and the proper water and thermal management.

## ΠΕΡΙΛΗΨΗ

Η παρούσα διπλωματική έχει ως αντικείμενο μελέτης τις κυψέλες καυσίμου μεμβράνης ανταλλαγής πρωτονίων (PEMFC), οι οποίες τροφοδοτούνται με υδρογόνο. Πιο συγκεκριμένα, θα μελετηθούν οι παράμετροι που επηρεάζουν την απόδοση και την ανθεκτικότητα των PEM κυψελών καυσίμου κατά τη διάρκεια της μακροχρόνιας λειτουργίας τους.

Αρχικά, γίνεται αναφορά στην ραγδαία αύξηση της ζήτησης των ενεργειακών αναγκών, καθώς και στο ότι τα ορυκτά καύσιμα που καλύπτουν αυτές τις ανάγκες μειώνονται και προκαλούν προβλήματα μόλυνσης στο φυσικό περιβάλλον. Οι Ανανεώσιμες Πηγές Ενέργειας (Α.Π.Ε.) είναι αυτές που τείνουν να αντικαταστήσουν τα ορυκτά καύσιμα.

Στη συνέχεια, παρουσιάζονται οι διάφορες ηλεκτροχημικές συσκευές για την αποθήκευση και παραγωγή ενέργειας. Αρχικά, παρουσιάζονται οι κυψέλες καυσίμου, στις οποίες γίνεται εκτενής αναφορά στα διάφορα είδη τους, στην ιδιότητά τους να πετυχαίνουν ιδιαίτερα υψηλές αποδόσεις και στις εφαρμογές τους. Ακολουθεί η ανάλυση των ηλεκτρολυτών, μπαταριών, πυκνωτών-υπερπυκνωτών και ηλεκτροχημικών αισθητήρων ως προς τα διάφορα είδη τους, αλλά και του μηχανισμού λειτουργίας τους.

Έπειτα, επικεντρωνόμαστε στις κυψέλες καυσίμου PEM και στον μηχανισμό λειτουργίας τους. Αναλύουμε τα πλεονεκτήματα και τα μειονεκτήματα των διαφόρων δομικών τους στοιχείων, με ιδιαίτερη έμφαση στην μεμβράνη, στο καταλυτικό στρώμα, στο στρώμα διάχυσης αερίων και στις διπολικές πλάκες.

Τέλος, συνεχίζουμε με την ανάλυση στις κυψέλες καυσίμου PEM, μελετώντας τις παραμέτρους που επηρεάζουν την απόδοσή τους και την αντοχή τους στην διάρκεια της μακροχρόνιας λειτουργίας τους. Η μελέτη επικεντρώνεται στις συνθήκες λειτουργίας, στα δομικά στοιχεία, καθώς και στην ορθή διαχείριση του νερού και της θερμότητας.

# CONTENTS

Chapter 1 .....	14
INTRODUCTION .....	14
1.1 Energy and the Environment.....	14
1.2 Hydrogen Economy.....	15
Chapter 2 .....	18
BASICS OF ELECTROCHEMISTRY AND ELECTROCHEMICAL DEVICES .....	18
2.1 Electrochemistry Basics .....	18
2.1.1 Thermodynamics of Electrochemical Reaction .....	19
2.2 Energy Conversion and Storage Devices .....	20
2.2.1 Fuel Cells .....	20
2.2.2 Electrolyzers .....	31
2.2.3 Batteries .....	35
2.2.4 Supercapacitors .....	39
2.2.5 Electrochemical Sensors .....	42
Chapter 3 .....	45
PROTON-EXCHANGE MEMBRANE FUEL CELLS (PEMFC) .....	45
3.1 History Overview of a PEMFC .....	45
3.2 Working Principle of a PEMFC .....	46
3.3 Single cell, Stack, System .....	47
3.4 Key Elements of PEMFC .....	49
3.4.1 Proton-Exchange Membrane (PEM) .....	50
3.4.2 Anode and Cathode Electrodes .....	54
3.4.3 Bipolar Plates (BP) .....	58
3.4.4 Other Components .....	61
3.5 Thermodynamic and Kinetic Analysis of PEMFC .....	64
3.6 Cost Reduction and Applications of a PEMFC .....	65
Chapter 4 .....	68
PARAMETERS INFLUENCING LONG-TERM PERFORMANCE AND DURABILITY OF PEM FUEL CELLS .....	68
4.1 Introduction.....	68
4.2 Operating Conditions.....	69

4.2.1	Temperature, Pressure, and Relative Humidity (RH).....	69
4.2.2	Startup, Shutdown, and Load Cycling.....	71
4.2.3	Impurity Effects.....	74
4.2.4	Reactant Starvation.....	79
4.3	Parameters Influencing each Component's Performance and Durability .....	80
4.3.1	Membrane .....	81
4.3.2	Catalyst Layer.....	85
4.3.3	Gas Diffusion Media (GDM).....	90
4.3.4	Bipolar Plates (BP).....	92
4.3.5	Sealing Materials (Gasket).....	94
4.4	Water Management.....	94
4.4.1	Fuel Cell Flooding.....	95
4.4.2	Dehydration of Membrane.....	97
4.5	Thermal Management.....	98
4.5.1	Cooling Methods.....	99
Chapter 5	.....	100
CONCLUSION	.....	100
References	.....	102

## List of Figures

Figure 1.1. The distribution of fuel sources in the global primary energy supply [2].	15
Figure 1.2. Classification of hydrogen production [4].	16
Figure 2.1. A simple electrochemical cell [6].	18
Figure 2.2. (a), (b) A galvanic and an electrolytic cell [7,8].	19
Figure 2.3. Process of energy conversion from different devices [14].	21
Figure 2.4. Basic components of a simple fuel cell. [17].	22
Figure 2.5. The basic steps of FCs' function [17].	24
Figure 2.6. Representation depicting the working mechanism of an AFC [21].	26
Figure 2.7. Representation depicting the working mechanism of a PEMFC [21].	27
Figure 2.8. Representation depicting the working mechanism of a SOFC [21].	29
Figure 2.9. Closed-loop of pollution-free energy economy[17].	31
Figure 2.10. A simple electrolyzer [36].	32
Figure 2.11. Schematic illustration of the operating principle of an AWE [45].	33
Figure 2.12. Schematic illustration of the operating principle of a PEM electrolyzer [45].	34
Figure 2.13. Simple anatomy of a battery [59].	35
Figure 2.14. Simple anatomy of a supercapacitor [79].	39
Figure 2.15. Classification of a supercapacitor [83].	42
Figure 2.16. Comparison of different types of Supercapacitors [86].	42
Figure 2.17. Comparison of different electrochemical devices [87].	42
Figure 2.18. A simple electrochemical sensor [94].	43
Figure 3.1. Working principle of PEM fuel cell [120].	47
Figure 3.2. A PEM fuel cell stack [125].	47
Figure 3.3. (a). A PEM fuel cell system, (b) A five–cell stack and its major subsystems [127].	47
Figure 3.4. Key components of a PEMFC (1 = end plates, 2 = current collectors, 3 = flow field plates, 4 = sealing materials, 5 = gas diffusion media, 6 membrane electrode assembly) [127].	49
Figure 3.5. Chemical formula of Nafion [128].	50
Figure 3.6. Different types of membrane [129].	50
Figure 3.7. A schematic representation of an electrode assembly [126].	54
Figure 3.8. A schematic representation of a CL and a GDL [144].	56
Figure 3.9. The two substrates that make up the gas diffusion media [147].	58
Figure 3.10. Various types of flow field configuration [152].	60
Figure 3.11. Presentation of other components of the fuel cell stack [155].	63
Figure 3.12. Methods of stack assembly [156],[157]: (a) bolt fastening type; (b) steel belt fastening	

type. ....	64
Figure 3.13. Applications of fuel cells [167]. ....	67
Figure 4.1. PEMFC performance degradation rate caused by different operation conditions [180].	71
Figure 4.2. Initial performance of the stack, $T_c=75$ , $T_f=75$ and $T_o=70$ °C, $P=1$ atm, $U_f=0.5$ and $U_o=0.25$ [182]. ....	74
Figure 4.3. Effects of CO concentration on a stack cell performance [184]. ....	76
Figure 4.4. The impact of CO temperature and pressure on cell performance at different concentrations of CO contamination [184]. A=20 cm <sup>2</sup> , GORE-SELECT® Membrane (25m), anode catalyst: Pt alloy at 0.45 mg•cm <sup>-2</sup> , cathode catalyst: Pt at 0.4 mg•cm <sup>-2</sup> . (a) P=202kPa; (b) T=70 °C.	76
Figure 4.5. Effects of long-term NH <sub>3</sub> exposure on H <sub>2</sub> -air fuel cell performance at 80 C. 30 ppm NH <sub>3</sub> (g) were injected into the anode feed stream [185]. ....	77
Figure 4.6. The time-dependent changes of the anode and cathode potential under starvation conditions [186]. ....	80
Figure 4.7. Membrane's lifepath in a fuel cell [187]. ....	81
Figure 4.8. Main factors influencing mechanical failure [187]. ....	83
Figure 4.9. Schematic representation of the structure of a catalyst layer [199]. ....	86
Figure 4.10. Ostwald Ripening. [209]. ....	87
Figure 4.11. The consequences of higher compression on the GDM [215]. ....	91
Figure 4.12. Water transport mechanisms inside of PEMFC [222]. ....	95
Figure 4.13. Effect of cathode flooding on PEMFC performance [223]. ....	96
Figure 4.14. Polarization curve for HTPEMFC (PBI membrane) and for LTPEMFC (Nafion membrane) [224]. ....	98
Figure 4.15. Cooling methods of PEMFC [224]. ....	99

## List of Tables

Table 1.1. Advantages and disadvantages of RES. ....	15
Table 2.1. Classification of fuel cells by temperature [17]. ....	25
Table 2.2. Fundamental traits of various fuel cell types [21]. ....	27
Table 2.3. Essential features of various types of batteries [75-78]. ....	33
Table 2.4. Examples of electrochemical transducers [97]. ....	44
Table 3.1. Subsystems and its devices of a PEMFC system [125]. ....	49
Table 3.2. Basic characteristics of the key components of a PEMFC [124]. ....	50
Table 3.3. DOE technical targets for PEMFC bipolar plates in 2020 [153]. ....	61
Table 4.1. Specification of the stack.....	73
Table 4.2. Origin of common fuel and air impurities [175]. ....	74
Table 4.3. Influence of potential cycling on initial ECSA [210]. ....	87
Table 4.4. Highly favorable electrocatalysts with advanced CO tolerance capabilities [170]. ....	90
Table 4.5. Coating materials for metallic BPs and their characteristics [219]. ....	93

# Chapter 1

## INTRODUCTION

### 1.1 Energy and the Environment

From the beginning of mankind and the use of wood and stone to produce fire for heating, to the fossil fuels that spurred the industrial revolution, energy played a key role in our development as species. However, its production and use have the following obstacles: cost, environmental impact, and the exhaustion of the used resources. As people's standard of living and energy needs continue to increase, there is a legitimate need to replace fossil fuels (oil, gasoline, etc.) with other forms of energy production.

It is true that the evolution of the standard of living of mankind was based on the exploitation of large quantities of fossil fuels such as oil and gasoline. This abuse sometimes has mild consequences such as acid rain and sometimes serious consequences such as global warming. Pollution of the environment is increasing at an uncontrolled rate, which means that countries are taking action to combat it.

The energy we consume in any sector of our lives can be produced from: conventional fuels (fossil fuels) divided into two categories, hydrocarbons and carbons, biofuels, nuclear fuels, and renewable energy sources (RES). Renewable energy sources are divided into (i) Solar energy, (ii) Wind energy, (iii) Geothermal energy, (iv) Hydroelectric energy, (v) Tidal energy/power, (vi) Biomass, (vii) Electromagnetic energy. There is a tendency for RES to become more and more popular by trying to replace conventional fuels [1]. However, in the poorest countries, the use of fossil fuels remains at the same level. Although RES are eligible for the production of "clean energy", they currently have a small global energy supply. This is due to the problem they present in their storage as well as the high cost which is required by the various technologies, their installation, and their transport. Since, through RES, a variable amount of energy is produced, due to the weather phenomena, sometimes we have an excess amount of energy and sometimes a quantity that is not sufficient. This is the reason why we need to find more efficient storage methods. The figure 1.1 shows the share of renewable energy in electricity generation in the year 2016.

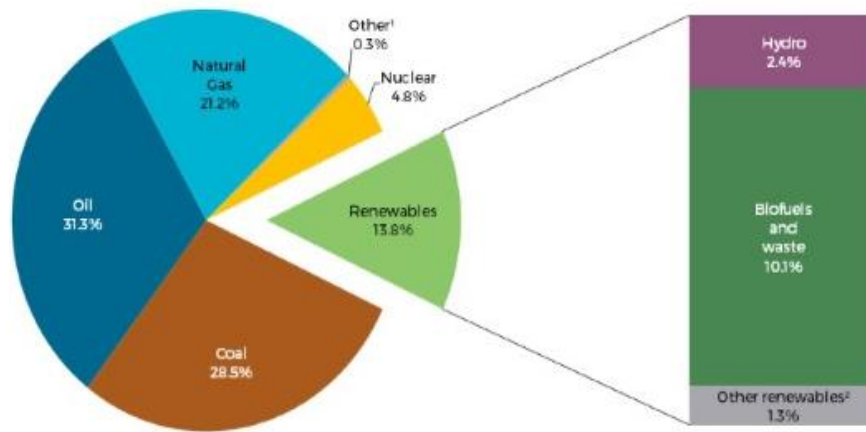


Figure 1.1. The distribution of fuel sources in the global primary energy supply [2].

Table 1.1 Advantages and disadvantages of RES.

<u>ADVANTAGES</u>	<u>DISADVANTAGES</u>
RES are very environmentally friendly, as they do not pollute the atmosphere, having zero CO <sub>2</sub> emissions.	Their rate of return is around 30%, resulting in large initial capital for their implementation should be required.
They are inexhaustible sources of energy, unlike fossil fuels that are exhaustible.	The integration of renewable energy into existing electrical grids can be challenging due to technical constraints and grid stability issues.
The cost of renewable energy technologies has been decreasing steadily over the years, making them more affordable and competitive compared to traditional energy sources.	The installation of large-scale renewable energy systems such as solar and wind farms can require significant amounts of land and other resources, which can have environmental impacts
The development of RES creates jobs in various sectors such as manufacturing, installation, and maintenance of renewable energy technologies.	Hydroelectric power stations cause decomposition of under water plants contributing to the greenhouse effect.
They can provide energy self-sufficiency.	The development and growth of the renewable energy industry depend on government policies and incentives, which can change over time and affect the viability of renewable energy projects
Most governments and international organizations support and finance them.	Due to the constant changes observed in weather phenomena, the production of electricity through RES presents huge fluctuations.

## 1.2 Hydrogen Economy

The aim of the European Union is a cleaner planet and a climate-neutral Europe. This can be accomplished by renewing energy sources and creating an integrated energy system accompanied by improved access for businesses and consumers to clean, affordable and safe energy. The EU has to deal with the fact that 75% of greenhouse gas emissions come from energy production and

consumption, and that it still relies on imports for 58% of energy consumption, mainly oil and natural gas.

This is the reason why a hydrogen strategy for a climate-neutral Europe has been proposed in order to achieve climate neutrality by the year 2050. Hydrogen is the most common element in the universe and in normal ambient conditions (STP) is a colorless, odorless, tasteless, non-toxic non-metal and highly flammable diatomic gas with the chemical formula  $H_2$ . It also produces 119 972 kJ/kg which makes it the element with the highest energy content per unit weight, about three times more than that of conventional gas. For this reason, it can be a fairly efficient method of energy storage and makes it an additional solution for the utilization of the excessive energy which is produced through RES.

Its categorization, as shown in Figure 1.2, is based on its method of production and on its greenhouse gas emissions: in "Grey Hydrogen" which is derived from fossil fuels and emitting  $CO_2$  into the atmosphere, in "Blue Hydrogen" which emits  $CO_2$  with the difference that it is either collected and stored in the soil or used in the creation of other objects and in "Green Hydrogen" which is produced through the electrolysis of  $H_2O$  and the use of electricity from RES and does not emit greenhouse gases. It is a fact that hydrogen covers only 2% of the EU's energy mix and only 4% of it is "Green Hydrogen". The goal is for the energy mix to be 20% hydrogen by the year 2050, mostly of which will be 'Green Hydrogen', in order to contribute significantly to the resolution of greenhouse effect [3].

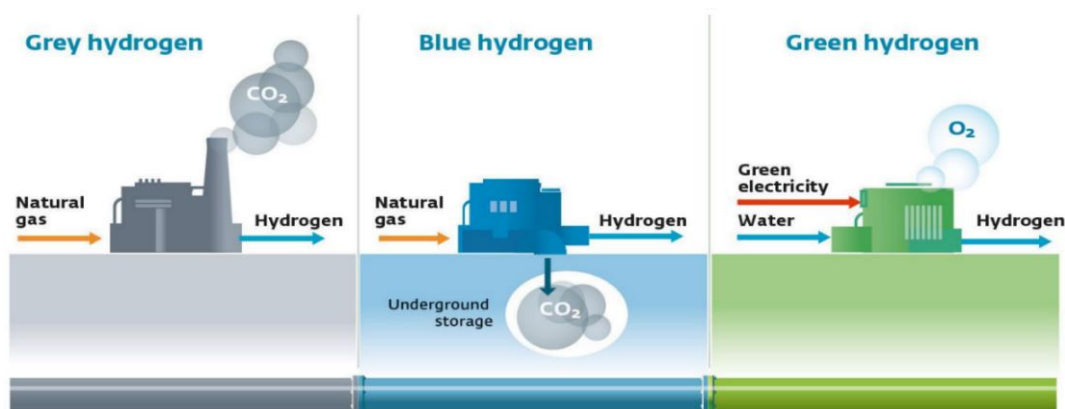


**Figure 1.2. Classification of hydrogen production [4].**

Hydrogen can be produced by a number of key technologies: reforming of hydrocarbons with steam, gasification of heavy hydrocarbons, gasification of biomass, nuclear processes, and electrolysis of water. Hydrogen is currently mainly produced using fossil fuels and reforming natural gas with steam. However, this will have to change, and its production will have to be done by electrolysis, using energy, which has produced from renewable sources.

Presently, hydrogen is mainly for industrial use. The 50% of the hydrogen produced is consumed for the production of ammonia ( $NH_3$ ), while 37% is consumed by refineries [5]. Applications of

hydrogen as an alternative fuel are found in a variety of suitably modified technologies, such as gas boilers, internal combustion engines, gas turbines and catalytic afterburners.

The product of hydrogen combustion is water, but when we have very high temperatures, nitrogen oxides are also produced. Hydrogen can be a quite efficient method of energy storage and makes it an additional solution for the utilization of the excessive energy which is produced through RES.

Fuel cells are a very important and relatively recent technology which is an electrochemical generating device of electricity, with water as the only by-product. Their function closely resembles conventional batteries with the basic difference that it has no restriction on fuel depletion.

## Chapter 2

### BASICS OF ELECTROCHEMISTRY AND ELECTROCHEMICAL DEVICES

#### 2.1 Electrochemistry Basics

The scientific term electrochemistry refers to either the production of electricity from chemical actions or the production of chemical energy from electricity. This connection takes place thanks to the electrical charge (anions, cations, electrons, etc.) which, when in an electrochemical system, are transferred. The most common electrochemical system is the electrochemical cell, as shown in Figure 2.1 are:

- A porous diaphragm or membrane with the primary role of facilitating the movement of ions from the anode to the cathode, while not allowing the movement of electrons across the membrane from the anode to the cathode.
- An electrolytic medium, which does not take part in the reactions, simply allows the movement of ions between the electrodes and can be either a liquid or solid polymer.
- The anode and cathode electrodes which are either conductors or semiconductors.
- An external source through which the electrons pass.

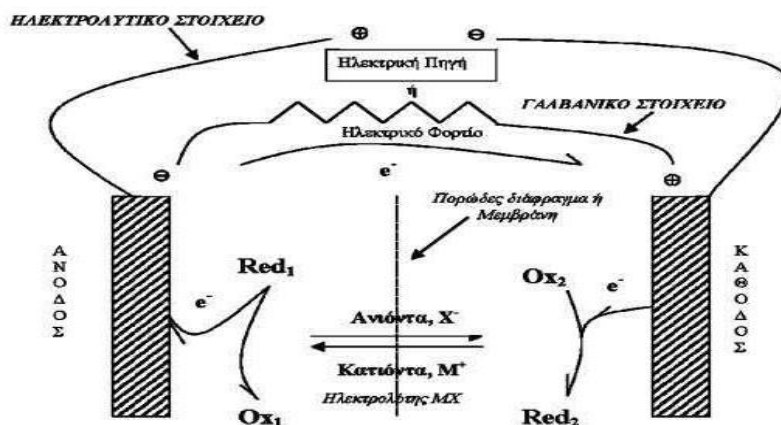
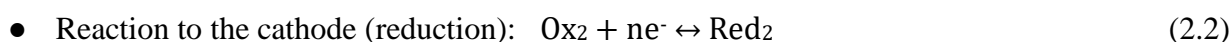
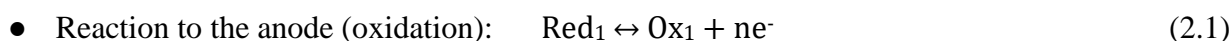


Figure 2.1 A simple electrochemical cell [6].

In a nutshell, the production of electricity is achieved by the movement of ions and the exchange of electrons between them and the flow of electrons through the external circuit. The reactions that take place are redox reactions, namely:



The term redox refers to the reaction between two conjugate pairs of oxidant-reductant that involves electron transfer from the reductant to the oxidant. Also, although the reaction is bidirectional it is practically in the direction from the stronger oxidant and reductant to the weaker one.

Looking at figure 2.1, the separation of the electrolytic element and the galvanic element (voltaic) is important (Figure 2.2). In the electrolytic element the electrical energy is converted into chemical energy, the anode has a positive sign while the cathode has a negative sign and finally an external current is consumed which makes the reaction forced. On the contrary, in the galvanic cell we have electricity generation from chemical, the cathode has a positive sign while the anode has a negative sign and is characterized as a spontaneous reaction. This is because one of the two elements loses electrons more easily than the other [8].

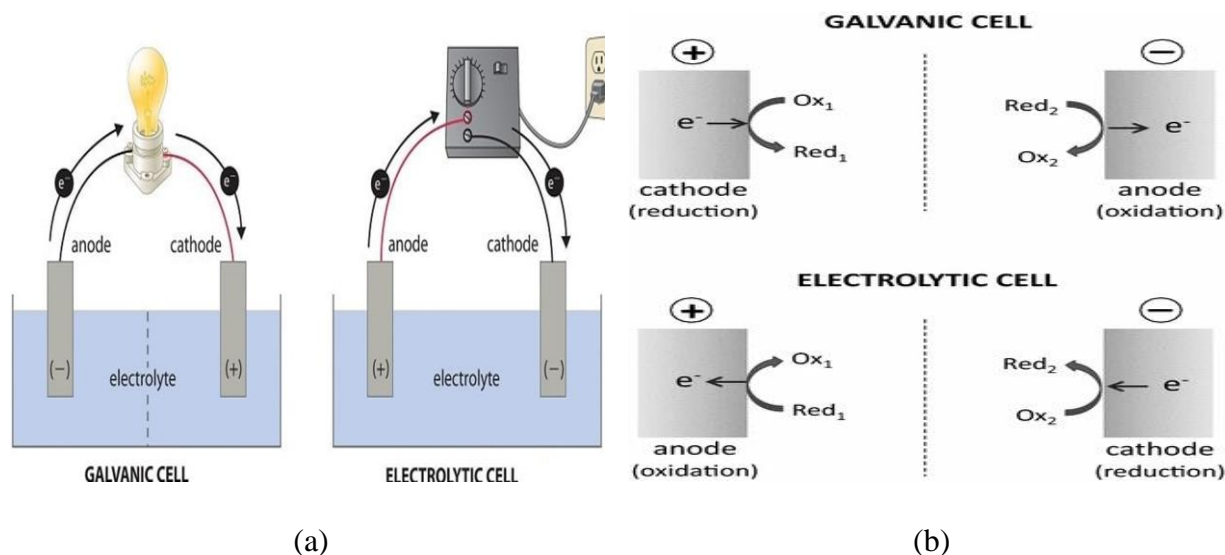


Figure 2.2. (a), (b). A galvanic and an electrolytic cell [7,8].

### 2.1.1 Thermodynamics of Electrochemical Reactions

When examining electrochemical systems, it is customary to consider them at constant temperature (T) and pressure (p). In such circumstances, the most practical thermodynamic functions are the Gibbs energy (G) and the enthalpy (H). The Gibbs energy (G) is calculated as the sum of the internal energy (U) and the product pressure (p) and volume (V), reduced by the product of temperature (T) and entropy (S) i.e.,  $G = U + pV - TS$ . Similarly, the enthalpy is obtained by the internal energy to the product of pressure and volume, without accounting for entropy i.e.,  $H = U + pV$ .

The Gibbs free energy is a state function and a fundamental concept in thermodynamics. When we talk about the transition of a system from state A to state B, the change in Gibbs free energy, denoted as  $\Delta G$ , represents the energy difference between these two states, without matter how the system reached its current state or how quickly it approached equilibrium. The following relationship holds:

$$\Delta G = Q - W_u \quad (2.3)$$

Where, Q is the heat exchanged with the environment, and  $W_u$  the useful work done on or by the system. The state of equilibrium is characterized by the minimum value of Gibbs energy, and the condition for equilibrium is expressed as  $\Delta G = 0$  [8,9].

The specific values of thermodynamic functions in systems containing various components are contingent upon the nature and quantity of those components. We can differentiate between two types of components: “pure” components, which form separate phases with constant composition, and components that are part of phases with variable composition. For a system consisting only of pure components the Gibbs energy is as follows:

$$G = \sum N_k \cdot G_k \quad (2.4)$$

Where,  $G_k$  is the specific molar Gibbs energy of component  $k$  and in J/mol and  $N_k$  is the number of moles of this component in the system. While, for a system consisting of variable components the Gibbs energy is as follows:

$$G = N_k \cdot \mu_k \quad (2.5)$$

Where,  $\mu_k$  is called the chemical potential of the component  $k$  in J/mol and is given by the equation:

$$\mu_k = \frac{dG}{dN_k} = \mu_k^0 + RT \cdot \ln p_k = \mu_k^0 + RT \cdot \ln c_k \quad (2.6)$$

Where  $p_k$  and  $c_k$  are the partial pressure and molarity respectively. Solutions in which the concentration dependence of chemical potential obeys the Eq. (2.6), as in the case of ideal gases, otherwise the concentration dependence of chemical potential is more complicated [9,10].

## 2.2 Energy Conversion and Storage Devices

In today’s world, the challenges we face on a global scale, such as the depletion of fossil fuels, climate change, and rapidly growing energy demand, make it necessary to develop more efficient clean energy technologies for energy storage and conversion. These technologies can be mechanical, magnetic, thermal, and electrochemical conversion and storage systems. Electrochemical devices are the most feasible, the most sustainable, the most environmentally friendly, and the most reliable. The most important electrochemical devices are fuel cells, batteries, capacitors, supercapacitors, and electrolytes, which are already in use or will be in use soon in several important sectors. Finally, it is necessary to make some improvements to these electrochemical devices in order to enable their use in new diverse application areas, as well as to overcome challenges such as cost, reliability, and safety, which hamper their commercialization [11].

### 2.2.1 Fuel Cells

Fuel cells are devices that utilize electrochemical processes to convert chemical energy into electrical energy. Therefore, they generate electricity by omitting the intermediate steps of heat generation and mechanical work, which are present in most conventional electricity generation devices. The omission of these steps puts fuel cells in an advantageous position in terms of their efficiency and their impact on the environment. Figure 2.3 shows schematically the process of converting energy from different devices [12,13].

The main difference between a fuel cell and a battery is that as long as the fuel cell is fed with fuels it produces electricity, while the battery to produce electricity is consumed.

Internal combustion engines, like fuel cells, convert chemical energy into electricity. In a conventional internal combustion engine, the fuel is burned by releasing heat. Considering the simplest example such as the combustion of hydrogen, we have the following reaction:



In the combustion of hydrogen, we have oxidation of hydrogen molecules to produce water and release heat. On an atomic scale, hydrogen-hydrogen bonds and oxygen-oxygen bonds disintegrate and reshape hydrogen-oxygen bonds over a few picoseconds on a subatomic scale. This disintegration and reformation of these bonds is done by electron transfer between the molecules. However, the energy contained in electrons during their transport is only recoverable as heat due to the very fast and very small-scale reconfiguration of the bonds. So, in order to produce electricity from an internal combustion engine, heat must be produced first, and then mechanical energy to end up in the production of electricity. The fuel cell manages by separating the hydrogen and oxygen reactants with an electrolyte to make the electrons usable and produce electricity directly from the chemical energy of the fuel [13,14].

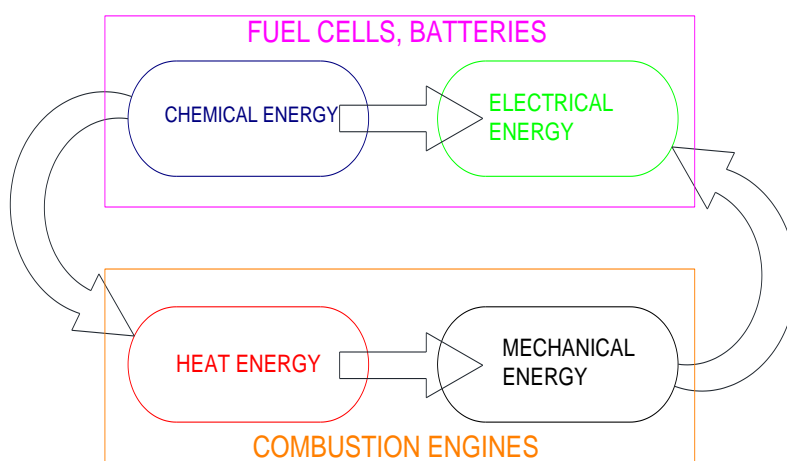
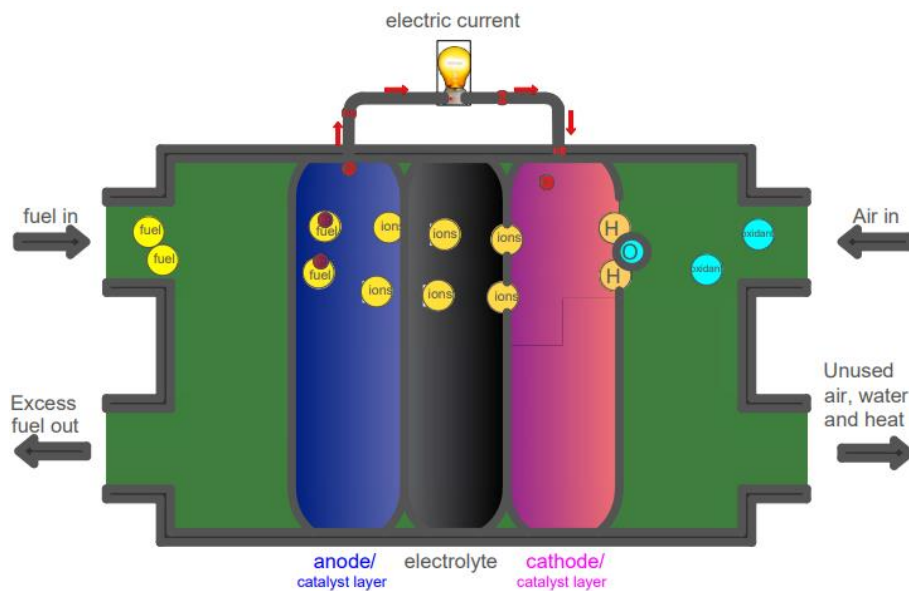


Figure 2.3 Process of energy conversion from different devices [14].

### Components and materials of a simple fuel cell.

A fuel cell is continuously powered by fuel at the anode and continuously by an oxidant (usually air oxygen) at the cathode. The anode and cathode are the negative and positive electrodes respectively. Electrochemical reactions take place in these electrodes. The electrolyte (membrane) separates the anode electrode from the cathode electrode, ensures that the two separate reactions will occur in isolation from each other, and only allows the transfer of ions through it. Thus, the electrons, which have been released by the oxidation of the fuel in the anode electrode, cannot penetrate the electrolyte, causing them to be transferred to the cathode electrode through an external circuit. The role of each component is detailed briefly below while Figure 2.4 shows schematically the basic anatomy of a simple fuel cell [12,15].



**Figure 2.4 Basic components of a simple fuel cell [17].**

1. Anode:

The anode is the electrode where the fuel is oxidized, producing electrons and ions. They are made of a porous material, usually carbon, and platinum.

2. Cathode:

The cathode is the electrode where the oxidant is reduced, consuming electrons and ions. They are made of a porous material, usually carbon, and platinum. Both electrodes are susceptible to the presence of various impurities that may be present in the inputs, potentially leading to their degradation and adversely impacting the overall performance.

3. Electrolyte:

The electrolyte is a critical component that plays a vital role in the cell's operation. Its main role is to be the medium for the transport of ions between the two electrodes, the anode, and the cathode, allowing the electrochemical reaction to take place. Additionally, the electrolyte must be conductive to allow this movement of ions, but it must also be impermeable to prevent the mixing of the reactants at the electrodes because the oxidation/reduction reaction must not take place on the same side, since that can harm the cell. The electrolyte must also be stable in the fuel cell's operating conditions, such as high temperatures and corrosive environments. The material which is made can be liquid or solid depending on the type of fuel cell [18].

4. Gas Diffusion Layer (GDL):

The GDL is an essential component of a fuel cell that is located between the electrode and the reactant gas channels. There are a lot of functions that must do. Firstly, GDL provides a porous and conductive layer that enables the flow of reactant gases to reach the electrode. Due to this porous structure of the GDL, the distribution of gases is uniform on the surface of the electrode, enabling the effective

realization of electrochemical reactions. Secondly, the electrons produced by the electrochemical reactions in the electrode are collected by the GDL, which acts as a current collector and transferred to the external circuit. The GDL must have a low electrical resistance to minimize the power losses that can occur due to resistance in the current path. Additionally, it plays a vital role in the water management of the fuel cell. The GDL must allow water to be transported away from the electrode, while the electrochemical reactions produce water as a by-product, to avoid flooding and ensure a continuous supply of reactant gases to the electrode. Moreover, the electrochemical reaction also produces heat as a by-product. The GDL can help facilitate heat transfer by providing a conductive pathway for the heat to be removed from the electrode and transferred to the cooling system of the fuel cell. The porosity of the GDL also allows for the efficient transfer of heat away from the electrode and into the coolant flow, which helps to maintain stable operating temperature. To perform these functions, GDL materials are typically made from carbon-based materials. It is also very important to have a high surface area to provide an efficient reactant distribution, and the carbon structure must be porous to allow for the transport of gases and water. Finally, must also be durable, stable in the fuel cell's operating conditions and have a good mechanical strength.

#### 5. Catalyst layers:

The main function of the catalytic layers is to catalyze the reactions between the fuel and oxidant gases that are supplied to the fuel cell. At the anode the catalytic layer promotes the oxidation of the fuel, while at the cathode it promotes the reduction of the oxidant. Also, due to their large surface area they help to increase the reaction rate and the overall efficiency. Finally, the porous structure of the catalytic layers provides the possibility of efficient transport of the reactants and products to and from the electrode surface, minimizing transport losses and increasing the power efficiency of the fuel cell. The materials used are usually metals, and especially Pt and its alloys, which have high catalytic activity and stability [19].

#### 6. Bipolar plates:

Bipolar plates are structures that contain very thin grooves or channels in order to diffuse the reactants throughout the surface of the cell. The shape, size and design of the flow channels can significantly affect the efficiency of the fuel cell. They are also responsible for the removal of waste heat from the fuel cell, which helps to maintain a consistent operating temperature. Moreover, they provide a conductive pathway for the flow of electrons between adjacent cells in the stack. The plates are designed with small holes or slots that allow the electrodes from different cells to come into contact with one another, creating a continuous flow of electrons from the anode to the cathode. The plates need to be made of materials with chemical stability, corrosion resistance, hydrophobicity, compressive strength, and electrical conductivity, thermal conductivity. Typically, their materials are made of non-porous graphite, metals such as aluminum, stainless steel, nickel,

and titanium, as well as polymer composites. Last but not least, the bipolar plates must be designed very carefully to minimize the contact resistance between adjacent cells in the stack, otherwise it can cause a voltage drop across the stack and reduce the efficiency of the cell [16,20].

## Basic operation of a fuel cell

The basic steps of a fuel cell's function in order to produce electricity efficiently are mentioned below:

1. Feeding the reactants to the fuel cell.
2. Electrochemical reactions.
3. Transfer of electrons through an external circuit and ionic conductivity through the electrolyte.
4. Product removal from the fuel cell.

The above steps are shown schematically in Figure 2.5.

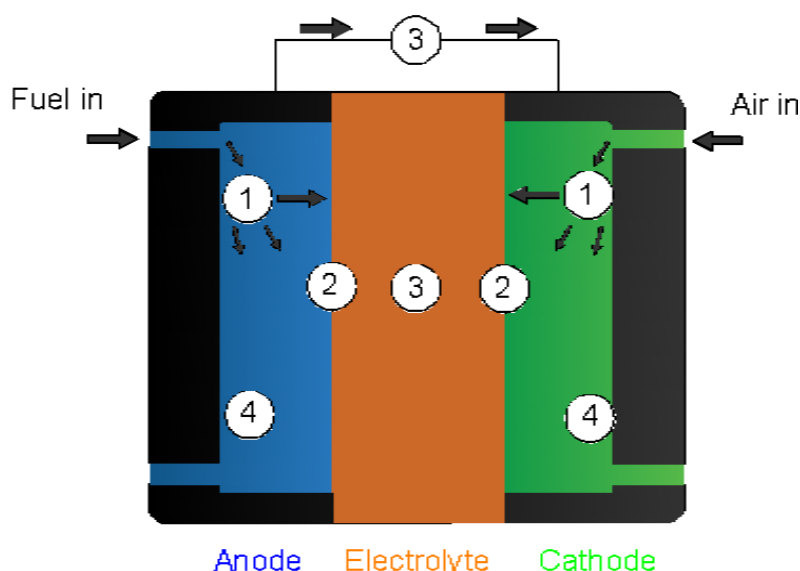


Figure 2.5. The basic steps of FCs' function [17].

### 1. Feeding the reactants to the fuel cell.

As already mentioned, in order for a fuel cell to produce electricity it must be continuously powered by fuel and oxidants. The transfer of these reactants to the fuel cell is not so simple and easy. For the efficient and correct feeding of the cell, in addition to the porous electrode structures which are required to increase the surface area of the reaction and ensure good access of the reactants, bipolar plates and gas diffusion layer are also used.

### 2. Electrochemical reactions

Immediately after the reactants are fed into the electrodes, the electrochemical reactions take place. Electrochemical reactions are directly related to the efficiency of the fuel cell. Fast electrochemical

reactions result in high electricity production. Therefore, catalysts are used to increase the speed of electrochemical reactions. Appropriate catalyst selection leads to increased fuel cell efficiency.

### 3. Ionic and electronic conductivity.

Electrochemical reactions that take place in the electrodes, either produce or consume ions and electrons. The ions and electrons which are produced in one electrode should be consumed in the other electrode. Thus, it is necessary to transfer from the electrode in which they are produced (anode) to the electrode in which they are consumed (cathode). For this transfer they follow two separate routes. Transfer of electrons is easier, as long as an electrically conductive path (e.g., a wire) exists. The ions are transferred from the anode electrode to the cathode electrode or vice versa via the electrolyte. Compared to the transfer of electrons, this process is much less efficient. For this reason, electrolytes should be manufactured as thin as possible, so that the ionic conductivity becomes more effective and eventually the cell functions more efficiently.

### 4. Product removal from the fuel cell.

In addition to electricity, fuel cell reactions also produce other products, such as water and CO<sub>2</sub>. If these products are not removed, they will flood the fuel cell blocking the fuel and oxidants from reaching the electrodes to react. This would render the cell useless and create a serious problem. However, feeding the cell with reactants automatically helps to remove the generated products by solving this problem very easily [17].

## Different types of fuel cells

There are several types of fuel cells, each incorporating different materials and operating conditions and being more suitable in different application areas. The Table 2.1 categorize the six most common types of fuel cells based on their operating temperature as follows [17]:

**Table 2.1. Classification of fuel cells by temperature [17].**

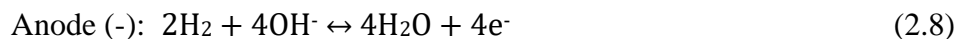
Low temperature fuel cells	High temperature fuel cells
Alkaline Fuel Cells (AFC)	Phosphoric Acid Fuel Cell (PAFC)
Polymer Electrolyte Membrane Fuel Cell (PEMFC)	Solid Oxide Fuel Cell (SOFC)
Direct Methanol Fuel Cell (DMFC)	Molten Carbonate Fuel Cell (MCFC)

### Alkaline fuel cells (AFC)

Alkaline fuel cells (AFC) are electrochemical devices, which operate at efficiencies between 60% – 70% and with typical operating temperatures between 50°C and 100°C, with an optimum temperature of 80°C. They are also responsible for providing power from a few tens of kW to a few

hundred kW. Figure 2.6 shows schematically the operating principle of an AFC, while Table 2.1 presents some basic elements of this type of cell.

AFCs use aqueous solution as an electrolyte, most often potassium hydroxide (KOH) because it is the most conductive of all alkaline solutions. The electrochemical reactions that take place in an alkaline fuel cell when hydrogen is used as a fuel are as follows:



In cathode, oxygen reacts with water according to reaction (2) and produces hydroxyl ions, which are transferred through the electrolyte to the anode where they react with hydrogen to produce water and electrons according to reaction (1). The electrons are transferred to the cathode via an external circuit as shown in Figure 2.6.

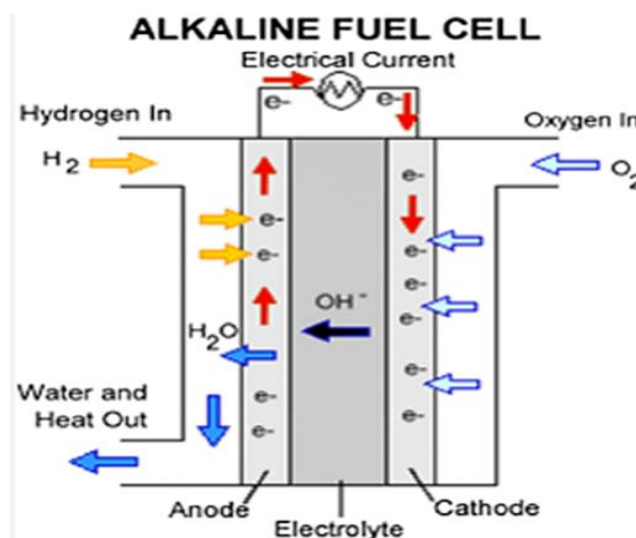


Figure 2.6: Representation depicting the working mechanism of an AFC [21].

The main disadvantage of an AFC is the fact that the KOH solution which is used as an electrolyte is sensitive to the presence of CO<sub>2</sub>. This problem is a huge limitation in the choice of oxidant since the most commonly used oxidant that is air contains CO<sub>2</sub> [21-23].

### Polymer electrolyte membrane fuel cell (PEMFC)

Polymer electrolyte membrane fuel cell are compact and the light electrochemical devices which function at efficiencies between 40% - 70%, with typical operating temperatures from 50°C to 120°C if a Nafion membrane is used and from 120°C to 220°C if another membrane type is used. They are responsible for providing more power than AFCs, which can range from 100 kW to 500 kW. Table 2.2 shows some key elements of PEMFC, while Figure 2.7 schematically presents the operating principle of this type of cell [24].

**Table 2.2. Fundamental traits of various fuel cell types [21].**

	PEMFC	PAFC	AFC	MCFC	SOFC	DMFC
Electrolyte	Polymer membrane	Liquid H <sub>3</sub> PO <sub>4</sub> (immobilized)	Liquid KOH (immobilized)	Molten carbonate	Ceramic	Polymer membrane
Charge carrier	H <sup>+</sup>	H <sup>+</sup>	OH <sup>-</sup>	CO <sub>3</sub> <sup>2-</sup>	O <sup>2-</sup>	H <sup>+</sup>
Operating temperature	50°C- 220°C	150°C- 220°C	50°C -100°C	650°C	600-1000°C	50- 90°C
Catalyst	Platinum or Palladium	Platinum	Platinum	Nickel	Nickel, Nickel oxides	Platinum
Cell components	Carbon based	Carbon based	Carbon based	Stainless based	Ceramic based	Carbon based
Fuel compatibility	H <sub>2</sub>	H <sub>2</sub>	H <sub>2</sub>	H <sub>2</sub> , CH <sub>4</sub>	H <sub>2</sub> , CH <sub>4</sub> , CO	CH <sub>3</sub> OH

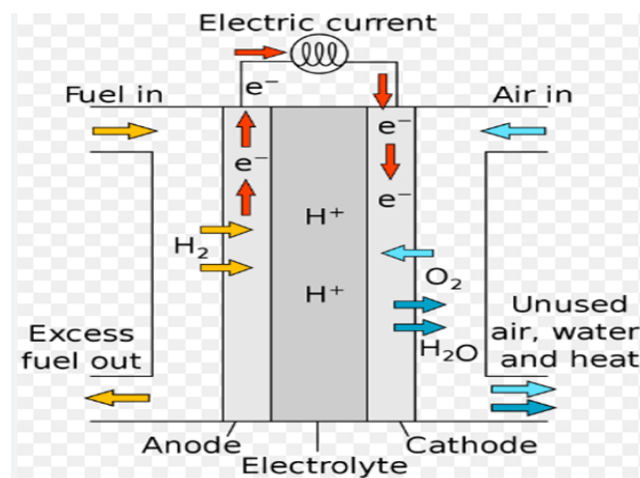
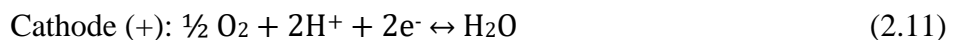


**Figure 2.7. Representation depicting the working mechanism of a PEMFC [21].**

PEMFCs use a thin polymer membrane as an electrolyte, which is usually the Nafion (DuPoint) membrane. The electrodes are made of noble nickel or carbon metals and coated by a catalyst (such as platinum or palladium) to increase efficiency. The electrochemical reactions that occur in PEMFCs electrodes when hydrogen is used as a fuel are as follows:



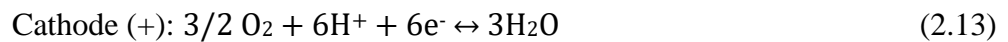
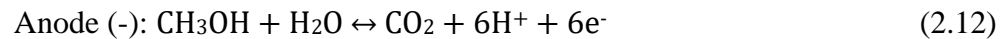
At the anode hydrogen disintegrates forming protons and electrons according to reaction (3). The protons are transferred through the electrolyte to the cathode while the electrons through the outer circuit where they react with oxygen, according to the reaction (4) producing water.

PEMFCs are considered a promising future technology if they are able to reduce the dependence of their electrodes on catalysts such as platinum without reducing their efficiency. This will allow them to become commercially competitive [21,25,26].

## Direct methanol fuel cell (DMFC)

Direct methanol fuel cells operate at efficiency ranging from 20% to 30%, with typical operating temperatures from 50°C to 90°C. They are also responsible for providing power from 100 mW to 1 kW, i.e. they produce a small amount of energy but for a long time. Table 2.1 shows some key elements of Direct methanol fuel cell.

DMFCs are similar to PEMFCs, as both have polymer material (usually Nafion) as electrolyte and the charge which is carried through the electrolyte is the protons ( $H^+$ ). In addition, as in PEMFCs, platinum catalysts are used in both electrodes in DMFCs. The electrochemical reactions that take place in this type of cell are the following:



Liquid methanol oxidizes at the anode in the presence of water, according to reaction (7), producing  $CO_2$ , protons and electrons. Then the protons and electrons through the electrolyte and the external circuit respectively are transferred to the cathode, where according to reaction (8) they are reduced by producing water. Direct methanol fuel cells are suitable for small to medium applications [21,22,25,27].

## Solid oxide fuel cell (SOFC)

Solid oxide fuel cells operate at efficiencies between 50% - 60% with typical operating temperatures between 600°C and 1000°C, i.e., at temperatures higher than any other type of fuel cell. They are responsible for providing a lot of power that can range from a few tens to a few hundred MW, depending on the stack in which they will combine and form. Table 2.1 shows some key elements of this fuel cell type. SOFCs have a thin solid ceramic membrane (0.1mm thick) as an electrolyte, usually from Perfluorosulfonic acid polymer (Nafion), yttria ( $Y_2O_3$ ) -stabilized zirconia ( $ZrO_2$ ), and the charge carried through the electrolyte is oxygen ions ( $O_2^-$ ). The anode electrode consists of a combination of yttria stabilized zirconia (YSZ) and nickel oxides (NiO). The cathode electrode is made of ceramics with a perovskite structure, such as lanthanum strontium manganite (LSM), or lanthanum calcium manganite (LCM). In addition, nickel catalysts or nickel oxides are used instead of high platinum cost [28].

Due to the high operating temperatures, SOFCs have great advantages, but they also have to face some challenges. Initially there is a significant restriction on the choice of electrode materials, and it is quite time-consuming to start them. It is also common to accumulate carbon dust or graphite at the anode preventing the fuel from reaching the catalyst. However, they show flexibility in the choice of fuel. A variety of fuel options such as methane, methanol, ethanol and gasoline are considered feasible for the operation of SOFCs. These crude fuels are reformed by steam before

being fed into the fuel cell producing hydrogen-rich gases (H<sub>2</sub>, CO, CH<sub>4</sub> mix). Figure 2.8 below shows schematically the operating principle of a SOFC [21,22,25].

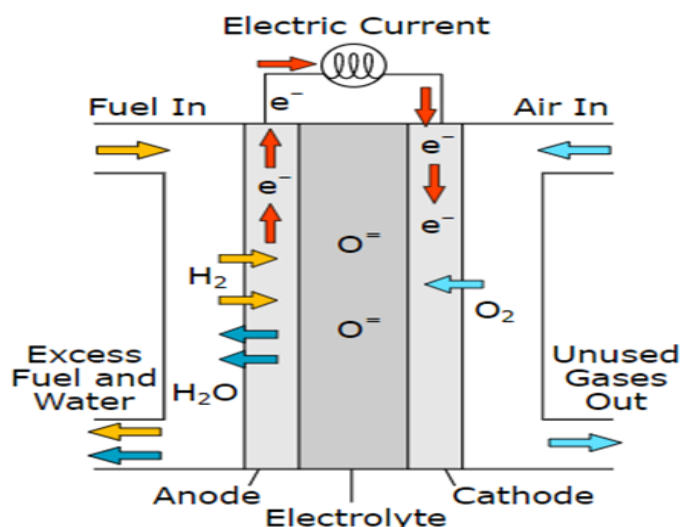


Figure 2.8. Representation depicting the working mechanism of a SOFC [21].

### Phosphoric acid fuel cell (PAFC)

Phosphoric acid fuel cells function up to 80% efficiency, with operating temperatures ranging from 150°C to 220°C. They are responsible for generating power up to approximately 100 MW. Table 2.1 shows some key elements of the PAFC.

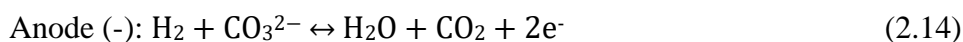
The operating principle of PAFC is similar to that of PEMFC, with the difference that phosphoric acid fuel cells use a highly concentrated liquid phosphoric acid (H<sub>3</sub>PO<sub>4</sub>) saturated in a silicon carbide matrix (SiC) as an electrolyte.

The easy construction, the low fluidity of the electrolyte, the fact that CO<sub>2</sub> does not affect the electrolyte, or the efficiency of the cell are some of the advantages of PAFC.

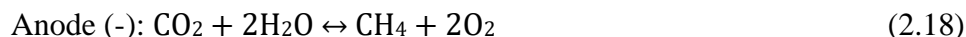
However, the high concentration of H<sub>3</sub>PO<sub>4</sub> in the electrolyte creates freezing problems when the cell is switched off, requiring an auxiliary heating installation to maintain a temperature above 40°C [21].

### Molten carbonate fuel cells (MCFC)

The molten carbonate fuel cells operate with efficiencies that can reach up to 50% - 60%, and with operating temperatures between 600°C and 650°C, lower than those required in a SOFC. They are responsible for generating up to 100 MW of power. Table 2.1 shows the basic building blocks of the cell. MCFCs employ an electrolyte composed of a molten salt mixture, which consists of carbonates salts (sodium or magnesium) suspended within a porous and chemically inactive ceramic matrix of lithium aluminum oxide (LiAlO<sub>2</sub>). The electrochemical reactions that take place are the following:



Internal Reform Reactions:



MCFCs can use carbon oxides as fuel by reforming them inside of the fuel cell into hydrogen or hydrogen-rich gases, in accordance with reactions (11), (12), (13). Therefore, this type of cell is not susceptible to monoxide or carbon dioxide poisoning.

However, the main disadvantages of MCFCs are their low life expectancy and the production of CO<sub>2</sub> products other than water which can be harmful to the environment [21,25].

### **Advantages and disadvantages**

Fuel cells have several advantages as they combine positive elements of various energy conversion devices. Initially, they generate electricity all the time, just like internal combustion engines, while their operation is based on electrochemistry, just like batteries. Their most important advantage is that by using the appropriate fuel, they do not emit unwanted exhaust gases, producing only water as a product. In addition, fuel cells do not contain any moving structural parts, and as a result are reliable with a fairly long-life expectancy and economical maintenance. The fact that they are made up of stable structural parts makes their operation sufficiently quiet. Another very important advantage of fuel cells is that they allow easy and independent scaling of both their power (determined by the size of the cell) and their capacity (determined by the size of the fuel tank of the cell). Thus, fuel cells are suitable devices both for the supply of one watt of power (mobile phone) and for the supply of many MW of power (power plant). The fast feedback of the fuel cells makes them ideal devices for many and varied applications. Finally, as already mentioned, fuel cells are much more efficient than conventional internal combustion engines, as they are not limited by the Carnot cycle, since they have the ability to convert chemical energy directly into electricity [29-31]. For every advantage that a fuel cell develops, there are still challenges and obstacles that need to be overcome in order to become popular and competitive in the international market. Initially, while hydrogen is in abundance in the universe, in order to be able to feed a fuel cell, it must be used solid. Solid hydrogen is found by various methods such as electrolysis of water or extraction from fossil fuels. The electrolysis of water is a costly process, while the extraction of hydrogen from fossil fuels creates undesirable pollutants. Another challenge that needs to be faced is the limited hydrogen fuel stations in order to facilitate the commercialization of the fuel cell in the transport sector. Another serious problem for which a solution should be proposed immediately is the way hydrogen is

transported and stored. Considering that hydrogen is a quite flammable material and has a very low volumetric energy, its transportation and storage are very difficult and dangerous procedures [17].

## Fuel cells and the environment

The greatest advantage of a fuel cell is the fact that it does not burden the environment with pollutants. However, using fossil fuels to produce hydrogen the above advantage is negated, and the cell ceases to be better than the current energy conversion system based mainly on internal combustion engines. Therefore, the use of fuel cells in combination with electrolyzers and renewable energy conversion technologies (such as wind and solar energy) create a closed-loop of pollution-free energy economy. This closed power system on a sunny, windy day generates electricity that is either used directly or converted through electrolytes into hydrogen and stored in this form so that it is converted back into electricity from a fuel cell on a cloudy, windless day. The function of this closed power system is shown schematically in Figure 2.9 [17,32].

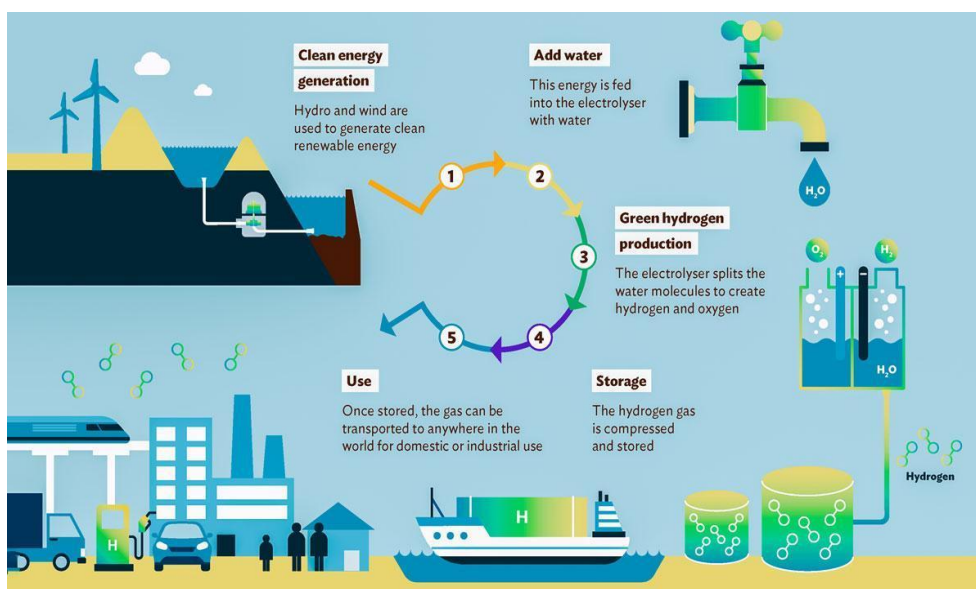


Figure 2.9. Closed-loop of pollution-free energy economy [17].

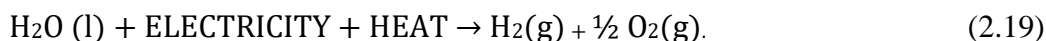
### 2.2.2 Electrolyzers

#### Introduction

An electrolyzer is an electrochemical device that uses electrical energy to separate the components of water, hydrogen, and oxygen through a process called electrolysis. Hydrogen production systems through water electrolysis, which are powered by renewable energy sources, are the only systems that produce huge amounts of hydrogen without the emission of polluting gases and without the consumption of fossil fuels. For this reason, these systems are expected to attract great interest if they manage to reduce the huge amounts of electricity they consume [33-34].

## Basic operation of a simple electrolyzer

As in all electrochemical devices, an electrolyzer consists of two electrodes, separated from each other by an electrolyte. Electrodes are electron conductors, while the electrolyte which is between the electrodes is an ion conductor and an electron insulator. The reactions that take place in each electrode vary depending on the nature of the electrolyte. However, a general form of the reactions taking place in the electrodes of electrolyzer can be described by the following reaction.



By supplying electrical power from a source of continuous current and heat to the electrolyzer, the water decomposes into hydrogen and oxygen. It is a redox reaction, which happens in the electrochemical element. In the process of electrolysis, the electrons are taken or released from the ions on the surface of the electrodes producing a multi-phase system of gases – liquids – solids. In the negative electrode (cathode) the reduction takes place, and the hydrogen is produced. The electrons flow through the external circuit to this electrode and polarize it negatively. In the positive electrode (anode) oxidation occurs and oxygen is produced. The electrons leave this electrode and polarize it positively. It can easily be observed that the roles of the electrodes are reversed compared to the technology of a fuel cell. The principle of operation and the basic structural parts of the main electrolyzers are schematically described by Figure 2.10 [35-44].

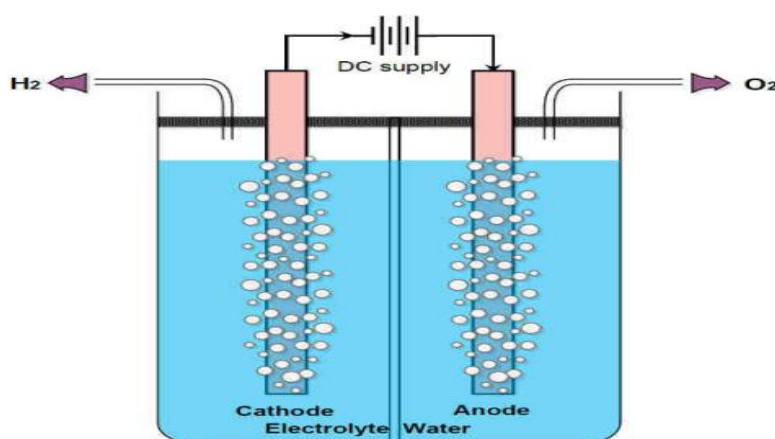


Figure 2.10. A simple electrolyzer [36].

## Different types of electrolyzers

As with fuel cells, electrolyzers are classified into some basic categories based on the electrolyte that is used. These basic classifications are as follows:

1. Alkaline water (AW) electrolyzers.
2. Proton exchange membrane ĩ polymeric membrane (PEM) electrolyzers.
3. Solid oxide (SO) electrolyzers.
4. Molten carbonate (MC) electrolyzers.

## 5. High - temperature steam (HTS) electrolyzers [45].

Some of the above types of electrolyzers are still in the laboratory stage. Alkaline water electrolyzers are currently the only type of electrolyzer that is sufficiently developed. Progress has also been made in proton exchange membrane (PEM) electrolyzers. These two types of electrolyzers are the only ones currently commercially available [46-47].

### Alkaline water electrolyzers (AWE)

Alkaline electrolysis of water is the simplest and most reliable way to produce hydrogen. The direction of the reactions at the electrodes is the reverse of that in an alkaline fuel cell. Alkaline water electrolyzers have a life expectancy of 15 years, they operate with efficiency between 47% and 82%, with typical operating temperatures between 65°C and 100°C and are recognized as a mature technology. Figure 2.11 shows schematically the principle of operation of an alkaline water electrolyzer [36,45].

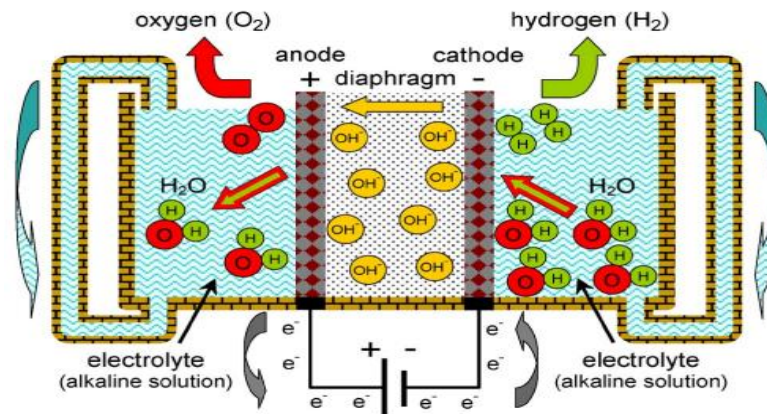
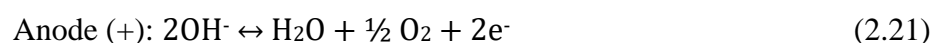


**Figure 2.11. Schematic illustration of the operating principle of an AWE [45].**

In this type of electrolyzer the two electrodes are separated from each other by a gastight diaphragm. This diaphragm prevents the reconstruction of hydrogen and oxygen and the short circuit of electrodes. Diaphragm – Electrode assembly is immersed in an aqueous electrolyte [48-49]. The electrolyte is an aqueous solution containing either KOH, NaOH, or NaCl with a typical concentration of 20-40 % w/t to increase ionic conductivity. The electrochemical reactions that happen in an alkaline water electrolyzer are as follows:



Therefore, the general reaction (2.8) is divided into two half reactions (2.9), (2.10), which take place in the electrodes. As shown in Figure 2.5 the water is reduced to cathode according to reaction (2.9) producing hydrogen and hydroxyl anions. The hydrogen gas is emitted while the hydroxyl anions are transported through the ionic conductive electrolyte to the anode where according to reaction (2.10) they close the circuit [36,45].

## Proton exchange membrane electrolyzers

The polymeric membrane water electrolysis, although commercially available, has some drawbacks, which need to be faced in the short term. These problems are due to their high installation costs, shorter life expectancy compared to alkaline electrolyzers and limited hydrogen production capacity. PEM electrolyzers operate at efficiencies between 48% and 65% with typical operating temperatures below 80°C and are mainly used for small-scale production devices. An interesting feature of PEM electrolyzers is that they can operate under variable power supply conditions producing very high purity hydrogen. Figure 2.12 shows schematically the principle of operation of a PEM electrolyzer [50].

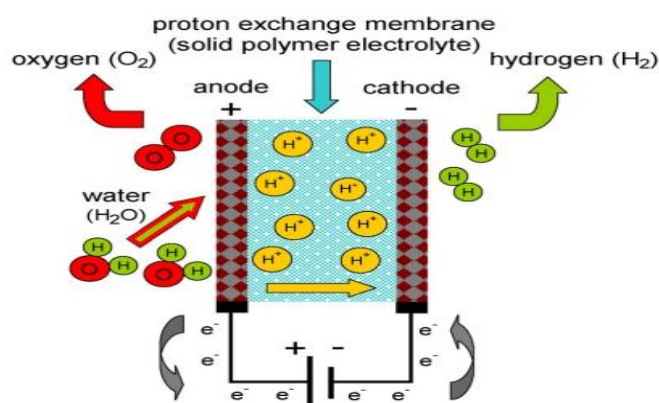
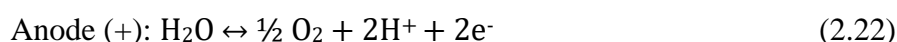


**Figure 2.12. Schematic illustration of the operating principle of a PEM electrolyzer [45].**

In a PEM electrolyzer the electrodes are separated by a membrane, which has the properties of both the diaphragm and the electrolyte. Perfluorosulfonic acid polymeric membranes are used in this type of electrolyte, the most commonly used being Nafion® [51]. The presence of functional groups of the sulfonic acid type (-SO<sub>3</sub>H) is responsible for the conductivity capacity of the protons (H<sup>+</sup>). Electrodes typically consist of noble metals such as platinum and iridium. The anode (positive electrode), the cathode (negative electrode) and the membrane compose the so-called membrane electrode assembly (MEA). The other components of a PEM electrolyzer are the gas diffuser, the gasket, the bipolar plates and the interconnector. The gas diffuser and the gasket enable the electric current to flow between the bipolar plates and the electrodes. Bipolar plates help to transfer water to the anode and to discharge the produced hydrogen and oxygen gases. The electrochemical reactions that happen in a PEM are as follows:



Water is oxidized according to reaction (2.11) to the anode producing oxygen, electrons, and protons. The protons are transferred through the membrane to the cathode where according to the

reaction (2.12) they are reduced producing hydrogen which creates bubbles and is discharged from the cathode, thus closing the circuit [36,45].

### SO electrolyzers, MC electrolyzers, HTS electrolyzers

Solid oxide, molten carbonate, and high temperature electrolyzers are all water electrolysis systems, or rather steam electrolysis systems that operate at high temperatures (600°C – 900°C, 650°C – 700°C, 800°C - 1000°C respectively) [52]. These three types of electrolyzers are still at a laboratory stage. Electrolysis at high temperatures is favorable due to its thermodynamics. Initially with the increase in temperature the requirement of electrolyzer for electricity is significantly reduced. In addition, the ionic conductivity of the electrolyte and the rate of electrochemical reactions occurring in the electrodes are increased. Therefore, the operating characteristics of these types of electrolyzers make the technology of steam electrolysis for the production of hydrogen at high temperatures particularly attractive when a high temperature heat source is available [36,45].

### 2.2.3 Batteries

A battery is an arrangement of electrochemical elements connected in series or parallel to each other that stores chemical energy and generates electricity. The battery as shown in Figure 2.13 consists of two charged electrodes, the anode (negatively charged electrode) and the cathode (positively charged electrode). Between the anode and cathode is an electrolyte which enables ions to be transferred between them. It is usually a liquid or gel substance containing salts, acids, or other conductive materials. It is the movement of electrons from the anode, where oxidation takes place, to the cathode, where reduction takes place that is responsible for the production of electricity [53-58].

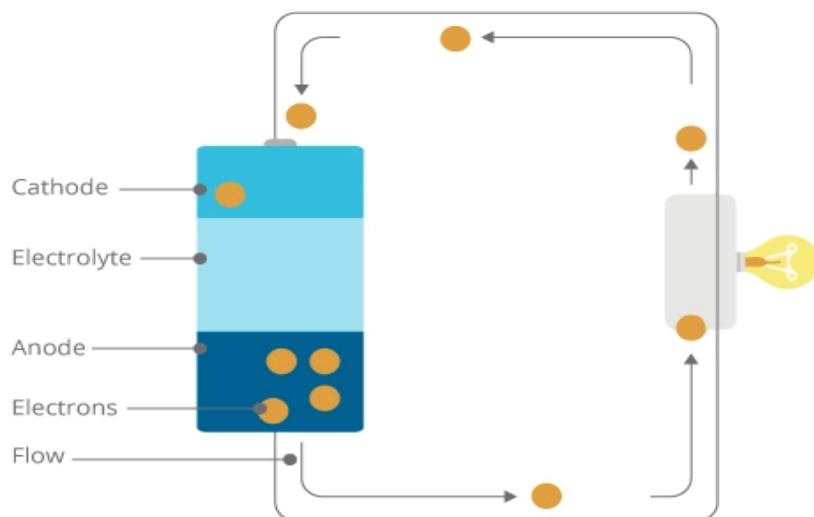


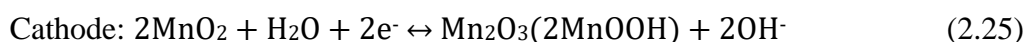
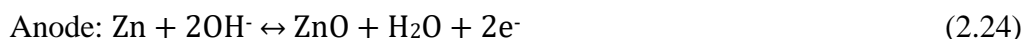
Figure 2.13. Simple anatomy of a battery [59].

Batteries are divided into Primary batteries and Secondary batteries based on the times used. Primary or non-rechargeable batteries have limited capacity and have been designed for single use

without being able to be recharged. They have a higher initial output, and this is a reason they are used in devices that require high current drains, such as digital cameras and flashlights. On the other hand, secondary or rechargeable batteries are designed to be recharged and used several times. They have lower initial energy output but can be recharged and reused multiple times, making them more cost-efficient in the long term. Also, primary batteries have longer shelf-life than secondary batteries that can lose their charge over time, even when not in use. However, secondary batteries have the advantage of being more environmentally friendly because of their ability to be recharged and reused more than once, reducing the amount of waste generated.

There are many types of batteries, and they differ based on their chemistry, size, and applications. Here are some of the most common types of batteries [60-61]:

1. Alkaline batteries: Alkaline batteries owe their development to a pioneer named Lewis Urry, who was born in Canada in 1927. These are primary batteries that use an alkaline electrolyte to generate electric current. Commonly used primary batteries that have a zinc/manganese dioxide chemistry with a basic potassium hydroxide electrolyte. During discharge, zinc metal functions as the negative electrode, while the MnO<sub>2</sub> acts as the positive electrode as it shown in following equations:

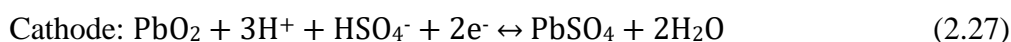
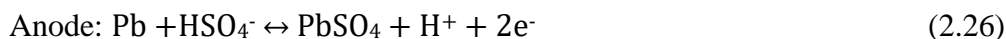


They have a voltage around 1.5V, a high energy density and long shelf-life that can last up to 5-10 years. Also, alkaline batteries have low cost and are widely available. This type is not considered as primary due to the high energy required to reverse the chemical processes involved. Attempting to recharge them would not only be impractical but also hazardous, as it would lead to a significant increase in the battery's temperature, making it dangerous to handle. Finally, they must dispose carefully because of toxic chemicals that can be harmful [62-63].

2. Lithium Primary batteries: These batteries are a type of primary battery that uses metallic lithium as the anode and a cathode made of a metal oxide or other materials. They have a high energy density, long shelf life that can last up to 5-10 years and can supply voltages in the range between 1.5V to 3.7V. The most common cathode material is manganese dioxide merged an organic solution with a lithium salt electrolyte. These batteries are commonly used in devices which require long-lasting power, such as digital cameras, watches, and remote controls. One of the main advantages of lithium primary batteries is their high energy density, allowing them to provide more power for longer periods of time. They are also lightweight and have a low self-discharge rate, making them suitable for long-term storage. However, lithium primary batteries are expensive compared to other types of batteries and contain

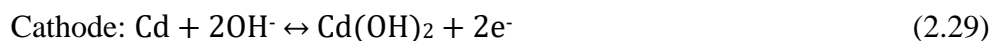
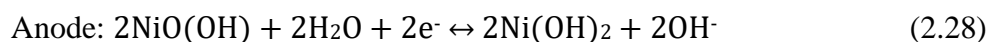
hazardous materials, including lithium and organic solvents that can be difficult to dispose safely. They can also pose a risk of fire or explosion if not handled properly. Moreover, attempting to recharge them can be dangerous, as they can overheat and even explode [64].

3. Lead acid batteries: Lead-acid batteries revolutionize portable power and fall into the classical category invented by French physicist Gaston Plante in 1859. These are types of secondary batteries that consist of six cells, each with a nominal voltage of 2 volts. Each cell is made up of a lead dioxide cathode, a sponge metallic lead anode, and an electrolyte solution that is about 37 % w/w sulfuric acid. When a lead-acid battery is charged, the lead dioxide on the cathode and the lead on the anode react with the sulfuric acid to produce lead sulfate and water. This process releases electrons, which flow through an external circuit and generate electricity. When the battery is discharged, the lead sulfate on the cathode and anode is converted back into lead dioxide and lead, respectively, and the sulfuric acid is regenerated. The electrochemical reactions that happen in a Lead-acid battery are as follows:



They have low energy density, and the self-life can range from several months to several years, seldom exceeds 4 years and can be recharged for 300-400 cycles, depending on how well it is maintained and stored. They also have a low cost compared to other types of batteries. Additionally, they are easy to recycle but they are heavy and bulky, which means it is difficult to use in portable devices [60,65-66].

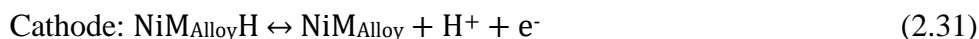
4. Nickel-Cadmium batteries (Ni-Cd): These are types of secondary batteries that use nickel oxide hydroxide as an anode electrode and metallic cadmium as a cathode electrode and an alkaline electrolyte and have a nominal cell potential of 1.2V. The electrochemical reactions that happen are as follows:



They are offering several advantages as higher energy density (50-75Wh/kg) than lead acid batteries, long life (2000-2500 cycles) and they can also operate in extreme temperatures. However, cadmium makes up about 15-20 % w/w of a Ni-Cd battery and is considered a very toxic heavy metal, which bioaccumulates in the environment and is very hazardous for human health. Overall, Ni-Cd batteries are not environmentally friendly because of the danger for cadmium to be released if the battery is not disposed carefully and due to this has actively been replaced by NiMH and Li-ion systems since the mid-1990s [60,67-68].

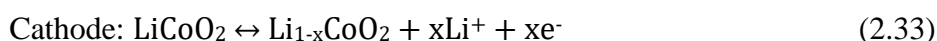
5. Nickel Metal Hydride batteries (NiMH): These are type of secondary batteries that uses a hydrogen-absorbing alloy instead of cadmium as the negative electrode, nickel oxide

hydroxide as the positive electrode and usually 28% potassium hydroxide as the alkaline electrolyte. The reactions that occur are as follows:



The main reason for their development is the environmental concerns about the danger of cadmium. They have higher energy density and longer life than Ni-Cd batteries. The volumetric energy density of NiMH batteries is similar to that of lithium-ion batteries, but their self-discharge rate is higher at 30% per month and has a low internal resistance, allowing them to deliver a near-constant voltage until they are almost completely discharged. Modern NiMH batteries contain catalysts to deal with gases produced during overcharging, which enables them to have a reasonable shelf life, but still not as good as other batteries. Improper disposal of NiMH batteries poses less environmental hazard than Ni-Cd batteries because they do not contain toxic cadmium. Currently, more than two million hybrid cars worldwide are running with NiMH batteries and many of these are manufactured by Panasonic (PEVE) and Sanyo [67-68].

6. Lithium Ions Batteries (Li-Ion): Lithium-ion batteries are a type of rechargeable battery that use lithium ions to transfer charge between the anode and cathode. The anode typically consists of porous carbon or graphite that is intercalated with lithium ions, while the cathode can be made of materials such as lithium cobalt oxide, lithium iron phosphate, or lithium manganese oxide. The reactions that occur are as follows:



Unlike traditional batteries that use metallic lithium as the anode material, which is highly reactive and requires nonaqueous electrolytes, Li-ion batteries use lithium-ion intercalation compounds that are safer and can be used with nonaqueous electrolytes. This has allowed for the development of high energy density batteries with specific energy densities of 150-250 Wh/kg. Moreover, they have slow loss of charge when not in use and also low maintenance cost. However, Li-ion batteries have higher internal resistance compared to other rechargeable batteries such as Ni-Cd and NiMH batteries, which reduces their ability to deliver current. Additionally, they are very sensitive to high temperatures and there is the risk of fire or explosion. Nowadays, Li-ion batteries are becoming increasingly popular in military, electric vehicle, and aerospace applications due to their high energy density [69-74].

These are just a few of the most common types of batteries. There are many other types of batteries such as zinc-carbon batteries, silver-zinc batteries, lithium polymer batteries and more. Table 2.3 shows the basic characteristics of these types of batteries.

**Table 2.3. Essential features of various types of batteries [75-78].**

	Alkaline	Lithium primary	Lead acid	Ni-Cd	NiMH	Li-Ion
<b>Discharge rate</b>	Low	Medium	Low	Very high	High	High
<b>Rechargeable</b>	No	No	Yes	Yes	Yes	Yes
<b>Shelf-life(years)</b>	5-10	10-15	2-5	3-5	3-5	2-3
<b>Nominal V per cell</b>	1.5	1.5	2	1.2	1.2	3.6

## 2.2.4 Supercapacitors

A Supercapacitor (SC), also known as ultracapacitor, is basically a device used for storage and delivery of electric energy quickly and efficiently. A SC, as we can see in Figure 2.14, consist of two electrodes, which usually made of activated carbon, a positive electrode (anode) and a negative electrode (cathode), separated by a membrane, which is called a separator, and an electrolyte. Electrolyte is the means that allows the flow of ions between the electrodes. On the other hand, separator's role is to prevent the electrodes from coming into a touch with each other and causing a short circuit. There are also current collectors, which are conductive materials that collect the charge from electrodes and transmit it to external circuit. Finally, the SC has an enclosure of a non-conductive material, which can protect it from physical damage, relative humidity, dust, and acts as a barrier to prevent accidental contact, with the internal components, reducing the risk of electrical shock or injury, ultimately improving its performance and reliability [79-81].

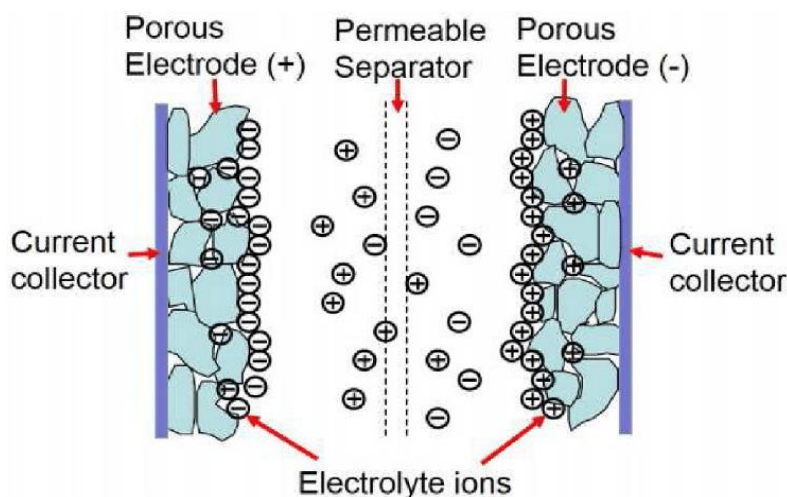


**Figure 2.14. Simple anatomy of a supercapacitor [79].**

Supercapacitor is a combination of two other devices, batteries, and a normal capacitor. It has higher capacity value but lower voltage limits than a normal type of capacitor. Supercapacitors store energy via two mechanisms [80-82]:

- Electric Double Layer Capacitance: Is the primary mechanism that involves separation of positive and negative charges at the Helmholtz double layer electrode-electrolyte interface, creating an electric double layer. Supercapacitors are often made with high surface area

carbon materials because the amount of charge, which can be stored in the double layer is proportional to the surface area of the electrode. Electric double layer capacitance offers fast charge and discharge rates, high power density and a long cycle life.

- Pseudocapacitance: Allows reversible redox reactions at the electrode-electrolyte interface and because of this provides a higher energy density than the electric double layer but it is still lower than that of batteries. Electrode material to facilitate pseudocapacitance is often metal oxides and conducting polymers.

The properties of a SC can be represented by the following equations:

$$C = \epsilon_0 \cdot \epsilon_r / d \cdot A \quad (2.34)$$

$$E = C \cdot \frac{V^2}{2} \quad (2.35)$$

$$P_{max} = \frac{V^2}{4R} \quad (2.36)$$

Where:

**C**: capacity

$\epsilon_0$ : absolute air permeability

$\epsilon_r$ : absolute permeability for the dielectric medium

**A**: the area of the electrodes

**d**: the distance between the two electrodes

**V**: the cell voltage

**E**: the energy density

**P**: the power density

Supercapacitors can be classified in different ways based on various factors such as construction, materials used and operating voltage. Here, as shown in Figure 2.15, are the three main types, based on the energy storage mechanism [82-85]:

1. Electric double layer capacitor (EDLCs): Is the simplest and most common type of supercapacitor based on the interface double-layer theory put forward by German physicist Helmholtz. It consists of two carbon-based electrodes, an electrolyte, and a separator and the energy is stored electrostatically or non-Faradaically, and there is no transfer of charge between electrode and electrolyte but utilize an electrochemical double layer of charge to store energy. The key feature is the large surface area of the carbon electrodes that provides a large interface for the formation of an electric double layer. The two layers of charges creates a large capacitance, allowing EDLCs to store and release energy more quickly than a simple capacitor, because the distance between the two layers of charge in supercapacitor is much smaller than that in traditional capacitor. Typically, the energy density ranges from 1 to 30 Wh/kg and the cycle life are typically high, because EDLCs do

not rely on chemical reactions to store energy, unlike batteries. Finally, compared with the rechargeable batteries the EDLCs can be charge more than  $10^6$  times.

2. Pseudocapacitor: Pseudocapacitors differ from EDLCs in that they rely on fast reversible faradic redox reactions to store charge, rather than solely on the electrostatic force. This leads to higher energy densities and capacities within a certain potential range on or near the surface of the electrode. Transition metal oxides are commonly used as electrode materials due to their abundance, easy preparation, and environmentally friendly nature. However, using a single metal oxide as an electrode can result in low conductivity and poor cycling stability. To address this issue, coupled metal cations are often utilized to improve metallic conductivity and electrochemical activity. Binary metal oxides, such as  $\text{NiMnO}_4$ ,  $\text{NiCo}_2\text{O}_4$ ,  $\text{MnCoO}_3$ ,  $\text{NiMoO}_4$ , and  $\text{CuCoO}_4$ , are widely studied. Summary, pseudocapacitors store charge Faradaically, allowing for greater capacitances and energy densities than EDLCs. However, they have some drawbacks such as mechanical instability and low cycle life due to changes in electrode size during charging and discharging.

3. Hybrid Supercapacitor: Is a combination of EDLC and pseudocapacitor to achieve better performance and characteristics. They can use both faradaic and non-faradaic processes for charge storage, making them superior to EDLCs in terms of power and energy density. Positive materials in hybrid supercapacitors are transition metal oxides or conducting polymers, while activated carbon is used as the negative material or power sources. The charge storage mechanism of hybrid supercapacitors combines fast and reversible faradic redox reactions with reversible adsorption of ions of active materials, resulting in relatively high energy density in combination with high specific capacitance compared to that of pseudocapacitors and EDLCs (Figure 2.16). Hybrid supercapacitors have wide applications in portable supplies, memory backup systems, electric vehicles, and emergency backup power because of their long battery life, higher power density, and smaller volume.

Overall, supercapacitors are used in a wide range of applications, mostly because of their high-power density (Figure 2.17) and long cycle life. Especially, compared to traditional batteries, SCs can charge and discharge much faster, making them an ideal for applications that require quick bursts of energy, such as applications in electric vehicles (EVs). Additionally, SCs can operate in a wide range of temperature relatively with batteries, and they are less affected by aging and degradation. However, as we can see in the Figure 2.17 SCs have lower energy density than batteries, which means that can't store as much energy as batteries and for that reason researchers are trying to develop new materials for them to succeed greater energy densities.

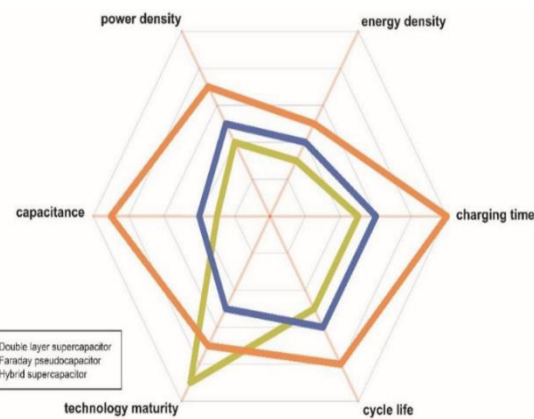
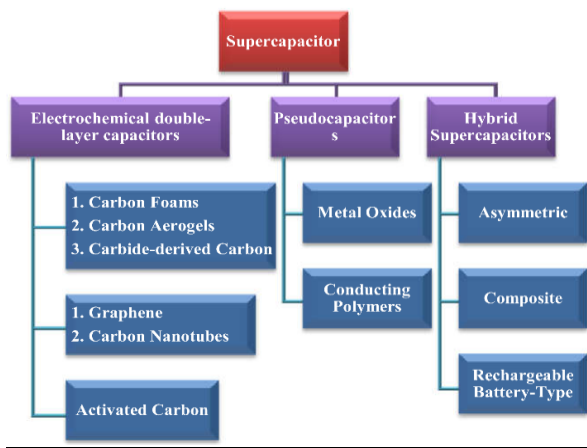


Figure 2.15. Classification of a supercapacitor [83]. Figure 2.16. Comparison of different types of Supercapacitors [86].

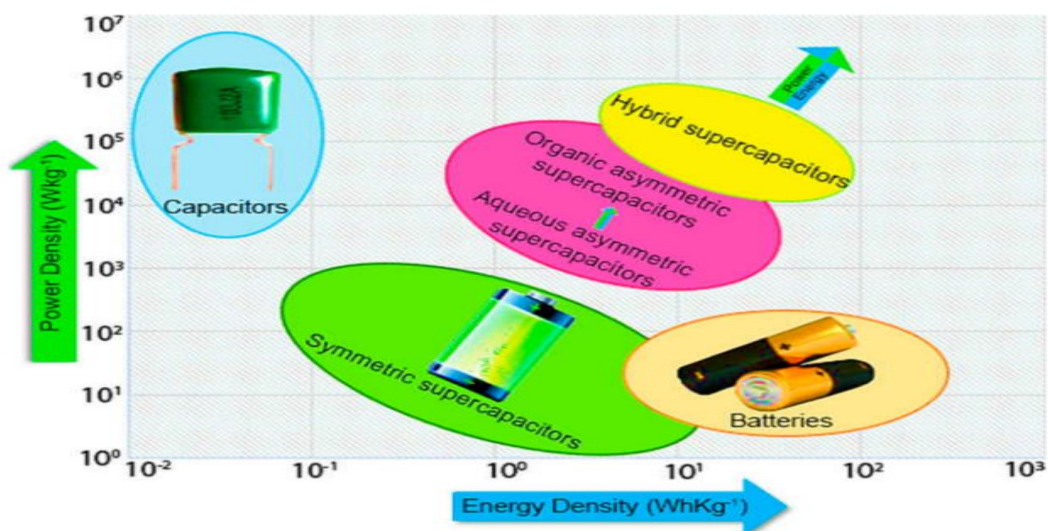
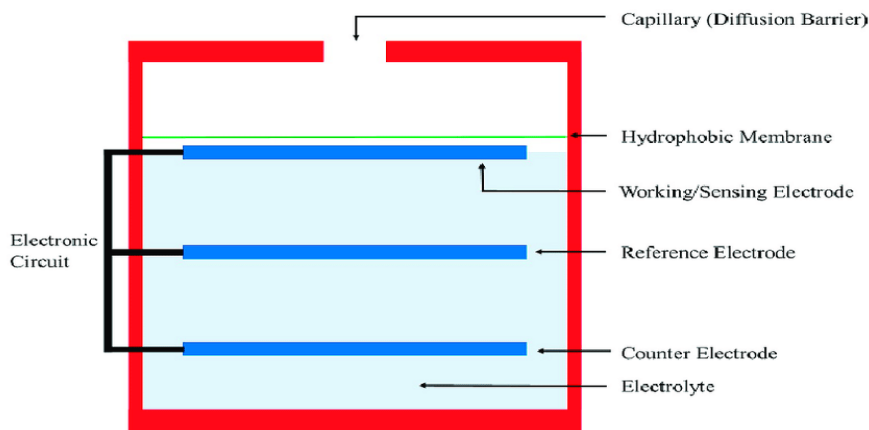


Figure 2.17. Comparison of different electrochemical devices [87].

## 2.2.5 Electrochemical Sensors

An electrochemical sensor is a type of sensor that detect the concentration of a specific chemical, usually oxygen, in a liquid or gas sample, by producing an electrical signal. Electrochemical sensors are accurate and can measure oxygen levels down to the parts per million (ppm) level. This ability makes them an excellent choice compared to thermal and optical sensors. Typically consist of four components (Figure 2.18): a working electrode, a reference electrode, a counter electrode, and an electrolyte. In addition, some electrochemical sensors also have a gas-permeable membrane. The working electrode is responsible for detecting the chemical species of interest, the reference electrode provides a stable voltage reference against which the working electrode's potential can be measured, and the counter electrode which is responsible for the flow of electrons. All three of them usually are made of noble metals. The electrolyte allows the transfer of ions between the working and reference electrodes, completing the electrochemical circuit [88-93]. Depending on the used

electrolyte, electrochemical sensors can be applied in a temperature range of  $-30^{\circ}\text{C}$  up to  $1600^{\circ}\text{C}$ . The electrochemical sensors, which work with aqueous or liquid electrolytes, are usually used up to  $140^{\circ}\text{C}$ , while sensors which work with solid electrolytes operate in the temperature range  $>500^{\circ}\text{C}$ . Finally, in the sensors, which have a gas-permeable membrane, membrane can allow gas molecules to diffuse into the sensor and usually are made of a thin polymer material [94-95].



**Figure 2.18 A simple electrochemical sensor [94].**

There are a lot of types of electrochemical sensors that depends to certain applications or fields of study. These is a brief explanation of the most common types [95-97].

1. **Potentiometric sensors:** Potentiometric sensors have been widely used since 1930s due to their simplicity and low cost and they can measure the potential difference between two electrodes in a solution. They can be classified into three categories: (i) Ion-selective electrodes, which use membrane that can be made of glass, polymers, or other materials, and its composition determines the selectivity of the electrode. Ion-selective electrodes are the most common type of potentiometric sensors and typically used for measuring pH, and metal ions. (ii) Coated-wire electrodes consist of a metal wire coated with a thin layer of selective membrane, The wire acts as the working electrode, and a reference electrode is used to measure the potential difference between the two electrodes. Coated-wire electrodes are used for measuring a wide range of analytes, including metal ions, halides, and biogenic amines. (iii) Field-effect transistors are a semiconductor material as the sensing element. The gate of the transistor is coated with a selective membrane that interacts with the analyte. When the analyte binds to the membrane, it changes the electrical properties of the semiconductor, causing a change in the transistor's output current voltage. Field-effect transistors are commonly used for measuring pH, glucose, and other analytes. Overall, potentiometric sensors have a widely use, because of their low cost, simple instrumentation, long lifetime, high selectivity, and good mechanical stability [98-103].
2. **Amperometric sensors:** This type of sensors measures the current produced by redox reaction between the analyte and a working electrode, producing an electrical current. The working electrode

is typically made of a noble metal such as platinum, gold or silver, and the redox reaction occurs at its surface. The current is measured by a current-to-voltage converter, and the output signal is proportional to the analyte concentration. Amperometric sensors are used to detect a wide range of analytes, including gases, organic compounds, and ions. Their main advantages are the high sensitivity, which allows them to detect analytes at low concentrations, the fast response time, which makes them perfect for real time monitoring applications, and also can be miniaturized and integrated with electronic devices, making them a perfect choice for portable and wearable applications. However, they have low mechanical stability, their materials have high cost and can be affected by interference from other substances in the sample, and their performance can be influenced by factors such as temperature and pH. Proper calibration and validation of the sensor are necessary to ensure accurate and reliable measurements [104-106].

3. **Conductometric Sensors:** This type of sensors can measure changes in electrical conductivity due to the presence of an analyte in a solution. Conductometric sensors can be used to detect a wide range of analytes, including ions, gases, and organic compounds. The main advantage is their simplicity, as they do not require a reference electrode or a specific redox reaction like other electrochemical sensors. For this reason, they are also inexpensive and can be easily miniaturized, making them perfect for portable and wearable applications. However, conductometric sensors can be influenced by factors such as temperature, pH, and the presence of interfering substances in the sample [107-113].

In table 2.4, examples of electrochemical transducers that are often employed for measurements are reported as well as instances of analytes that have been measured.

**Table 2.4 Examples of electrochemical transducers [97].**

	<b>Transducer</b>	<b>Transducer Analyte</b>
<b>Potentiometric</b>	Ion-selective electrode, gas electrode, glass electrode, metal electrode	K <sup>+</sup> , Cl <sup>-</sup> , Ca <sup>2+</sup> , F <sup>-</sup> , H <sup>+</sup> , Na <sup>+</sup> , CO <sub>2</sub> , NH <sub>3</sub> redox species.
<b>Amperometric</b>	Carbon electrode, chemically modified electrodes.	O <sub>2</sub> , sugars, alcohols, phenols, oligonucleotides.
<b>Conductometric</b>	Interdigitated electrodes, metal electrode.	Urea, charged species, oligonucleotides.

Electrochemical sensors are widely used in many branches of industry and in a variety of applications, because of their good selectivity, repeatability, accuracy, and the relative low cost. Most commonly they are used for environmental monitoring of air quality, for oxygen monitoring in the medical sector, and for detection of explosive gases and toxic vapors. Overall, electrochemical sensors play a crucial role in various applications and the choice of the type depends on the specific application [114].

## Chapter 3

### PROTON EXCHANGE MEMBRANE FUEL CELLS (PEMFC)

#### 3.1 History Overview of a PEMFC

In the 1800s, scientists William Nicholson and Anthony Carlisle described the process of splitting water into hydrogen and oxygen. In 1839 the Welsh chemical physicist and lawyer William Grove, based on the theory of W. Nicholson and A. Carlisle, made the first attempt to create a fuel cell, who after a series of experiments realized that this reaction could be exploited to produce electricity in a larger scale and introduced the concept of the fuel cell in his paper 'On the Gas Voltaic Battery' in 1839. Grove's work laid the foundation for the development of modern fuel cell technology [115-116].

Before the invention of the PEMFC, which was carried out in the early 1960s by Dr. Willard Thomas Grubb and Dr. Leonard Niedrach of General Electric, the existing types of fuel cells, such as SOFCs, faced several difficulties in implementation due to their cost and large size. Initially, PEMFCs had a polystyrene sulfonate membrane for the electrolyte and then in 1966, it was replaced by the ionomer Nafion, a new type of membrane made of tetrafluoroethylene sulfonate-fluorovinyl ether copolymer, which has more efficiency and durability than polystyrene sulfonate. PEMFCs were initially developed for use in the NASA Gemini series of spacecraft. However, they were replaced by AFCs in the Apollo program and the Space Shuttle. In the mid-1970s, General Electric improved PEM water electrolysis technology for undersea life support, leading to the US Navy Oxygen Generating Plant. In the early 1980s, this technology was used by the British Royal Navy for their submarine fleet [117].

Even though fuel cell systems were successful in space programs, they cannot be used for common applications because of their high cost, due to the use of expensive materials and the need for very pure hydrogen and oxygen. Early fuel cells also required inconveniently high operating temperatures, which was problematic in many applications. However, around 1990, fuel cells became more affordable thanks to significant innovations. For example, catalyst loading decrease and thin film electrodes made fuel cells competitive against combustion engines. Today, PEMFC production is mainly for the Toyota Mirai. According to a report by Allied Market Research published in 2020, the global proton exchange membrane fuel cell market was valued at \$645 million in 2018 and is projected to reach \$2.24 billion by 2026, growing at a CAGR (Compound Annual Growth Rate) of 17.2% from 2019 to 2026 [118]. The report suggests that the increasing demand for clean energy sources and favorable government policies towards sustainable energy would drive the growth of the PEMFC market in the coming years.

### 3.2 Working Principle of a PEMFC

PEM fuel cells have attracted scientific society because of their simplicity, rapid start-up and wide application in various fields, such as portable electronic devices and transportation. As a result, research activities for the development of PEM fuel cells have increased exponentially, which is very favorable for their future development. This technology is the best in its class due to its low operating temperature, high power density and high energy efficiency. However, the low durability and high costs of a PEM fuel cell have limited implementation for extensive applications [51].

The operating principle of a PEM fuel cell follows the four steps which are already presented in chapter 2 (figure 2.5), i.e., it follows the basic function of a fuel cell, while the reactions taking place in its electrodes have also been presented in chapter 2 (reactions 2.11 and 2.12). However, a more detailed description of the operating principle of a PEM fuel cell is necessary at this point [122].

To generate electricity directly from the chemical energy of a fuel through a PEM fuel cell it is necessary to follow in sequence the following steps:

1. Hydrogen and oxygen are fed through the flow field channels of the anode and cathode, at the anode and cathode respectively.
2. Immediately after entering the cell, the reactants flow through the porous gas diffusion layer, microporous layer and backing layer and eventually diffuse into the catalyst layer of anode and cathode respectively.
3. In the anode catalyst layer, hydrogen undergoes oxidation and decays (according to reaction 2.11, HOR) producing protons and electrons.
4. The protons are transported through the proton exchange membrane to the cathode catalyst layer, while the electrons are channeled to the anode current collector and then through the external circuit to the cathode current collector, eventually ending up in the cathode catalyst layer.
5. In the cathode catalyst layer, the electrons recombine with the protons and with the oxygen molecules, which have been fed by the cathode flow channel, form (according to reaction 2.12, ORR) pure water as the only by-product of the reaction.
6. Water is removed from the cathode catalyst layer through the gas diffusion layer and the microporous layer.
7. Finally, the heat generated, mainly due to the reaction of oxygen reduction (reaction 2.12), in the cathode catalyst layer is removed with the help of bipolar plates.

The net result of the above steps is an electron current through an external circuit – direct current (DC) [120-121].

Figure 3.1 illustrates all the steps of the operating principle of a PEM fuel cell.

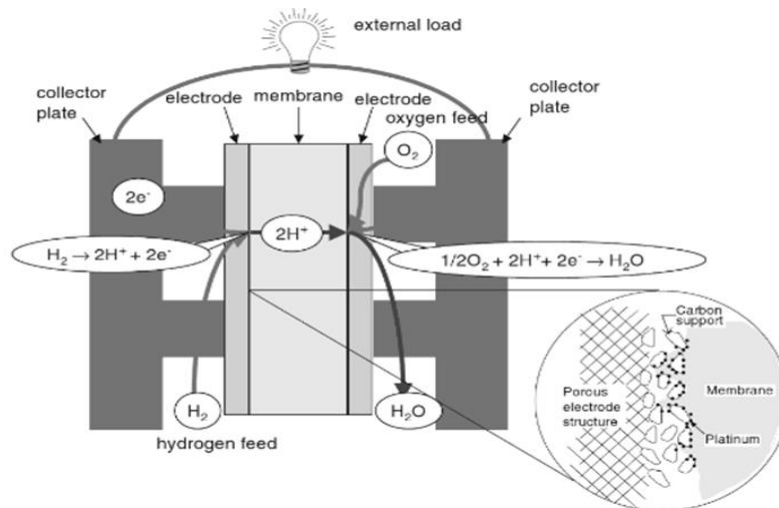


**Figure 3.1. Working principle of PEM fuel cell [120].**

### 3.3 Single cell, Stack, System.

#### Single PEM fuel cell

A single fuel cell contains only an anode electrode and a cathode electrode. Therefore, all fuel cell images shown so far (figures 2.00, 2.01, 2.02, 2.03 etc.) show a single cell of a different type at a time. A single PEM fuel cell usually operates at a voltage of 0.5 V to 0.7 V. Modern PEM fuel cells can achieve current densities of 1 A/cm<sup>2</sup> at voltages around 0.6 V under typical operating conditions. That is, they are capable of producing one ampere of current per square centimeter of the active surface of the electrodes. Single PEM fuel cells are mainly used in small-scale applications, as they are lightweight, efficient and emit only water as a by-product [123,125].

#### PEM fuel cell stack

As mentioned above, a single PEM fuel cell can produce less than one Volt of voltage, which is not sufficient to power many industrial devices. Thus, to produce useful voltage single PEM fuel cells are stacked with the help of high conductivity bipolar plates in a fuel cell stack. This can be achieved by parallel formation, by series formation or by a combination of these two formations. A stack of PEM fuel cells is shown schematically in Figure 3.2.

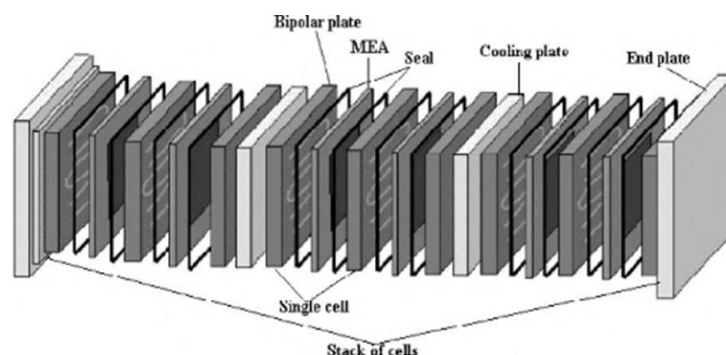


**Figure 3.2. A PEM fuel cell stack [125].**

The potential power from a PEM fuel cell stack depends on the number and size of the separate fuel cells that make up the stack and the surface of the proton exchange membrane.

Flow field design is extremely important for a fuel cell stack, as it can be instrumental in maximizing efficiency, minimizing pressure drop between the inlet and outlet of the flow field, and equable fuel distribution. For this reason, for the design of the flow field of a fuel cell, considerations such as flow rate, water management and heat management should be taken into account.

Finally, it may be equally important to properly assemble a PEM fuel cell stack. By employing a proper assembly, such as ensuring tightness between the PEMFC stack components, achieving uniform pressure distribution across the base, and minimizing contact resistance on the surface, leakage can be prevented. At present, there are two methods of assembling the stack, the bolt fastening type, and the steel belt fastening type [124-125].

### **PEM fuel cell system.**

For the practical operation of a PEM fuel cell stack, it requires its cooperation with other subsystems and structural elements, in order for them to operate together as a single system. Such subsystems may be the hydrogen reformer or a hydrogen purification subsystem, air supply subsystems, water management subsystems and thermal management subsystems. An integrated PEM fuel cell system is shown in Figure 3.3a, while Figure 3.3b presents a 5-cell stack with three main subsystems, fuel delivery, air delivery and thermal management [125].

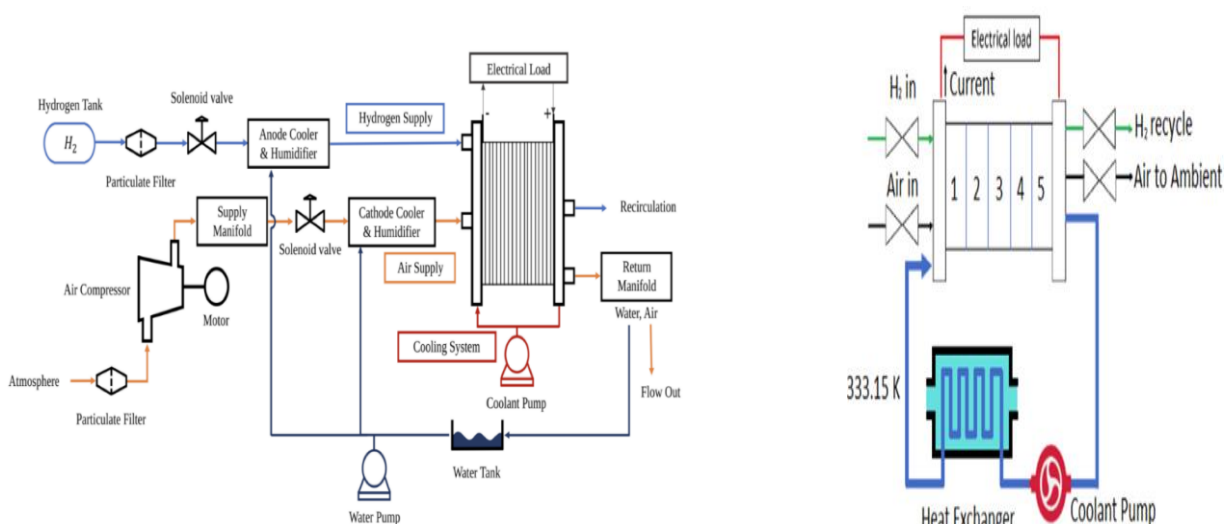


**Figure 3.3 (a). A PEM fuel cell system, (b) A five – cell stack and its major subsystems. [127].**

The hydrogen reformer is necessary in a fuel cell system where a non-hydrogen fuel is used, as this fuel must be reformed to form a hydrogen-rich anode feed mix. Air supply subsystems usually include compressors, air blowers or air filters. Water is the product of a reaction in every PEM fuel cell system, while the gaseous reactants entering the cell must first be moistened. Therefore, it is important that every PEM fuel cell system has a water management subsystem. Finally, redox reactions in addition to water

also produce heat. All fuel cell systems require careful temperature management of the stack, so a heat management subsystem is also often necessary. It is noteworthy that the exact setting of fuel cell systems varies, depending on the type of cell, the choice of fuel and the application. Table 3.1 shows several necessary devices in a PEM fuel cell system, and the subsystems which they belong [125].

**Table 3.1. Subsystems and its devices of a PEMFC system [125].**

Air management	Fuel management	Thermal management	Water management	Power units
Compressor	Gas metering	Coolant	Water tank	AC/ DC converter
Heat exchanger	Humidifier	Pump	Water separator	Power conditioner
Sensors	Heat exchanger	Heat pipes/ Heat spreader		Controller
Conduits/ hoses	Recirculation pump	Radiator		Wires
Flow controller/ valves	Sensors	Heat exchanger		
Humidifier	Conduits/ hoses	Ports and hoses		

### 3.4 Key Elements of PEM Fuel Cell.

The PEM fuel cell consists of the membrane electrode assembly (MEA), which is located between the bipolar plates (BP), on which the flow field channels are grooved or placed, sealed with gaskets, enclosed at both ends by the current collectors and fastened with various bolts and nuts. MEAs have the proton exchange membrane, which is surrounded by the anode electrode on one side and the cathode electrode on the other side. The anode and cathode electrodes consist of anode and cathode catalyst layers (CL), anode and cathode microporous layers (ML), anode and cathode gas diffusion layers (GDL), and anode and cathode backing layers (BL), respectively. Of course, depending on the manufacturing process of the cell, the catalytic surface may be part of the membrane and not the electrode. A detailed description of all the building blocks mentioned is presented below. Figure 3.5 shows the key components of a PEM fuel cell, and Table 3.2 shows some basic characteristics of these components [124].

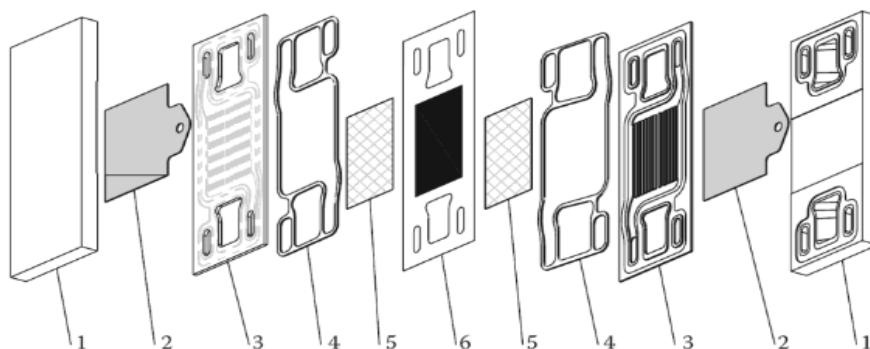


**Figure 3.4. Key components of a PEMFC (1 = end plates, 2 = current collectors, 3 = flow field plates, 4 = sealing materials, 5 = gas diffusion media, 6 membrane electrode assembly) [124].**

**Table 3.2. Basic characteristics of the key components of a PEMFC [124].**

	Thickness	Density (g/cm <sup>3</sup> )	Typical materials
<b>Polymer electrolyte membrane (PEM)</b>	0.01 – 0.1 mm	around 2	Nafion®
<b>Catalyst layer (CL)</b>	100 nm – 0.05 mm	around 0.4	Carbon-supported catalyst, ionomer porous composite and PTFE
<b>Gas diffusion backing layer (GDBL)</b>	0.1 – 0.4 mm	0.3 – 0.5*	Carbon fiber-based porous paper
<b>Microporous layer (MPL)</b>	around 0.05 mm	0.3 – 0.5	Carbon black and PTFE binder
<b>Bipolar plate (BP)</b>	0.3 – 2 mm	1.7 – 8**	Carbon-based composites or metals

### 3.4.1 Proton-Exchange Membrane (PEM)

As previously reported, the PEMFC had originally a polystyrene sulfonate membrane, but the need for greater practicality led scientists to fabricate membranes from a perfluorocarbon-sulfonic acid ionomer, with typical thickness of 0.01 mm - 0.1 mm. This is essentially a copolymer of tetrafluoroethylene (TFE) and various perfluorosulfonic monomers. The best known is Dupont's Nafion®, which uses perfluorosulfonic ethyl-propyl-vinyl-fluoride-ether (PSEPVE), a hydrophilic and perfluorinated membrane, with the chemical formula of the Figure 3.6. Additionally, the Figure 3.7 shows the different types of membrane.

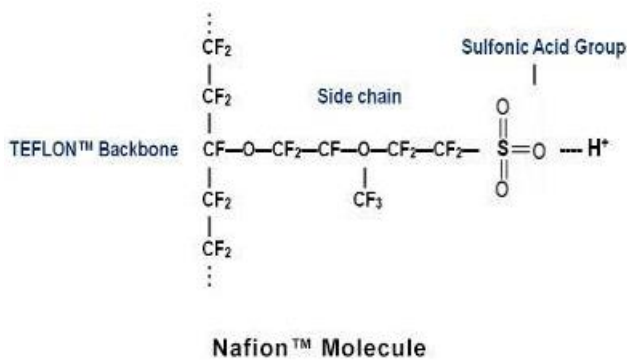


**Figure 3.5 Chemical formula of Nafion [128].**

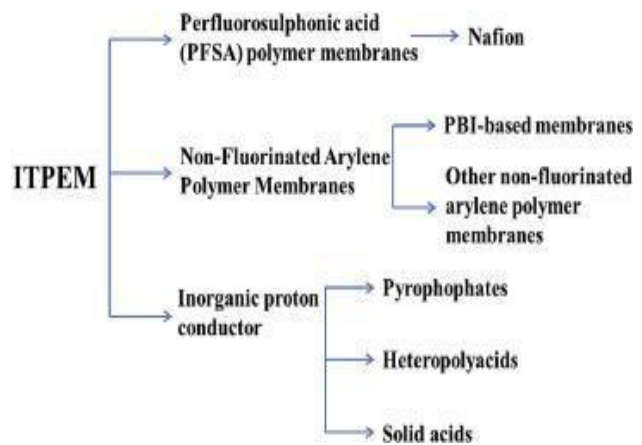


**Figure 3.6 Different types of membrane [129].**

The membrane in a PEMFC plays a key role in facilitating the electrochemical reactions ((3) and (4)) that generate electricity, being responsible for a multitude of functions. In more detail, the functions are as follows:

- **Ion conduction:** Is one of the most important functions of the membrane in a PEMFC. In a fuel cell the membrane selectively conducts protons (H<sup>+</sup>) from the anode to the cathode, while blocking the flow of electrons. The ion conduction mechanism of the membrane is based on the principle of proton exchange. The membrane is made of a polymer electrolyte material, which contains acid groups that can dissociate into protons (H<sup>+</sup>) and anions

(negatively charged ions). The protons are transported through the membrane via a process known as Grotthuss hopping, which involves the transfer of protons from one water molecule to another in the membrane [81,94]. The ion conductivity of the membrane depends on several factors, including the nature of the polymer electrolyte, its molecular structure, and the degree of hydration. For example, the sulfonic acid groups in Nafion® dissociate into protons and sulfonate ions, and the protons are transported through the membrane via Grotthuss hopping. Regarding the degree of hydration, membrane must be hydrated for proton transport through the membrane to be possible. However, excessive hydration can lead to flooding and reduced performance. The membrane is designed to maintain an optimum level of hydration, which depends on several factors such as temperature, humidity, and the flow rate of reactant streams. In addition, to the membrane, the electrodes in a PEMFC also play a critical role in the ion conduction process. The anode is usually coated with a catalytic material, which facilitates the oxidation of the hydrogen fuel into protons and electrons. The protons are then transported through the membrane to the cathode, where they combine with oxygen and electrons to form water. Overall, the ion conduction properties of the membrane in a PEMFC are critical to the efficient and reliable operation of the fuel cell [130].

- Separation of reactants: Another important function of the membrane in a PEMFC is the separation of reactants. In a fuel cell, the anode and the cathode compartments are separated by the membrane, which allows the selective transport of protons and blocks the transport of electrons. This separation ensures that the fuel and oxidant streams remain separate and do not mix, which could lead to unwanted reactions and reduced efficiency. In a few words the membrane acts as a physical barrier that prevents the crossover of reactants and products between the anode and cathode compartments. The anode compartment contains the fuel, hydrogen, and the cathode compartment contains the oxidant, oxygen, or air. The fuel and oxidant streams are fed into the fuel cell at different locations, and they flow through separate channels in the anode and cathode plates, respectively. The membrane must have high selectivity to prevent the crossover of reactants and products. The selectivity of the membrane is determined by its molecular structure and properties, such as the size and charge of the ions that it can transport. The membrane must also be durable and stable under the operating conditions of the fuel cell, such as high temperatures and humidity. In addition to the membrane, other components in the fuel cell can play a vital role in the separation of reactants. For example, the gas diffusion layer (GDL) is very important for the separation of reactants as we will see below. Overall, the separation of reactants is a critical function of the membrane in a PEMFC. The membrane must have high selectivity and durability to ensure the efficient and reliable operation of the fuel cell [118,131].

- Electron-blocking: The membrane is designed to allow the transport of protons across the membrane while blocking the transport of electrons. This allows the electrons generated at the anode during the electrochemical reaction to flow through the external circuit, where they can do useful work, such as powering a motor or generating electricity. PEM is a highly resistive material, which means that it offers significant resistance to the flow electrons, that prevents the electrons from flowing through the membrane and forces them to travel through the external circuit. Additionally, PEM is selectively permeable to protons, that allows the transport of protons across the membrane while blocking the transport of other ions, such as negatively charged ions or electrons. Finally, the PEM is typically coated with a thin layer of catalyst material, such as platinum, on both sides. This catalyst layer helps to promote the electrochemical reaction and enhances the transfer of protons across the membrane [118,130].
- Water management: To manage water in a PEMFC, the membrane must be designed to allow for efficient transport of water and protons while preventing flooding and dehydration. The membrane must also be able to maintain a humid environment in the cell to prevent the membrane from drying out and losing its proton conductivity. One approach to water management is to use a membrane that is hydrophilic, meaning it has high affinity for water and another approach is to use a membrane that is hydrophobic, meaning it repels water. The most common membrane, Nafion®, is a hydrophilic membrane. This hydrophilic nature allows it to absorb and transport water from the cathode to anode in the PEMFC. However, too much water can accumulate in the cell, leading to flooding and reduced performance. To prevent flooding, the Nafion® membrane is typically coated with a thin layer of a hydrophobic material, such as polytetrafluoroethylene (PTFE) on the cathode side, which is a synthetic fluoropolymer of tetrafluoroethylene. It is a highly non-reactive and thermally stable plastic, commonly known by the brand name Teflon. The water content within a membrane is typically quantified either as the weight ratio of water to polymer or as the ratio of water molecules to sulfonic acid groups in the polymer,  $\lambda = N_{\text{H}_2\text{O}} / N_{\text{SO}_3\text{H}}$  [131]. The upper limit of water retention by a membrane is primarily determined by the membrane processing and the condition of the water used for equilibration. For example, a Nafion® membrane equilibrated with liquid water can hold up to approximately 22 water molecules per sulfonate group, while the maximum water uptake from the vapor phase, corresponding to 100% relative humidity in the surrounding gas, is about 14 water molecules per sulfonate group [80]. Regarding the maintenance of proper humidity levels, the PEMFC system may include a humidifier or water management system that helps to supply and regulate the amount of water in the cell [132].

- Chemical stability and compatibility: The chemical stability of PEMFC membranes is influenced by their chemical structure and functional groups, with fluorinated backbones such as Nafion® exhibiting high stability due to their resistance to chemical attack. However, the stability of the membrane is also affected by the operating conditions of the fuel cell, such as temperature, pressure, and fuel type, with higher temperatures and pressures accelerating chemical degradation and reducing the membrane's lifetime. Oxidative and reductive species present in the fuel cell environment, such as oxygen and hydrogen, can also contribute to membrane degradation. Stabilizing agents like cerium oxide can be added to improve chemical stability by scavenging free radicals and preventing chemical reactions. The chemical compatibility of the membrane is critical for preventing unwanted chemical interactions with other fuel cell components. If the membrane swells excessively due to chemical interactions with other components, it can impede proton transport and reduce fuel cell performance. Surface treatments or coatings can be used to improve the chemical compatibility of the membrane, such as perfluorinated coatings that have been shown to enhance compatibility. Researchers are also investigating new materials and design strategies, like composite membranes made from multiple layers of different materials, to improve chemical stability and compatibility [118, 130, 131].
- Thermal stability: The operating temperature of a PEMFC range from 50° C to 220° C. The membrane must be able to maintain its structural integrity and proton conductivity under the high operating temperatures. Exposure to high temperatures can lead to thermal degradation of the membrane, resulting in reduced proton conductivity, mechanical strength, and water uptake, that can lead in reduced performance and shorter lifespan. To ensure thermal stability, membranes are typically made from high-temperature-resistant materials, such as perfluorinated sulfonic acid polymers like Nafion®, or aromatic polymers like polybenzimidazole (PBI). Membrane additives can also be used to improve thermal stability, such as phosphoric acid or phosphoric acid derivatives. Moreover, the design of the fuel cell can also play a role in thermal management, as the heat generated during operation can be used to maintain the desired operating temperature and reduce thermal stress on the membrane [118,131].
- Mechanical strength and durability: A durable and mechanically robust membrane is essential for maintaining the integrity of the fuel cell and avoiding any leakage of reactants or products. The must withstand the mechanical stresses of assembly and operation, such as pressure, temperature changes, and deformation, without cracking or tearing. Additionally, the membrane must also have good resistance to degradation caused by the harsh conditions within the fuel cell, such as the presence of reactive oxygen and hydrogen species and high

temperatures. Without these properties, the membrane can fail prematurely, leading to decreased performance and reduced lifespan of the fuel cell [118,130].

Researchers are constantly exploring new materials and design strategies to improve the properties and the cost effectiveness of PEMFC membranes, including the development of partially fluorinated and non-fluorinated membranes. One approach is to use alternative materials such as organic polymers or composite membranes that can provide similar or superior performance to traditional fluorinated membranes at a lower cost. Another approach is the development of more efficient and sustainable manufacturing processes.

### 3.4.2 Anode and Cathode Electrodes.

As already mentioned, an electrode assembly of a typical PEM fuel cell consists of several layers such as the catalyst layer (CL), the gas diffusion backing layer (GDBL) and the microporous layer (MPL). The catalyst layer is required to facilitate electrochemical reactions, the transport of reactants, the transport of electrons and the transport of protons. The gas diffusion backing layer and microporous layer are required to conduct the electrons and heat, transport the gaseous reactants, and enable the water management of the cell. GDBL and MPL are placed between the catalyst layer and bipolar plates. Figure 3.8 shows the porous layers of which an electrode assembly is composed [126].

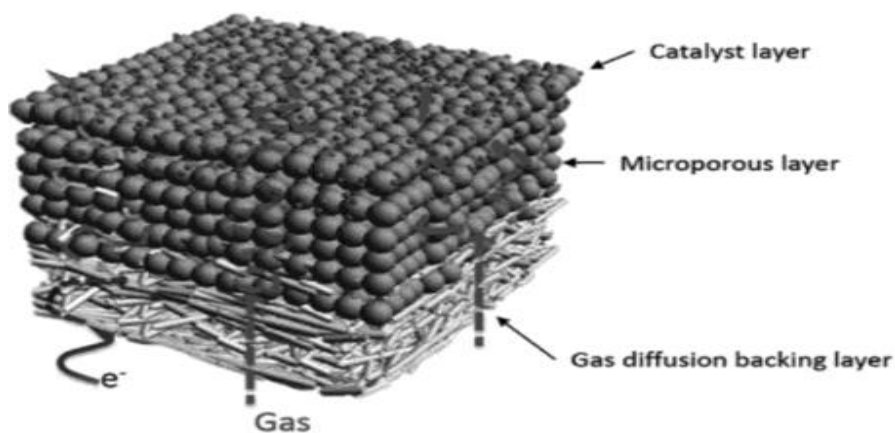


Figure 3.7. A schematic representation of an electrode assembly [126].

#### Catalyst layer

Electrochemical reactions occur on the surface of this layer. As it is known, electrochemical reactions involve gaseous reactants, electrons, and protons. Therefore, the reactions take place in one piece, where all three species have access, namely the catalytic surface. To access the electrons to the catalytic surface, the catalyst particles need to be electrically connected in some way to the bipolar plates, where the electrons are transported through the external circuit. For proton access to the catalytic surface, it is important that the catalyst is in contact with the ionomer membrane (proton exchange membrane). Finally, for the access of the gaseous reactants to the catalytic surface, the

catalyst layer should be porous, as the gaseous reactants are only transported through voids. At the same time, the water product must be removed from the catalyst layer, as otherwise the electrode will be flooded and as a result the access of oxygen to the catalytic surface will be blocked [133-135].

To achieve all of the above, but also to achieve high rates of HOR and ORR, and to improve the overall performance, the interface where the electrochemical reactions take place must be carefully designed. The best catalyst for both oxygen reduction and hydrogen oxidation is considered to be platinum. Pt offers satisfying properties but is rare, expensive, and prone to carbon monoxide poisoning. For this reason, huge research activity is focused on finding an alternative catalytic material. An alternative is the creation of platinum alloys such as Pt – Co, Pt – Ni, Pt – Fe etc. that show good catalyst kinetics. Another alternative is to use other metals which are less valuable as a catalyst, such as ruthenium or palladium. The last useful approach may be the use of non – precious metal catalysts (NPMC), which can perform encouragingly but are not stable in the acid operating conditions of the cell [136-137].

To increase the rate of electrochemical reactions and therefore, the efficiency of the fuel cell, catalytic surface matters and not the weight of the catalyst. In conclusion, it is important to have small platinum particles, about 4nm or smaller, (or other catalytic material) dispersed over a large surface (active surface of the catalyst). In the early stages of development of PEM fuel cells, up to 28 mg Pt/cm<sup>2</sup> were used, while from the late 1990s onwards, using a supported catalyst structure, this amount was reduced to 0.3 – 0.4 mg Pt/cm<sup>2</sup>. The content of Pt/C should be between 10 and 40 % for optimum efficiency. The supporting material of platinum consists of larger particles, about 40nm, and is typically carbon powders. Thus, the platinum is spread over the supporting material creating a large active catalyst surface, resulting in a reduction in catalyst loading and at the same time in power increase. The most widely used support material is a carbon powder called VulcanXC72® by Cabot. It is very important that the support material can withstand the acidic conditions of the fuel cell environment, which is why carbon is preferred [138-139].

Essentially the typical structure of a catalyst layer consists of catalyst particles, supported by nanoscale carbon powders, soaked in ionomer thin belts. The ionomer material acts as a binder, promotes the transfer of protons, and absorbs oxygen to the surface of the catalyst in the cathode for the reduction reaction. An excess amount of ionomer will reduce gas diffusion pathways and block oxygen access to the catalytic surface of the cathode. Therefore, the content of ionomer material should be 30% Nafion® loading which is considered to be optimal.

Finally, for the removal of the water product from the PEM fuel cell, it is added to the catalytic layer polytetrafluoroethylene (PTFE). PTFE is hydrophobic and expels water from the catalyst layer to an area of the cell where it can evaporate or be stored [140-143].

Figure 3.9 shows a catalyst layer schematically and distinguishes all the nanoparticles that make it up.

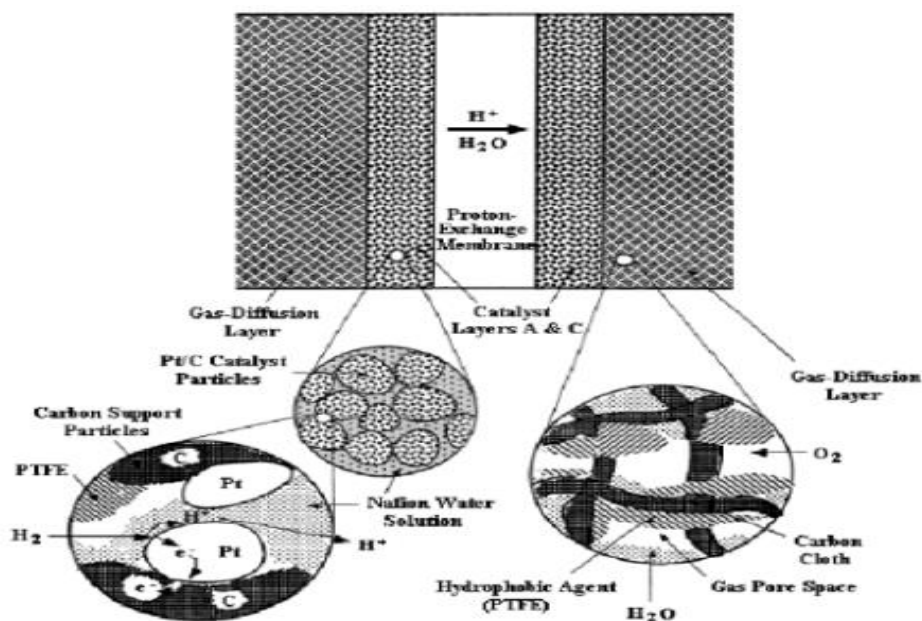


Figure 3.8. A schematic representation of a CL and a GDL [144].

The optimum thickness of the catalyst layer in a PEM fuel cell depends on electrochemical kinetics and transport properties. Platinum-based catalyst layers have an optimum thickness between 1  $\mu\text{m}$  to 10  $\mu\text{m}$ . Non - precious metal catalyst layers have an optimum thickness between 30-100  $\mu\text{m}$  to be able to provide comparable kinetics to that of precious metals. However, as the thickness of the catalyst layer increases, the transfer resistances of the protons and electrons also increase, and as a result the overall efficiency decrease. For the design of an efficient PEM fuel cell a catalyst layer with a reasonably small thickness (about 10  $\mu\text{m}$ ) and a large active catalyst area is ideal [139].

### Gas diffusion media (GDM)

As mentioned above, the gas diffusion media consists of two layers, the gas diffusion backing layer and the microporous layer. These two layers, as shown in Figure 3.8, are placed between the catalyst layer and the bipolar plates and although they do not participate directly in electrochemical reactions, they perform some very basic functions for the PEM fuel cell. Initially, gas diffusion media is a diode for reactants to access the entire active surface of the catalyst, not just the one adjacent to the flow field channels of bipolar plates. Conversely, they are also a diode for the removal of water product and electrochemical heat reactions from the catalyst layer to the flow field channels of bipolar plates and bipolar plates respectively. Another important function of GDMs is that they allow electrons to access the interface of electrochemical reactions by electrically connecting the catalytic surface to the bipolar plates or some other current collector. Finally, GDM provides mechanical support to the MEA while protecting catalyst layers from corrosion, which can be caused by flows

or other factors. Gas diffusion media must be sufficiently porous (with a porosity rate varying between 70-80 %), be electrically and thermally conductive, composed of small particles as catalyst layers, and typically have a thickness of 0.2 mm to 0.5 mm. The two separate layers are detailed below [136,145].

### **Gas diffusion backing layer (GDBL)**

The gas diffusion backing layer is a macroporous layer (in many books and articles it is mentioned as that), which is placed between the microporous layer and the bipolar plates (figure 3.10). The macroporous layer can perform all the functions mentioned in the previous paragraph. The dimensions of GDBL depend on the species involved, i.e. oxygen, water, protons, electrons and heat, but the typical thickness of this layer is usually between 0.1 – 0.4 mm. GDBLs are typically made from highly porous carbon fiber-based materials, such as carbon paper and carbon cloth, and possess a pore size of about 10  $\mu\text{m}$ . However, the manufacturing process of GDBL from such carbon substrates is complex, while such carbon substrates have limited thermal and electrical conductivity. Research has shown that metallic GDBLs could be used as an alternative with much greater effectiveness. Metallic GDBLs offer greater conductivity compared to carbon fiber-based materials and ease of machining that makes the design of macroporous layers quite flexible. However, they are very susceptible to corrosion in the acidic environment of PEM fuel cell and need various coatings to obtain the necessary resistance to this problem [136,145].

### **Microporous layer (MPL)**

The second layer of gas diffusion media is a thinner microporous layer, which is placed between the macroporous layer and the catalyst layer (figure 3.10). MPL is a layer made of a mixture of carbon and hydrophobic PTFE and is mainly used when the catalyst layer is attached to the hydrophilic Nafion®, for better water management. In addition to the main functions which must perform as a gas diffusion media, the microporous layer has a few more responsibilities. Initially, it is necessary for water management in a PEM fuel cell, since this avoids the risk of flooding the catalyst layer that is connected to the hydrophilic Nafion® and is more prone to flooding. At the same time, it can help improve membrane moisture, allowing water to be transported from a hydrophobic MPL to a less hydrophobic MPL through the hydrophilic proton exchange membrane. In addition, it provides good adhesion between GDBL and CL and protects CL from the thick and rough structure of GDBL. The microporous layer is also composed of small particles (smaller than those of GDBL) and has a typical thickness of around 50 nm. A thicker MPL would create a flood risk of the catalyst layer, as increasing the thickness of the layer also increases the water transfer resistance [145-146].

Figure 3.10 schematically shows the two layers that make up the gas diffusion media.

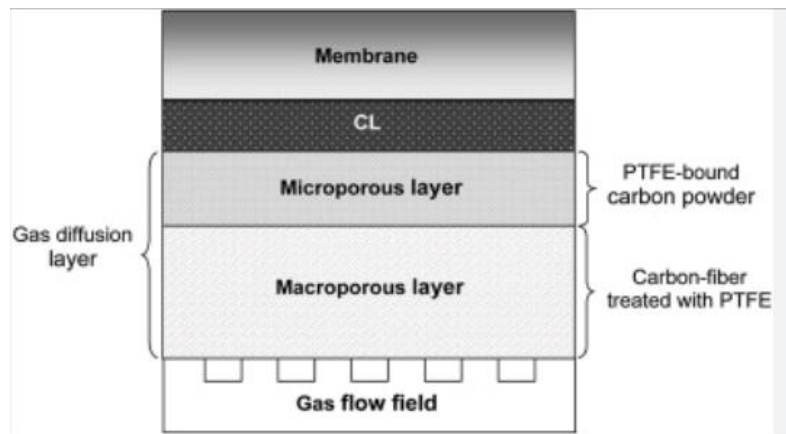


Figure 3.9. The two substrates that make up the gas diffusion media [147].

### 3.4.3 Bipolar Plates (BP)

Bipolar plates (BP) are an essential component in a fuel cell and are positioned between the membrane-electrode assembly (MEA) to form a stack. Also, BP account for the highest portion of fuel cell weight and almost half the total cost. The BP performs various essential functions such as providing structural support, impermeable to gasses, electrically and thermal conductivity, flow-field channels, corrosion resistance and low cost [148]. In more detail, the functions are as follows:

1. Provide structural support: The plates act as a barrier between the individual cells and provide mechanical support to prevent deformation or collapse of the stack. Additionally, they help to evenly distribute the compressive force exerted by the end plates and clamping mechanism, ensuring a consistent pressure across the entire surface area of the cell. The design of the BPs should also take into account the mechanical loads that the cell will be subjected to during operation, including the weight of the reactants and products, thermal expansion and contraction, and mechanical vibrations. The plates must be strong enough to withstand these loads without deforming or cracking, but also lightweight to minimize the overall weight of the stack. Moreover, the flow channels and distribution channels must also be carefully design because the shape, size, and orientation of them can affect the overall performance, efficiency, durability and the lifespan of the fuel cell [118, 149-150].
2. Impermeable to gasses: Gas crossover is a common problem that occurs in fuel cells when the membrane fails to separate the fuel and oxidant gasses efficiently. This leads to a decrease performance and to inefficient use of a fuel cell as we have analyzed in the membrane's functions. Hence, it is critical to have BPs that are impermeable to gasses to avoid these issues. In addition, to prevent gas crossover, having an impermeable BP is also essential for ensuring the correct stoichiometry of the reaction. The flow channels on the BP surfaces must be designed in such a way that they allow the required amount of fuel and oxidant gasses to react, without any additionally gasses coming in or out [118].

3. Electrically conductivity: If the conductivity is low, the resistance to electron flow increases, leading to higher losses of electrical power. On the other hand, if the electrical conductivity is too high, it can result in an excessive flow of current, which can cause corrosion and other forms of degradation to the bipolar plate. Therefore, the electrical conductivity of the BP should be optimized to achieve a balance between low resistance and stability. Typically, metals such as stainless steel and titanium have excellent electrical conductivity [151].
4. Thermal conductivity: During the operation of a fuel cell, a certain amount of heat is generated, and it is essential to dissipate it properly to maintain the optimal operating temperature of the cell. If the heat generated cannot be removed, it will cause a rise in temperature, which will have a detrimental effect on the performance and lifespan of the fuel cell. Therefore, the BPs is designed to have high thermal conductivity to transfer heat efficiently from the cell. The high thermal conductivity ensures that the heat is rapidly conducted away from the fuel cell, minimizing the temperature gradient across the cell. This function is crucial because a temperature gradient can create thermal stresses in the materials used in the cell, leading to deformation and mechanical failure. Additionally, the thermal conductivity of the BP also affects the thermal management of the fuel cell stack. The heat generated by each cell must be removed and dissipated to the environment to maintain the proper operating temperature of the entire stack. Bipolar plates with high thermal conductivity help to reduce the temperature difference across the stack, which enhances the efficiency and lifespan of the stack. Typically, metals such as stainless steel and titanium have excellent thermal conductivity [118,149].
5. Flow-field channels: The primary function of the flow-field channels in the BP is to act as a gas distributor to the active area of the PEMFC and promote the flow of reactants and products. They provide a direct path for the transport of the reactants to the catalyst layer and then to the ion-exchange membrane. The flow-field channels' structure influences the efficiency of the reactant delivery and removal of products. They must have also a specific geometry that provides a uniform that provides a uniform distribution of the gases throughout the catalyst layers. Till date, there are various flow field configurations that have been developed such as pin-type, series-parallel, serpentine, integrated, interdigitated, and metal sheets-based flow fields as shown in a Figure 3.11. The shape and the size of them determine the pressure drop across the BP and the efficiency of the fuel cell. The flow-field channels also contribute to the heat dissipation in the fuel cell. As the electrochemical reaction is exothermic, the generated heat needs to be removed from the cell. Thus, the design of the flow-field channels helps to transport heat from the cell to the coolant, promoting the uniform distribution of the heat in the cell and enhancing the performance [118,152].

6. Corrosion and ohmic resistance: The corrosive species present in the fuel cell can attack the surface of the bipolar plate, resulting in a loss of material and decreased performance of the fuel cell. For example, in a PEMFC, the anode side of the BP is exposed to hydrogen gas and the cathode side is exposed to oxygen or air. The high potential difference between the two sides can lead to corrosion of the BP, especially if it is made of a metal that is not highly resistant in corrosion, such as stainless steel. Another example is the corrosion of graphite bipolar plates, which can occur due to the presence of acids and water in the fuel cell. The acid can cause the graphite to become oxidized, resulting in the loss of material and decreased performance. Regarding, the ohmic resistance, must be low and steady. Ohmic resistance refers to the electrical resistance encountered by the flow of current through a conductor, which in this case is the BP. If the ohmic resistance is high, it can cause an increase in the internal resistance, which can reduce the overall output voltage. Furthermore, if it is not steady and fluctuates during operation, it can cause irregularities in the flow of current and voltage, which can affect the stability of the fuel cell [148].

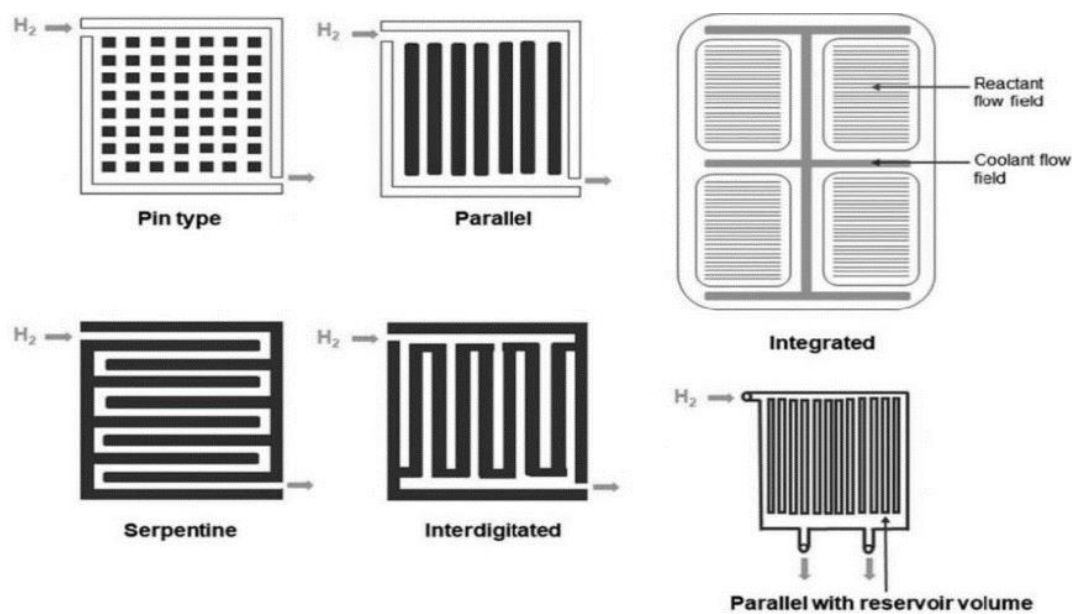


**Figure 3.10. Various types of flow field configuration [152].**

In general, two types of materials are used for bipolar plates in PEMFCs, namely metallic or carbon-based materials. Bipolar plates are exposed to extreme conditions such as a very corrosive environment inside a fuel cell, at a range of pH 2-3 and temperature 60-80°C. Typical metals such as steel, aluminum, titanium, or nickel will corrode in such an environment and shattered metal ions will diffuse into the ionomeric membrane, causing a reduction in ionic conductivity and fuel cell lifetime. In addition, a corrosion layer on the surface of bipolar plate would lead to an increase in electrical resistance. For this reason, it is necessary to coat these plates with a non-corrosive but electrically conductive layer, such as graphite, diamond-type carbon, noble metals, metal nitrides, organic self-assembling polymers, etc.

Scientists have mainly focused on graphite, a mineral polymorphic form of carbon, which in addition to its weight and volume practicality, which are not considered critical, has high corrosion resistance in wet and acidic environments, good chemical stability within a PEMFC, low contact resistance, low density (2.2 gr/cm<sup>3</sup>) and good thermal and electrical conductivity. However, graphite has low mechanical strength, which leads to a reduction in plate thickness and results in low volumetric power density. This makes it unsuitable for mobile and transport applications. Graphite is filled with resin to block pores to enhance gas impermeability. The fabrication of the flow field channels is incorporated into a computer numerical control machine, which is time consuming and costly, preventing large-scale production. To optimize the properties of graphite, attention must be paid to the nature degree of crystallinity, size, morphology and determine the filtration threshold. Graphite can be classified into natural graphite, which has higher crystallinity or synthetic graphite, which has lower crystallinity and lower electrical conductivity. The electrical conductivity of natural graphite varies depending on the geographical origin of the extraction, the grinding and sifting during processing and changes in particle size and morphology. Because of this wide range of possibilities, synthetic graphite is available in a variety of purity and degrees of crystallinity with variations in grain size, surface areas and electrical conductivity. Metallic bipolar plates have good thermal and electrical conductivity, excellent mechanical strength, low manufacturing costs, good gas permeability and possibility of making thin plates. For low-cost considerations, metals that have been considered include stainless steels, aluminum alloys and nickel alloys. It has been estimated that a 7 KW PEMFC stack at less than \$20/KW can be achieved by using stainless steel bipolar plates. The power/volume ratio also can be significantly improved due to their ability to be formed into thin (about 2mm) BP sheets. However, they also have some disadvantages, such as being chemically unstable in harsh environments and prone to corrosion, which results in increased corrosion resistance [118,149,151]. Therefore, the current drive for metallic BP research is the development of coated plates in which the surface coating will significantly improve the corrosion resistance and electrical conductivity of the plate to a level that satisfies the United States Department of Energy (DOE) criteria (Table 3.3), at an acceptable cost.

**Table 3.3 DOE technical targets for PEMFC bipolar plates in 2020 [153].**

<b>Property</b>	<b>Unit</b>	<b>2020</b>
Cost	\$KW <sup>-1</sup>	3
Weight	KgKW <sup>-1</sup>	0.4
H <sub>2</sub> permeation rate	cm <sup>3</sup> (cm <sup>2</sup> s) <sup>-1</sup>	1.3 * 10 <sup>-14</sup>
Corrosion at anode, cathode	μAcm <sup>-2</sup>	<1
Electrical conductivity	Scm <sup>-1</sup>	>100
Area specific resistance	Ω-cm <sup>2</sup>	0.01
Flexural strength	MPa	>25

### 3.4.3 Other Components

In PEM fuel cell, there are several other important components aside from the above. These include the current collector, sealing material and end plate material. The current collector plays a critical role in gathering the generated current within the fuel cell. It is typically attached to the bipolar plates. Its primary function is to facilitate the flow of electrons from the anode to the cathode through an external circuit. In a single cell or in a fuel cell stack, bipolar plates can act as current collectors. For an efficient current collector design, it should be lightweight, highly conductive, and possess good electrochemical and mechanical stability. Metals and alloys such as copper, titanium, aluminum, and stainless steel are commonly used as current collector materials. Conductivity can be improved by coating with other metals the surface of these materials. Stainless steel and copper are particularly advantageous as they are abundant, cost-effective, and easy to machine. However, their high density can negatively impact the specific power density of the PEM fuel cell. Recently, exfoliated graphite has been proposed as an alternative current collector material. Exfoliated graphite offers high conductivity and is lightweight compared to the previously mentioned materials. Its use can improve overall fuel cell performance. However, exfoliated graphite does have a drawback of low mechanical stability and requires protection. Therefore, it is crucial to protect exfoliated graphite with another material that does not compromise its performance, while also improving the mechanical strength of the current collector [118].

The sealing material is very important for a PEMFC as it plays a crucial role in preventing the leakage of reactants, products, and coolants. It is positioned between the membrane and bipolar plates to ensure a tight seal. The sealing material needs to possess certain key properties such as good gas impermeability, affordability, ease of machining, as well as high thermal, electrochemical, and chemical stability. The commonly used materials for fabricating sealing components in PEM fuel cells include PTFE (Polytetrafluoroethylene), PTFE-based materials, and silicon elastomers. However, PTFE and PTFE-based materials can suffer from compressibility issues, which means that a high compression force is required to install them in the fuel cell. On the other hand, silicon elastomers raise concerns about potential decomposition over long-term operation of the fuel cell. The decomposed products of silicon elastomers can adhere to the catalyst layers (CLs) and adversely affect the overall performance of the fuel cell [118,154].

The end plates are also essential components in a PEM fuel cell system. Their primary function is to securely assemble the various components together, applying sufficient clamping force to prevent hydrogen leakage, while also ensuring the uniform contact pressure between the components. The contact pressure on the multiple interfaces between the BPs and the MEA is crucial as it can significantly impact the performance and durability of the fuel cell. The end plates are positioning at both ends of the fuel cell (Figure 3.12), namely the anode end and the cathode end. In a fuel cell designs that incorporate metal flow channels, the end plates may also serve the purpose of directing

the flow of gases. However, when graphite flow channels are used, a separate plate is typically employed as the end plate. This allows for more cost-effective and lightweight construction of the fuel cell. To meet these requirements, end plates are commonly made from materials such as aluminum and polymer-based composites. These materials offer a balance of strength, durability, and cost efficiency, making them suitable for use in the demanding environment of a fuel cell [118,155].

As already mentioned, challenges such as the leakage of the PEM fuel cell stack, the contact resistance at the interface and the nonuniform base pressure distribution can be prevented by an appropriate assembly. Stack assembly can be either bolt fastened (Figure 3.13a) or steel belt fastened (Figure 3.13b) The bolt fastening type is widely employed in both small and large stack assemblies due to its simplicity, ease of assembly, and high reliability. However, it can lead to uneven force distribution on the end plate due to local stress concentrations around the bolts. To improve the sealing performance, optimization of factors such as the number, size, installation sequence, and load of the bolts are necessary. On the other hand, the steel belt fastening type, features a more compact structure and is primarily used in large PEMFC stacks. This advanced fastening technique disperses the pressing force at the fastening points of the steel strip and the electrode stack, avoiding uneven force distribution on the local end plate. By modifying the dimensions and thickness of the steel strip, as well as strategically determining the distribution of the steel strips, the sealing performance can be effectively improved. In the future scientists should optimize these two assembly methods [156-157].

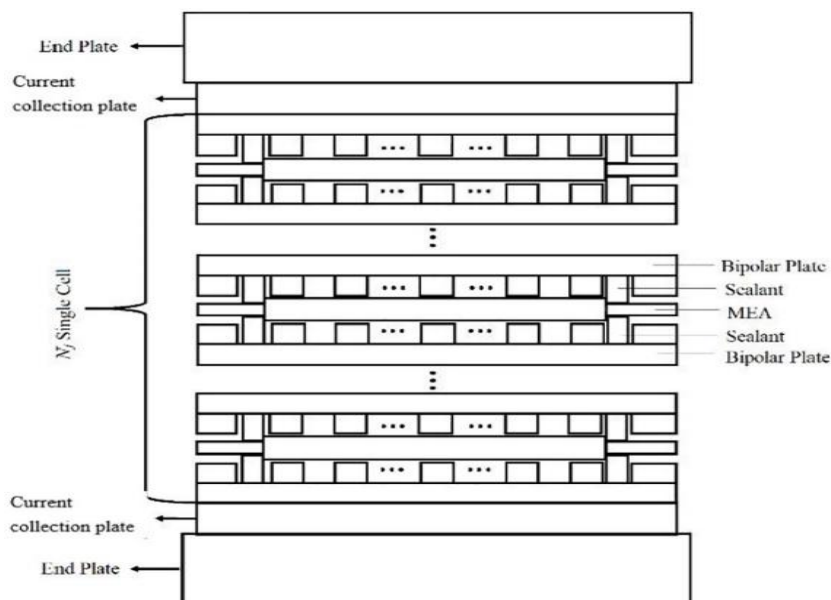


**Figure 3.11. Presentation of other components of the fuel cell stack [155].**

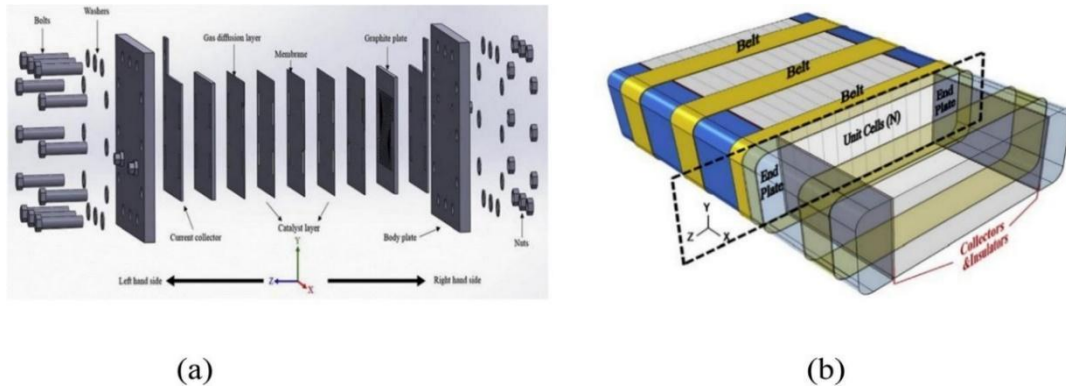
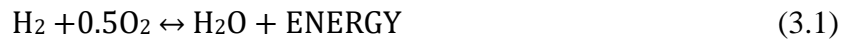


Figure 3.12. Methods of stack assembly [156], [157]: (a) bolt fastening type; (b) steel belt fastening type.

### 3.5 Thermodynamic and Kinetic Analysis of PEMFC

The overall electrochemical reaction that occurs in a PEMFC which is responsible for power generation is as follows:



#### Gibbs free energy

The change in Gibbs free energy ( $\Delta G_f$ ) of a reaction is the difference between the Gibbs free energy of the product and the Gibbs free energy of the reactants. The change in Gibbs free energy varies with both temperature and pressure is as follows:

$$\Delta G_f = \Delta G_f^0 - RT \ln(P_{\text{H}_2} P_{\text{O}_2}^{0.5} / P_{\text{H}_2\text{O}}) \quad (3.2)$$

Where,  $\Delta G_f^0 = n \cdot F \cdot E^0_{\text{cell}}$  is the Gibbs under stable pressure, temperature, and reversibility conditions. R is the universal gas constant (8.314 J/(kgK)), T the temperature in Kelvin,  $P_{\text{H}_2}$ ,  $P_{\text{O}_2}$ ,  $P_{\text{H}_2\text{O}}$  are the partial pressure in atm of hydrogen, oxygen, and vapor respectively, n is the number of electrodes which pass around the external circuit (according to the eq.(3)  $n=2$ ), F is Faraday constant (96485 coulombs) and  $E^0_{\text{cell}}$  is the voltage of the fuel cell.

#### Nernst equation

Electric potential for each cell of the PEMFC is described from the following equation:

$$E = -\Delta G_f^0 / (n \cdot F) + \Delta S / (n \cdot F) (T - T_0) - RT \ln(P_{\text{H}_2} P_{\text{O}_2}^{0.5} / P_{\text{H}_2\text{O}}) \quad (3.3)$$

By extension of the previous equation, the open circuit voltage known as Nernst voltage, which defines the maximum voltage produced by a cell is as follows:

$$V_N = \Delta G_f / n \cdot F = 1.229 - 0.85 \cdot 10^{-3} (T - T_0) + RT \ln(P_{\text{H}_2} P_{\text{O}_2}^{0.5} / P_{\text{H}_2\text{O}}) \quad (3.4)$$

Where:

$$E^0_{\text{cell}} = \Delta G_f^0 / n \cdot F = 237,200 \text{ J/mol} / 2 \cdot 96485 \text{ As/mol} = 1.229 \text{ V}$$

$T_0$ : standard-state temperature (298.15K)

$\Delta S$ : is the entropy change, which can assume that in the given reaction is constant.

Fuel cell's output voltage is lower than Nernst voltage due to 3 different voltage losses, which are activation loss, concentration loss and ohmic loss [159].

$$V_C = V_N - V_L, \text{ where: } V_L = V_{act} + V_{conc} + V_{ohm} \quad (3.5)$$

- 1) Activation loss: Activation losses refer to the voltage loss that occurs due to the slow kinetics of the electrochemical reactions taking place in the fuel cell. These reactions involve the transfer of electrons between the reactants and the electrode surface. For these reactions to occur, an activation energy barrier must be overcome, which requires a certain amount of voltage overpotential. This overpotential results in a loss of useful voltage that could be used to generate power [158-159].
- 2) Concentration loss: Concentration losses refer to the reduction in voltage caused by the change in reactant concentration at the electrode surface as the fuel is consumed. This can happen due to slow fuel diffusion through the porosity of the electrode, reactant and product diffusion through the electrolyte, and the removal of produced water. These factors can all contribute to a decrease in the concentration of reactants at the electrode surface, leading to a reduction in the voltage output of the fuel cell.
- 3) Ohmic loss: Ohmic losses refers to the resistive losses that occur when the current flows through the materials in the external circuit, the electrolyte, and the interfaces between the components of the fuel cell. These losses are directly proportional to the current density, and their relationship is linear. Ohmic losses are caused by the resistance of the materials to the flow of electrons and ions, and they increase with the thickness and length of the materials through which the current is flowing [158].

#### Theoretical and real PEMFC efficiency

$$n_{th} = \Delta G^{\circ} / \Delta H^{\circ} = 237.1\text{kJ/mol} / 286\text{kJ/mol} = 83\% \quad \text{and} \quad n_{real} = E_{cell} / E^{\circ}_{cell} \quad (3.6)$$

### **3.6 Cost Reduction and Applications of a PEMFC**

#### Cost reduction

The cost of a proton exchange membrane fuel cell (PEMFC) is a major barrier to the widespread adoption of this technology. Currently, PEMFCs cost around 550 dollars per kilowatt per unit [160]. For example, a car using a PEMFC system is 10 times more expensive than a car using an internal combustion engine (ICE). The cost of a typical PEMFC is made up of several components, including the membranes, platinum, electrodes, bipolar plates, peripherals, and the assembly process. The bipolar plates and the electrodes, which include platinum, account for about 80% of the total cost of a PEMFC. To reduce the cost of PEMFCs, Tsuchiya et al. [160] conducted a cost structure analysis and suggested the possibility of cost reduction through mass production of PEMFCs using the

learning curve analysis. According to their analysis, the typical performance of a single fuel cell has 0.6-0.7 V and 0.3-0.6 A/cm<sup>2</sup> cell current density, which equates to a power density of 2 kW/m<sup>2</sup> or more. Nevertheless, the single cell performance is higher than stack performance. If an automobile has a 50 kW rated output, then the cell area for 2 kW/m<sup>2</sup> of power density will need to be 25 m<sup>2</sup>, i.e., 278 cell layers with 30 cm x 30 cm cell area. In this case, the power density is expected to increase to the level of 5 kW/m<sup>2</sup> or more [161-162]. The analysis showed that the cost reduction to the level of an ICE is possible with mass production. However, the bipolar plates and the MEA still make up a large proportion of the stack cost even at the mass production stage.

### Applications of PEMFC

Fuel cells are widely regarded as a key technology for future applications, particularly in the context of transitioning to a hydrogen economy and replacing internal combustion engines. One of the primary reasons for their significance is their high efficiency and ability to operate with zero greenhouse gas emissions. This makes them an attractive alternative to conventional power sources, contributing to efforts in combating climate change and reducing air pollution. The major applications of fuel cells as shown in Figure 3.14, focus on transportation, distribute/stationary, portable power generation, and backup power [163]. The applications are more detailed below:

- 1) Transportation: In transportation, fuel cells can power vehicles, replacing traditional internal combustion engines. FCVs have already been developed and demonstrated by major automakers, showcasing the potential of fuel cells in providing clean and efficient transportation. Toyota made a significant contribution to the commercialization of PEM fuel cells with the introduction of their Mirai FCV in 2017. The Mirai fuel cell system incorporates advanced design and materials, allowing for impressive performance metrics such as a Pt-loading of 0.365 mg/cm<sup>2</sup>, 2 kW/kg, and 3.1 kW/l, resulting in a total power generation of 153 HP. Despite the challenges about cost reduction, the adoption of FCVs has been steadily increasing. By June 2018, nearly 5,000 FCVs were already in operation in the United States (U.S.) since their introduction in 2015. There are also more than 20,000 forklifts in the U.S. and more than 20 buses in four states, which are powered by PEM fuel cells. Moreover, hydrogen infrastructure has been expanding, with over 30 hydrogen gas stations already operational, and plans to establish 200 more stations in California by 2025. In addition to FCVs, airplanes, airships and marine are potential areas of PEMFC applications. These efforts support the growth and accessibility of hydrogen as a fuel source for fuel cell vehicles [164-165].
- 2) Stationary: Fuel cells have been successfully commercialized for stationary applications for over two decades. Stationary fuel cell systems are designed to provide power for stationary or fixed locations, such as residential buildings, commercial facilities, and remote or isolated

areas. The efficiency of stationary fuel cell systems varies depending on the specific technology and fuel used. Generally, these systems can achieve an efficiency of around 40% when using hydrocarbon fuels. Moreover, can be integrated with other renewable energy sources, such as photovoltaics (solar panels) and wind turbines, as well as energy storage systems like batteries and capacitors. This integration allows for primary or secondary power generation, depending on the availability the renewable energy sources. By combining different energy technologies, the overall efficiency and reliability of the stationary power system can be improved. Additionally, cogeneration, or combined heat and power (CHP), is another important aspect of stationary fuel cell applications. Cogeneration systems utilize the waste heat generated by the fuel cell for heating purposes, increasing the overall system efficiency, which can achieve up to 85% while simultaneously reducing energy consumption [166].

- 3) Portable: Portable power generation is rapidly growing application area for PEMFC. This includes providing continuous and reliable power for portable electronics, such as laptops, cell phones, and military communication devices. PEMFCs offer higher energy capacity and longer runtime compared batteries, making them suitable for meeting the fast-growing energy demands of modern portable devices. They can be fabricated in small sizes without sacrificing efficiency, making them ideal for portable power applications [150,163].
- 4) Backup power: PEMFCs are being explored for backup power solutions. They provide a reliable and efficient source of power during grid outages or emergencies. This is particularly crucial for critical infrastructure like banks and telecommunication companies, where the cost of power breakdowns can be extremely high. PEMFs ensure uninterrupted operation, contributing to maintaining the smooth functioning of essential services and reducing downtime [150].

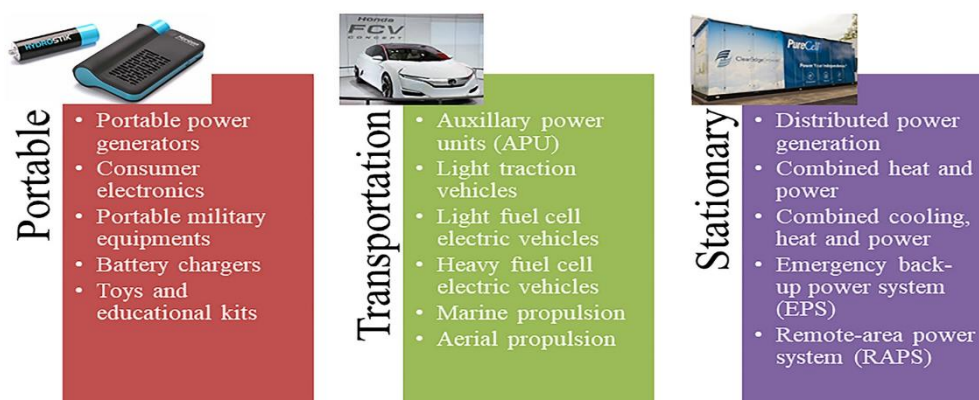


**Figure 3.13. Applications of fuel cells [167].**

## Chapter 4

### PARAMETERS INFLUENCING LONG-TERM PERFORMANCE AND DURABILITY OF PEM FUEL CELLS

#### 4.1 Introduction

The performance and durability of PEMFCs can be affected by several parameters. These interacting parameters lead to a degradation of PEMFC's components, thereby reducing its performance and service life. For this reason, it is important to study and understand these parameters in order to address them and ultimately increase the lifetime and performance of the next generation of PEM fuel cells. Before analyzing these degradation mechanisms, a brief description of them will be given below [168].

Initially, the performance and durability of PEMFCs is affected by the operating conditions. The cycled operation of the fuel cell creates more problems or makes the existing problems of PEMFC more intense than the operation in constant load. Impurity contamination, in particular CO contamination, should be considered unavoidable and it is a major problem of fuel cell operating conditions. The operating temperature and pressure, as well as the relative humidity of the reactants are also operating conditions that strongly affect the efficiency and service life of this type of fuel cell. Finally, the operation under gas starvation conditions, i.e., the operation under fuel or oxygen starvation conditions, degrades the performance of the cell. Gas starvation also creates the inversion of the cell, that is, the formation of oxygen at the anode and hydrogen at the cathode, which may result in the definitive failure of the fuel cell [169-170].

Water and thermal management are also parameters that affect the performance and durability of the proton exchange membrane fuel cell. Poor water management can cause either flooding or dehydration of membrane, which can cause other problems that hinder the smooth functioning of the cell. The same goes for thermal management. Thermal management is important when the fuel cell is called upon to operate or store at freezing temperatures. Exposure of the cell to subzero temperatures can cause problems such as internal thermal and mechanical strains, cracks in the membrane, detachment of the mechanical layers and loss of electrical contact, which have a significant influence on the performance and durability of the cell. On the other hand, the operation of the cell at high temperatures aggravates other degradation problems, such as corrosion. Therefore, it is obvious that water and thermal management should be excellent [168].

Finally, significant is the influence of the design and materials of each component on the performance and durability of the fuel cell. Optimal choice of materials and the most appropriate

design of the fuel cell, depending on its application, can improve the balance of heat and water of the fuel cell, with a consequent improvement in energy production efficiency and a prolongation of its service life. The components of MEA, i.e., the anode and cathode electrodes and the polymer membrane, are the most important components of PEMFCs. Poor design and selection of inappropriate MEA materials can lead to degradation of the MEA, which can lead to degradation of parameters such as electrochemical surface area (ECSA), hydrogen crossover current density ( $i_{H_2}$ ), Ohmic resistance ( $R\Omega$ ), double-layer capacitance (Cdl) and short-circuit resistance ( $R_e$ ), which lead to degradation of fuel cell performance and service life [169,171].

The electrochemical surface area (ECSA,  $m^2/g$  [Pt]) represents the electrochemical reactivity capacity of the catalytic layer. Therefore, the greater the ECSA, the greater the performance of the cell. Agglomeration/ sintering, corrosion and catalyst loss or contamination can reduce ECSA and subsequently cell performance. The hydrogen crossover current density ( $i_{H_2}$ ,  $mA/cm^2$ ) corresponds to the hydrogen permeability from the PEM to the unit of time and is used to measure the degree of aging of the membrane and evaluate the compact construction of the cell. The rate of  $i_{H_2}$  is proportional to the degree which the hydrogen crossover effect will affect the cell, which will be analyzed below. Ohmic resistance ( $R\Omega$ ) represents the sum of the resistance of the conductive element and the resistance of the membrane to electron transfer and ion transfer in a fuel cell respectively. The  $R\Omega$  parameter and the fuel cell efficiency are inversely proportional. The water level of MEA and the aging of the elements of MEA are factors that can increase this parameter. The state of the catalytic layer interface is characterized by the Cdl parameter. Finally, the  $R_e$  parameter characterizes the electron insulation of the MEA, and in particular of the PEM, i.e., the resistance of the membrane to electron transport. The more the short-circuit resistance parameter increases, the more the electron insulation of the membrane increases, and therefore the performance and durability of the cell increases. The above proves that the change of the MEA parameters can significantly affect the performance and service life of the fuel cell [169].

This chapter will analyze in detail all the key parameters and mechanisms that can degrade the performance and durability of PEM fuel cells, in order to be aware of the problems that will need to be addressed for more efficient next generation fuel cells.

## **4.2 Operating conditions**

### **4.2.1 Temperature, Pressure, and Relative Humidity (RH)**

The operating temperature significantly affects the electrical and thermal behavior of PEM fuel cells, which makes it an essential factor. The performance of PEM fuel cells can be greatly improved by varying the operating temperature within a range of 100°C to 200°C. Researchers such as Xia et al. [172],

studied the effects of operating temperature, and thickness of membrane and catalyst layer on the performance of high temperature proton exchange membrane (HTPEM) fuel cells. Xia et al.'s findings indicate that increasing the operating temperature from 120°C to 200°C leads to a substantial increase in fuel cell performance. However, the optimum operating temperature reported in the range of 160 °C to 180 °C provides high power density and reduces maintenance costs. Another study by Askaripour demonstrated the impact of fuel cell temperature on the polarization curve, by considering inlet gas temperatures of 75°C, 80°C, 85°C, and 90°C, showing that fuel cell performance improves significantly as cell temperature increases, particularly at moderate to high current densities [173]. Additionally, Hirpara et al. [174] explored the effect of operating temperature on the dynamic behavior of droplets within PEM fuel cells. Their study indicated that by increasing the operating temperature from 25°C to 75°C, the droplet cycle time decreased significantly from 14 seconds to 0.5 seconds. The Department of Energy (DOE) mandates that PEMFCs should be capable of starting up and operating at temperatures as low as -20°C, reaching 50% of their rated power within 30 seconds and consuming less than 5 MJ of energy (subfreezing effect) [175]. This requirement is crucial for automotive applications where quick startup and operation in cold conditions are necessary. Exposure to freezing temperatures after long-term shutdown can lead to ice formation, causing a 9% volume expansion that damages cell components, blocks gas passages, and covers the catalyst. Ice formation also increases CL porosity, resulting in membrane delamination, decreased cathode Electrochemically Active Surface Area (ECSA), and increased membrane resistance. Additionally, repeated freeze-thaw cycles cause CL delamination, loss of thermal and electrical contact, and rough membrane surfaces with pinhole formation. Ice formation and retained water can block bipolar plates, flow fields channels, and result in startup failures and electrode degradation due to fuel starvation [175]. Summarize, there must be a balance in the operating temperature, as a low temperature can lead to flooding and inhibition of the reaction gasses, while a high temperature can lead to dehydration and general degradation of the fuel cell. To ensure PEMFC longevity, addressing these issues is essential, including preventing ice formation, maintaining fuel cell performance, and avoiding irreversible degradation in sub-zero temperatures [176].

In addition to operating temperature, operating pressure plays a significant role in PEM fuel cell performance. Researchers have conducted experiments to investigate the impact of different operating conditions on fuel cell performance. Amirinejad et al. [177] studied a single PEM fuel cell with an active area of 5cm<sup>2</sup> and examined various operating conditions. Their findings demonstrated that higher backpressure on the cathode side resulted in better fuel cell performance compared to the anode side. This suggests that maintaining a higher pressure on the cathode side can enhance the cell's performance. Similarly, Wang et al. [106] observed improved PEM fuel cell performance under high-pressure conditions and their results support the notion that higher operating pressure can have a positive influence on fuel cell performance. The influence of pressure on PEM fuel cells can be attributed to several factors.

Higher pressure on the cathode side facilitates better oxygen supply and promotes more efficient oxygen reduction reactions, enhancing the overall cell performance. It can also improve reactant gas diffusion and enhance mass transport within the fuel cell, leading to more effective reactions at the electrodes. Furthermore, operating at higher pressures can increase the contact between reactant gases and the catalyst, enhancing the catalyst utilization and improving the fuel cell's power output. Higher pressure conditions can also help mitigate reactant crossover and improve reactant utilization efficiency. However, it is worth noting that operating at excessively high pressures may lead to increased parasitic losses, increased mechanical stresses on the fuel cell components, and higher system costs. Therefore, finding the optimal operating pressure that balances performance gains with system feasibility and durability is crucial [176].

Lower currents result in cooler and more humid cell conditions, while higher currents lead to hotter and drier cell environments. It has been observed that when the membrane is exposed to high relative humidity (RH) conditions, water uptake causes the ionomer to swell, which can create compressive stresses. These stresses can then transition into tensile residual stresses during drying, potentially contributing to mechanical failures of the membrane. Additionally, studies have indicated that drying processes can impose significant strain on the MEA, and the gradual reduction in ductility combined with constrained drying can result in mechanical failures. Moreover, relative humidity levels have been found to affect the rate of ECSA loss caused by platinum particle growth [176,179].

#### 4.2.2 Startup, Shutdown, and Load Cycling

In vehicular applications, fuel cells often operate under variable load conditions, which poses specific challenges to their durability and performance. Load fluctuations, including load changing, start-stop cycles, idling, and high-power demands, have a significant impact on the lifetime of fuel cells. Among these factors, frequent load changes contribute to the development of fuel cell performance, accounting for approximately 56% of the performance degradation, as depicted in Figure 4.1 [180].

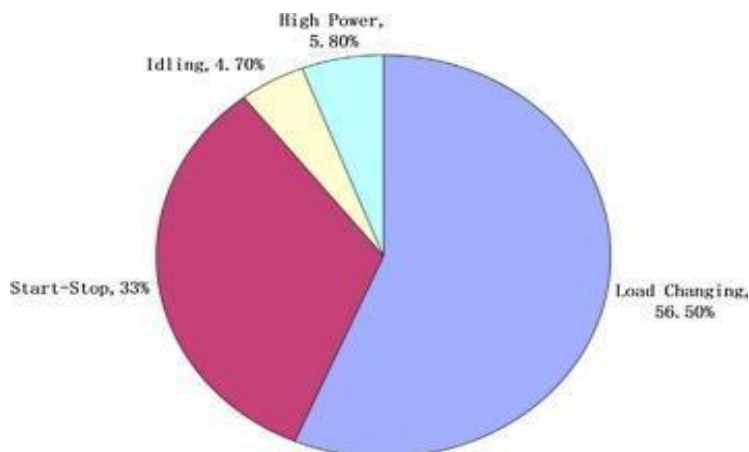


Figure 4.1. PEMFC performance degradation rate caused by different operation conditions [180].

The startup and shutdown cycles of a fuel cell have significant implications for its long-term performance and durability. During prolonged shutdown periods, the phenomenon of hydrogen crossover occurs, where hydrogen gradually diffuses from the anode to the cathode. This results in the anode flow channels being filled with air. When the fuel cell is subsequently started up, a transient state occurs where fuel is present at the anode inlet, but the anode outlet remains fuel starved. This localized fuel deficiency leads to a substantial rise in the cathode local potential, exceeding the threshold of 1.8 V. As a consequence, the fuel cell's efficiency and durability experience a significant degradation. In a study by R. Lin et al. [181], the effects of 1800 startup and shutdown cycles on fuel efficiency and MEA degradation were examined. The findings revealed notable changes in various performance parameters. The Electrochemically Active Surface Area (ECSA) of the fuel cell decreased from  $479.6 \text{ cm}^2 \cdot \text{mg}^{-1}$  (fresh MEA) to  $335.4 \text{ cm}^2 \cdot \text{mg}^{-1}$  after 1800 cycles, indicating a decrease in the catalyst's active area with rate of  $0.08 \text{ cm}^2 \cdot \text{mg}^{-1} \cdot \text{cycle}^{-1}$ . This reduction in ECSA has a direct impact on the fuel cell's electrochemical reactions, leading to decreased reaction rates and overall performance. Additionally, the ohmic resistance of the fuel cell increased by 35%, contributing to higher internal resistance and reduced power output. The charge transfer resistance of the cathode also exhibited a significant increase of approximately 90% relative to the fresh MEA. This rise in charge transfer resistance can be attributed to the decrease in ECSA, which hinders the efficient transfer of charge carriers and leads to reduced current density. The cathode catalyst layer suffered considerable damage as well, with a reduction in thickness by 60% and extreme carbon corrosion. These adverse effects on the MEA components, including decreased ECSA, increased resistances, and catalyst degradation, significantly impact the fuel cell's performance, leading to decreased power output and reduced overall efficiency [175,179].

Load cycling, characterized by rapid changes in the electrical load to meet variable power demands, poses additional challenges to fuel cell performance. During load-changing operations, the current density and cell potential of the fuel cell undergo frequent fluctuations. The cell potential can shift within a range of 0.6 to 1.0 V in most cases, causing potential swings at the cathode as the anode approaches the reversible hydrogen potential. Such potential shifts induce changes in the properties of the electrode materials, particularly the degree of oxide coverage on platinum and carbon surfaces. The presence of oxide layers on these surfaces can inhibit platinum dissolution at higher potentials, preserving the catalyst's integrity and ensuring sustained performance. However, load cycling can disrupt this protective oxide layer and potentially accelerate platinum dissolution, leading to catalyst degradation and reduced catalytic activity. In addition to potential changes, load cycling also affects fuel cell operation through water control issues. Sudden load reductions result in decreased gas flow rates, which in turn leads to a decline in the water content within the fuel cell. This decrease in water

content can cause bulk water retention within the cell, leading to flooding. The accumulation of excess water impedes the reactant gases access to the catalyst sites, reducing the fuel cell's reaction rates and overall performance. Conversely, sudden load increases result in increased gas flow rates, entraining a larger quantity of emitted water out of the fuel cell. This rapid removal of water can result in membrane dehydration, negatively impacting the ionic conductivity of the membrane and reducing the fuel cell's overall efficiency [175,179].

In summary, startup and shutdown cycles can have a detrimental impact on fuel cell durability, leading to decreased efficiency, degradation of the MEA, and damage to the cathode catalyst layer. Rapid load changes also affect fuel cell integrity by causing potential swings, altering electrode material properties, and leading to water control issues such as flooding or membrane dehydration. Understanding and mitigating these effects are crucial for ensuring the long-term performance and durability of PEM fuel cells in various applications.

S.-Y. Ahn et al. [182], studied the performance and the behavior of the stack in continuous operation. The characteristics of the stack are summarized in Table 4.1. The Figure 4.2 shows the initial performance of the stack at 75 C and 1 atm, with gas utilization of 0.5 for H<sub>2</sub> and 0.25 for O<sub>2</sub>. After being moisturized with humidified gases for 24 hours, the stack's performance was evaluated. The open circuit voltage (OCV) of the stack was measured to be 40.0 V, with an average OCV of 1.00 V per cell unit. As we can also see in Figure 4.2, when a load of 24 V was applied, the current and power reached 109.4 A and 2.63 kW, respectively. The stack achieved its maximum current and power of 128.5 A and 2.83 kW at 22 V.

**Table 4.1. Specification of the stack.**

<b>Area of electrode</b>	200 cm <sup>2</sup> (14.1 cm * 14.1 cm)
<b>Number of cells</b>	40
<b>Anode</b>	0.4 mgPt/cm <sup>2</sup>
<b>Cathode</b>	0.7 mgPt/cm <sup>2</sup>
<b>Preparation of electrode</b>	Screen printing method
<b>Electrolyte membrane</b>	Nafion 115
<b>Gas distribution</b>	Counter-flow (internal manifold)
<b>Humidification of gas streams</b>	External bubble humidifier

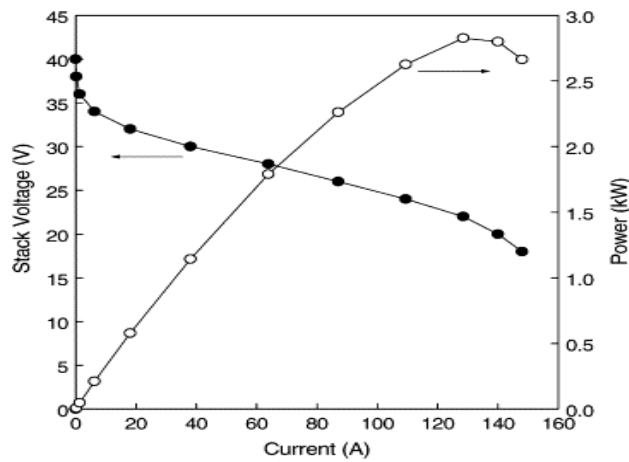


Figure 4.2. Initial performance of the stack,  $T_c=75$ ,  $T_1=75$ ,  $T_0=70^\circ\text{C}$ ,  $P= 1 \text{ atm}$ ,  $U_1=0.5$  and  $U_0=0.25$  [182].

### 4.2.3 Impurity Effects

Impurities in a Proton Exchange Membrane Fuel Cell (PEMFC) can have a significant impact on its efficiency and durability. Table 4.2 provides a summary of the most common impurities and their sources in both the hydrogen fuel stream and the air intake. During the reforming process of hydrocarbons fuels like crude oil, natural gas, and methanol, impurities such as carbon monoxide (CO), hydrogen sulfide (H<sub>2</sub>S), ammonia (NH<sub>3</sub>), and hydrocarbons are generated. These impurities can be attributed to the breakdown of these hydrocarbon fuels. Additionally, impurities like sulfur oxides (SO<sub>x</sub>), nitrogen oxides (NO<sub>x</sub>), and volatile matter are present in the air inlet due to carbon combustion and atmospheric conditions. Furthermore, fuel cell components may introduce impurities through corrosion processes or deicers used in the system [175].

Table 4.2. Origin of common fuel and air impurities [175].

	Sources	Potential Impurities
<b>Hydrogen fuel Impurities</b>	Crude oil	CO, NH <sub>3</sub> , H <sub>2</sub> S, HCN, hydrocarbons
	Natural gas	CO, NH <sub>3</sub> , H <sub>2</sub> S, HCN, hydrocarbons
	Methanol	CO, odorants, alcohols
	Biomass	Cations, aldehydes, alcohols, formic acid, NH <sub>3</sub> , H <sub>2</sub> S, HCN
	Water electrolysis	Anions, cations
<b>Air Impurities</b>	Fuel combustion pollution	SO <sub>x</sub> , NO <sub>x</sub> , hydrocarbons, soot, and particulates
	Ambient air, farming	NH <sub>3</sub>
	Natural sources	Ocean salts, dust
<b>Others</b>	Deicers	NaCl, CaCl <sub>2</sub>
	Fuel cell corrosion products	Cations, anions

## Fuel Impurities

The type and concentration of impurities present in the hydrogen are influenced by various factors including the specific reforming technique employed, the type of fuel utilized, and any post-treatment applied to the reformat stream. While alternative methods like electrolysis can be employed for hydrogen production, they come with their own impurity concerns, such as the presence of cations, and tend to involve higher production costs. As a result, a balance must be struck between the purity of the hydrogen and the associated costs when selecting the hydrogen production approach. Consequently, extensive research has been conducted to evaluate the durability and performance of fuel cells operating with hydrogen contaminated by impurities. The composition of reformat is directly influenced by the reforming process and the type of fuel employed. For instance, hydrogen produced through autothermal reforming of gasoline typically consists of approximately 45% H<sub>2</sub>, 20% CO<sub>2</sub>, and 35% N<sub>2</sub> as its major constituents. In the case of steam reforming of methanol, the resulting hydrogen is typically composed of 75% H<sub>2</sub> and 25% CO<sub>2</sub>. When natural gas is subjected to steam reforming, the hydrogen composition can reach approximately 80% H<sub>2</sub> and 20% CO<sub>2</sub>, alongside smaller quantities of trace impurities. Carbon monoxide (CO) has emerged as a significant issue in PEM fuel cells that utilize reformat H<sub>2</sub>-rich gas as fuel, especially when operating at conventional temperatures below 80 °C. The binding affinity of CO to Pt sites is widely recognized, leading to a decrease in the number of surface-active sites for hydrogen adsorption and oxidation. Baschuk Li [182] studied the poisoning of Pt electrocatalysts by CO and found that it is related to the concentration of CO, exposure time, cell operation temperature, and the type of anode catalyst [175, 179, 184].

The impact of CO poisoning on Pt electrocatalysts escalates with increases in CO concentration and exposure time. Figure 4.4 shows the curves of various CO concentrations as a function of cell voltage and current density. It is easy to see that even the slightest increase in CO concentration leads to a decrease in cell voltage and thus to a decrease in fuel cell performance. Obviously, over time the already existing CO leads to a further decrease in cell voltage, with all that implies. After 6 hours of exposure, a CO level of 50 ppm resulted in a voltage loss of less than 3%, whereas an 85% voltage loss was found when the CO level rise to 70 ppm [176]. Benesch and Jacksier [184] stated that the time taken for cell voltages to decay to a threshold value of 0.3 V was 1 hour when exposed to 50 ppm of CO, and 9 hours when exposed to 10 ppm of CO. Cell voltages did not drop below 0.3 V when the CO concentrations were lower than 5 ppm. It is worth to note that CO<sub>2</sub> is known to react via the reverse water-gas-shift reaction, producing CO.

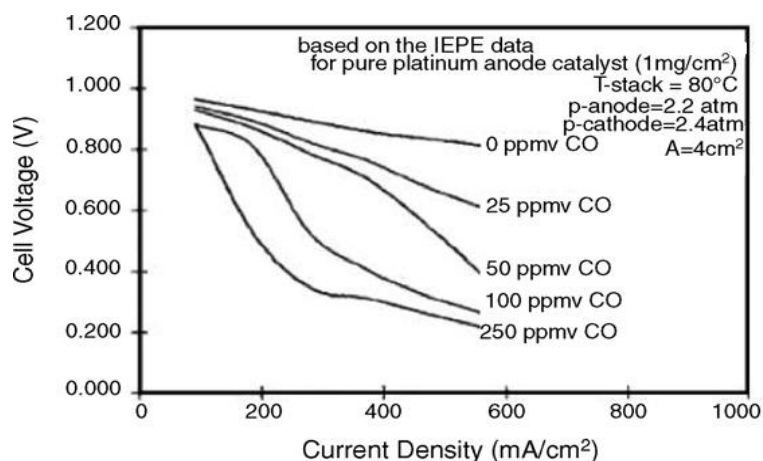


**Figure 4.3. Effects of CO concentration on a stack cell performance [184].**

At temperature below 80 °C, even trace amounts of CO can significantly impact performance. For example, there is a substantial performance drop, impacting both the efficiency and durability, observed when the anode is supplied with H<sub>2</sub> containing 250 ppm of CO at temperatures below 80 °C. Higher temperatures and humidity levels can effectively reduce CO coverage on the catalyst surface by promoting CO oxidation with an OHads group that refers to a surface-bound hydroxyl (OH) species that interacts with the catalyst surface in a fuel cell. This effect was observed in Polybenzimidazole (PBI) membrane-based fuel cells operated at 125, 150, 175, 200 °C with varying CO concentrations in the hydrogen, resulting in lower cell voltage drops at higher temperatures. Furthermore, the combined effects of CO concentration, temperature, and pressure on the fuel performance were investigated (Figure 4.5). Lower temperatures and higher CO concentrations consistently caused more significant performance drops, while the pressure effect differed between pure hydrogen and CO-containing hydrogen. Increasing pressure improved cell performance with pure hydrogen but had only a slight impact in the presence of 500 and 3000 ppm CO, particularly at higher current densities.

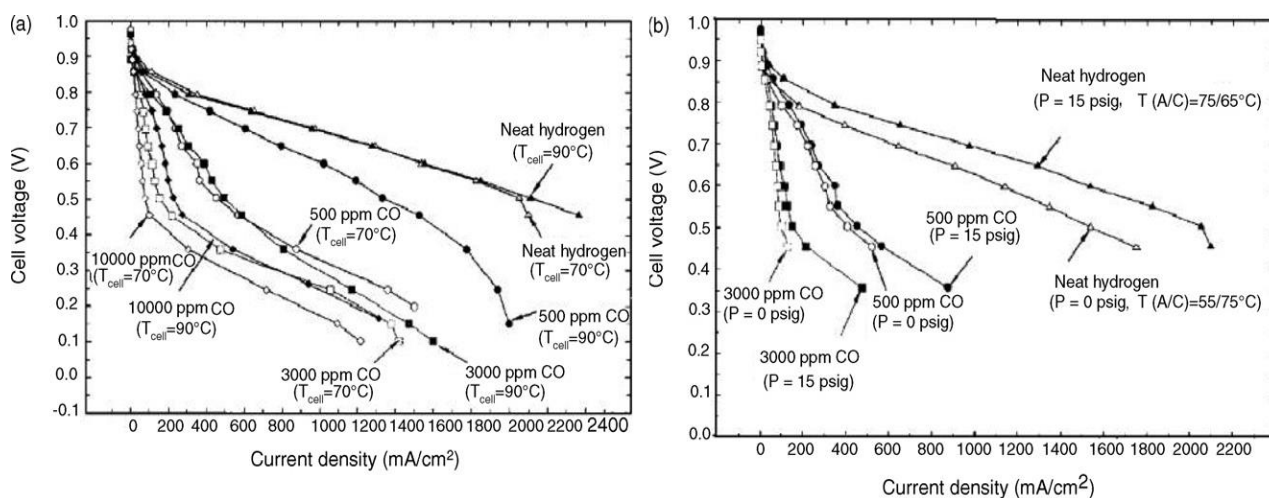


**Figure 4.4. The impact of CO temperature and pressure on cell performance at different concentrations of CO contamination [184]. A=20 cm<sup>2</sup>, GORE-SELECT® Membrane (25m), anode catalyst: Pt alloy at 0.45 mg•cm<sup>-2</sup>, cathode catalyst: Pt at 0.4 mg•cm<sup>-2</sup>. (a) P=202kPa; (b) T=70 °C.**

CO forms a strong bond with Pt and chemisorbs on the metal surface, leading to a decrease in the active surface area by occupying the Pt anode site. This chemisorbed CO hinders the adsorption of hydrogen onto the active Pt sites for hydrogen electro-oxidation (HOR), resulting in performance losses. Additionally, CO impurities in the anode can crossover to the cathode through pin-holes in the membrane, further impacting the cathode output. In the next section there is a more extensive analysis about the effects of CO in different types of anode catalysts [179,184].

Another common PEMFC contaminant is ammonia ( $\text{NH}_3$ ).  $\text{NH}_3$ , present in both the hydrogen fuel and air intake, mostly in hydrogen fuel, has a detrimental effect on fuel cell performance, even at trace amounts of 13 ppm. Higher concentrations of  $\text{NH}_3$  exacerbate the performance decrease, with simulated reformat cell performance dropping from 825 to 200  $\text{mA}/\text{cm}^2$  at 0.6 V. Short-term exposure to  $\text{NH}_3$  shows reversible effects (<1 hour), but long-term exposure causes irreversible negative effects, leading to only a partial recovery [175, 179, 184]. Figure 4.6 demonstrates this phenomenon in a test conducted with 30 ppm  $\text{NH}_3$ . High-frequency resistance measurements revealed an increase in resistivity from  $0.10 \Omega\text{cm}^2$  before  $\text{NH}_3$  exposure to  $0.25 \Omega\text{cm}^2$  after 15 hours. Interestingly, cyclic voltammetry analysis of the anode showed no noticeable  $\text{NH}_3$  adsorption onto the catalyst layer. This suggests that the degradation mechanism is primarily attributed to a loss of protonic conductivity rather than direct  $\text{NH}_3$  adsorption. More specific,  $\text{NH}_3$  impurities indirectly poison the catalyst by replacing  $\text{H}^+$  ions with  $\text{NH}_4^+$  through the reaction with ionomeric  $\text{H}^+$ , leading to a loss of protonic conductivity [185].

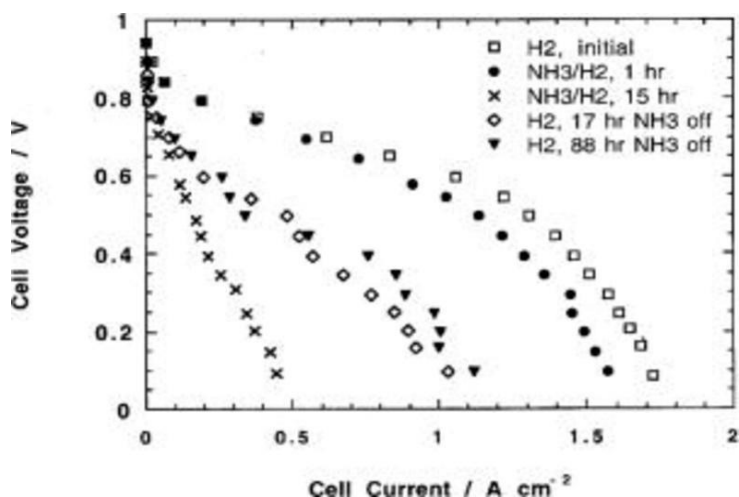


**Figure 4.5. Effects of long-term  $\text{NH}_3$  exposure on  $\text{H}_2$ -air fuel cell performance at 80 C. 30 ppm  $\text{NH}_3$  (g) were injected into the anode feed stream [185].**

In addition to CO and  $\text{NH}_3$ , hydrogen sulfide ( $\text{H}_2\text{S}$ ) can also have significant degrading effects, particularly through Pt catalyst poisoning. Even small amount of  $\text{H}_2\text{S}$  can lead to a substantial decrease in fuel cell efficiency. More specific, the presence of just 1 ppm of  $\text{H}_2\text{S}$  in  $\text{H}_2$  resulted in measurable performance loss within 4 hours. Of exposure and almost complete failure after 21 hours. The sulfur in  $\text{H}_2\text{S}$  forms a strong S-Pt bond upon adsorption onto the Pt catalyst. This chemisorption

hinders the adsorption of hydrogen onto active Pt sites, limiting the fuel cell performance. Moreover, the presence of H<sub>2</sub>S can reduce water levels at the anode, leading to lower membrane conductivity and further compromising PEMFC performance. Additionally, H<sub>2</sub>S causes rapid voltage drops, resulting in decreased fuel cell capacity. This mechanism is similar to CO poisoning [175, 179, 184].

Moreover, hydrocarbon impurities, such as methane and ethane, are commonly present in fuel streams as a result of reforming reactions. Methane, in particular, is a prevalent hydrocarbon impurity with levels typically ranging from 0.1% to 1% during reforming processes. Interestingly, methane does not exhibit a poisoning effect on fuel cells, especially in stationary systems that utilize reformed natural gas containing methane. Furthermore, hydrocarbons like benzene and toluene have shown no evidence of degrading fuel cell performance when exposed to the anode [175].

Finally, cationic ions originating from impurities in fuel cell components, fuels, and coolants can have detrimental effects on water management in fuel cells. These ions, which include alkali metals, alkaline earth metals, transition metals, and rare earth metals, directly impact the transport properties of the electrolyte membrane. For instance, iron ions from stainless steel end plates have been found to cause significant degradation to Nafion membranes, resulting in the loss of fluoride ions. The presence of these iron ions also leads to various performance losses, including kinetic losses at the cathode and anode, ohmic losses, and mass transport losses. Studies have shown that metallic ions, such as Cu<sup>2+</sup>, Fe<sup>3+</sup>, Ni<sup>2+</sup>, and Na<sup>+</sup>, present in sulfate salt solutions at concentrations of 100 ppm, can significantly decrease the ionic conductivity of Nafion 117 membranes, with ferric ions being particularly harmful. It has been observed that the displacement of H<sup>+</sup> ions with foreign cationic ions directly affects water flux and proton conductivity within the membrane, ultimately leading to membrane degradation [179, 184].

### **Air Impurities**

Popular atmospheric contaminants resulting from fossil fuel combustion, such as sulfur oxides (SO<sub>x</sub>) and nitrogen oxides (NO<sub>x</sub>), are exposed on the cathode side. The impact of sulfur dioxide (SO<sub>2</sub>) injected at the cathode of a fuel cell is similar to that of hydrogen sulfide (H<sub>2</sub>S) at the anode. The extent of performance degradation is dependent on the concentration of SO<sub>2</sub> in the bulk, with higher concentrations causing more significant decreases in performance. For example, a 2.5 ppm SO<sub>2</sub> concentration resulted in a 53% performance decrease, whereas a 5 ppm SO<sub>2</sub> concentration led to a 78% decrease. Once the impurity injection is stopped, the performance does not recover through normal operation, indicating irreversibility. The severity of the effect can be attributed to the strong chemisorption of SO<sub>2</sub> (or other sulfur species) onto the platinum (Pt) catalyst surface. However, it has been observed that electrochemical oxidation of adsorbed SO<sub>2</sub> during cyclic voltammetry (CV) can lead to full cell performance recovery. In addition to SO<sub>2</sub>, exposure to nitric dioxide (NO<sub>2</sub>) leads to a gradual decrease in performance over 30 hours of operation, with no further degradation thereafter. The severity

of the degradation is not strongly dependent on the bulk concentration of  $\text{NO}_2$ . Fuel cell performance can experience up to a 50% reduction, but complete recovery is observed within 24 hours when pure air is applied. Interestingly, the poisoning effect of  $\text{NO}_2$  does not involve catalyst surface poisoning species, as no detectable surface species are observed during CV. The presence of  $\text{NO}_x$  in the cathode's oxidant flow initially accelerates fuel cell performance, followed by a subsequent drop and stabilization.  $\text{NO}_2$  causes less severe performance loss compared to  $\text{SO}_2$ . Nitric oxide (NO) directly affects the catalyst and is primarily absorbed as NO, while  $\text{NO}_2$  reacts with ionomeric  $\text{H}^+$  to form  $\text{NH}_4^+$ , reducing protonic activity [175, 179, 184].

In addition to gas-phase contaminants, salts (mostly from ocean mists and road deicer) may contaminate the cathode air supply. Most common salts are sodium chloride ( $\text{NaCl}$ ) and calcium chloride ( $\text{CaCl}_2$ ). The presence of these salts in fuel cells leads to decreased efficiency and reduced component longevity. High concentrations of salt result in reduced hydrophobicity and increased liquid water retention in the GDL, ultimately hindering oxygen transport to the electrocatalyst, especially at high current densities. The exchange of  $\text{H}^+$  by cations ( $\text{Na}^+$ ,  $\text{Ca}^{2+}$ ) at the CL and membrane causes a decrease in proton conductivity and contributes to membrane degradation. Anions such as chloride ( $\text{Cl}^-$ ) decrease the ECSA of the cathode, primarily through site-blocking effects on the Pt surface and the formation of chloride complexes, leading to increased Pt dissolution. Additionally, chloride does not appear to block adsorption on catalyst surfaces, as observed in CV measurements, although it significantly influences the oxygen reduction kinetics of cathode electrocatalysts [175].

#### **4.2.4 Reactant Starvation**

Starvation is a significant parameter that can adversely affect the efficiency and durability of PEM fuel cells. During rapid load variations, fuel starvation arises from an insufficient provision of fuel or oxidant and can manifest as either localized or overall starvation.

Local starvation occurs when there is an insufficient supply of reactant gas in specific areas of the CL of the fuel cell. This can be caused by various factors, including poor cell and stack design, inadequate water management, poor thermal management, contaminant gasses, and blockages. On the other hand, overall starvation refers to the insufficient supply of reactant gas at the stack level, often caused by incorrect operation or control module failure. When local starvation occurs, it can lead to uneven fuel distribution and restricted access to reactants in certain regions of the CL. This results in performance degradation and potential damage to the fuel cell. Large-scale cells, such as those used in stack configurations, can experience different flow distributions between the inlet and outlet regions, further exacerbating the challenges of local starvation. Researchers have conducted studies to investigate the effects of local starvation on fuel cell performance. For example, Shen et al. found a rise in the voltage difference between the input and the output regions as current density increased, accompanied by a

decrease in air stoichiometry. These observations indicate that local fuel starvation can impact voltage distribution within the fuel cell. Moreover, localized fuel starvation can induce significant local potentials on the air electrode, potentially exceeding 1 V. When there is not enough fuel, the electrodes will have to increase their potential to bring the fuel cell to equilibrium. Insufficient fuel supply in specific regions can result from uneven cell-to-cell flow distribution, obstructions within channels, variations in channel depth tolerances, and impediments caused by water. Improper control of water, including the condensation of water vapor within anode channels, can further exacerbate fuel distribution challenges and cause harm to the cathode catalyst layers. [176,179].

In the case of overall starvation, multiple cells within a stack may experience fuel maldistributions, where some cells receive insufficient fuel to carry the current being pushed through them by adjacent cells. This can result in negative cell voltages, as the anode potential increases to positive levels and the carbon support in the catalyst layer is consumed instead of fuel. Without a sufficient anodic current source from hydrogen, the cell potential continues to rise until oxidation occurs. In this scenario, the carbon support of the catalyst layer undergoes oxidation, leading to permanent damage to the anode CL. This phenomenon can be damaging and reduce the overall performance and lifespan of the fuel cell. A diagram illustrating the changes in electrode potentials under starvation conditions is shown in Figure 4.7 [186].

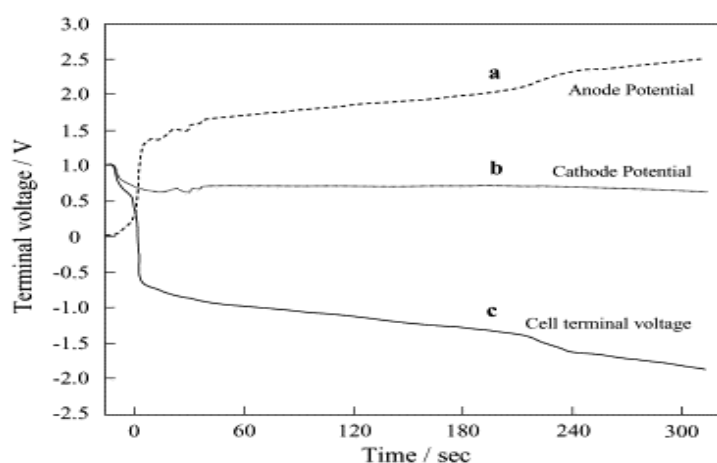


**Figure 4.6. The evolution of the anode and cathode potential over time under starvation conditions [186].**

Under conditions of fuel starvation, the anodic current is typically provided by carbon corrosion, leading to the formation of carbon dioxide. This process of carbon corrosion and subsequent damage to the anode CL is a result of the lack of fuel supply. Modeling studies have been conducted to investigate how poor hydrogen distribution can induce both oxygen evolution and carbon corrosion at the cathode of the fuel cell. These models have also predicted that the crossover oxygen through the membrane plays a role in controlling the total amount of current directed towards carbon corrosion.

### **4.3 Parameters Influencing each Component's Performance and Durability**

### 4.3.1 Membrane

As has already been said, a membrane It should possess high proton conductivity, enabling efficient transport of protons within the fuel cell. At the same time, it should have low electronic conductivity to minimize electron leakage, which can reduce overall cell efficiency. The membrane should also demonstrate chemical and thermal stability, ensuring long-term durability under the harsh operating conditions of the fuel cell. Effective water management is crucial, allowing the membrane to maintain appropriate hydration levels for optimal proton conduction without flooding or drying out. Additionally, mechanical durability is essential to withstand the mechanical stresses experienced during operation. However, the deterioration of PFSA membrane, which is the most common, properties are governed by mechanical, thermal, and chemical degradation.

#### Parameters leading to mechanical failure

The performance and durability of a PEM fuel cell rely on its ability to function effectively throughout its service lifetime. The life path of a PEM membrane can be divided into four keys processes: fabrication, assembly, short-time operation, and long-time operation, as it seems in Figure 4.8. The quality of the membrane fabrication plays a crucial role in determining its material properties and resistance to degradation. During the assembly process, the membrane is integrated into the fuel cell alongside other components like BP, sealing materials, and end plates. At the initial stages of fuel cell operation, the membrane experiences significant changes in stress due to variations in relative humidity and temperature, necessitating high mechanical flexibility within the confined cell environment. Extreme conditions can lead to membrane failure, posing a risk to the overall performance. Throughout long-term operation, the membrane is subjected to repetitive cycles of swelling and shrinkage, influenced by water absorption, thermal effects, gas pressure, and chemical exposure. Any mechanical failure in the membrane at any stage of its life path can lead to a decline in fuel cell efficiency. Various external and internal factors, such as fabrication quality, assembly procedures, components quality, chemical degradation, and operational factors can influence the occurrence of mechanical failure in the membrane [179, 187].

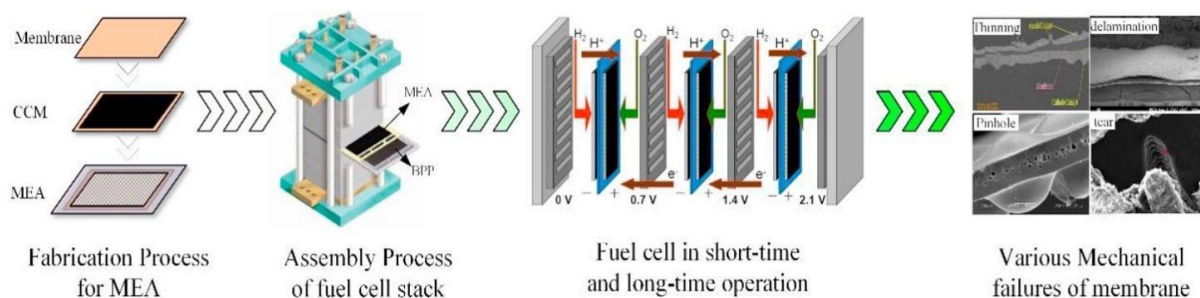


**Figure 4.7. Membrane's lifepath in a fuel cell [187].**

The first process in the life path of a PEM membrane focuses on the quality of manufacturing process. It is essential to achieve high-end qualities in terms of mechanical and geometric properties for the thin PEM. However, due to the challenges of mass production, defects can occur, such as micro pinholes, increased roughness, and thickness variation. These undesirable variables lead to non-uniform mechanical and chemical properties within membrane. Consequently, they have detrimental effects on both the durability of the membrane and the performance of the fuel cell. These effects manifest as reduced mechanical strength, the formation of hot spots, and vulnerability to radical attacks [187-188].

When assembling a fuel cell stack, multiple single cells are connected in series to fulfill the voltage and power requirements. The PEM is positioned between two BPs in a sandwich structure, forming the MEA. However, the assembly process and manufacturing errors of the components can introduce non-uniform mechanical stress or localized concentrated stress on the membrane. This is primarily influenced by the sealing edge and the arrangements of ribs and channels in the flow field, which are typically set at regular intervals. These fluctuating mechanical stresses in the membrane can be further exacerbated by manual assembly procedures and variations in component manufacturing. The accumulation of these stresses poses a risk of membrane tearing, compromising its integrity, and potentially leading to performance degradation and fuel cell failure [187].

During the operation of fuel cell, humidified reactant gases are supplied to the system at a specific temperature. This introduces pressure fluctuations and cyclic hygrothermal conditions to the constrained membrane. During startup or shutdown phases, in particular, the membrane experiences significant tensile and compressive stresses as a result of expansion and shrinkage. These stress variations can potentially lead to plastic deformation, where the membrane may undergo permanent changes if the applied compressive or tensile stress exceeds its yield strength. Additionally, environmental factors, such as freeze-thaw cycles and weak areas at the joint region between the membrane and the MEA frame can contribute to rapid membrane failure during short-term operation. These challenging mechanical conditions pose significant risks to the durability and performance of the membrane in a fuel cell system [187,189].

During the long-term operation of a fuel cell, the membrane is subjected to cyclic loading conditions. This cyclic loading, combined with the swelling and shrinkage of the membrane, leads to fluctuating mechanical stresses within the material. Over time, these stresses can result in the formation of wrinkles, creep, and fatigue, which weaken the membrane structure. As a consequence of long-term accumulation, the mechanical failure of the membrane occurs through the initiation and propagation of micro-pinholes or cracks, particularly within areas that are already defective. It is important to note that in real working environments, the mechanical failure process can be further exacerbated by delamination from the CL and chemical degradation [187,190].

Confirming all the above, ex-situ analysis of aged membranes has revealed several degradation features, including crazes, cracks, pinholes, thinning, and elongation of the membrane. The formation of these defects can be attributed to cyclic stress caused by repeated swelling and shrinking of the membrane during water sorption and desorption processes. Consequently, the electrical contact between the MEA and electrodes may be compromised, and crossover of gases increases. These effects result in lower open circuit voltage (OCV), higher ohmic losses, and a decrease in fuel cell performance. Moreover, as the crossover of reactants intensifies, local hotspots may develop, further accelerating the degradation process. Ultimately, these factors can lead to the catastrophic failure of the membrane [179, 191, 192]. Figure 4.9 summarizes the main factors influencing mechanical failure.

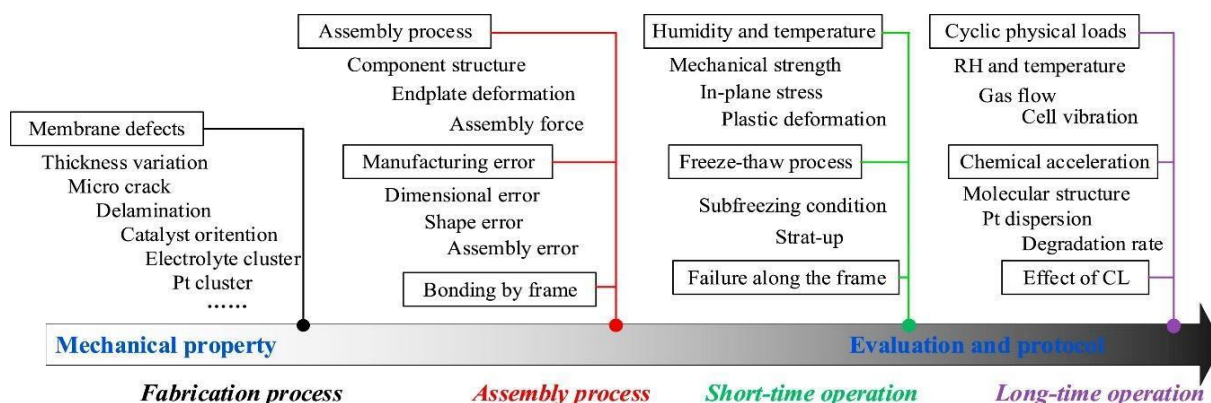


Figure 4.8. Main factors influencing mechanical failure [187].

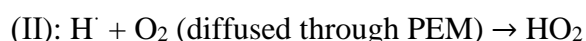
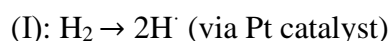
### Parameters leading to thermal failure

During typical operating conditions of fuel cells, approximately 80 °C, the impact of thermally triggered deterioration of the electrolyte is presumed to be negligible. Nevertheless, upon heating Nafion films to 95 °C, the formation of cross-linked sulfonic end-groups was detected, resulting in a decrease in conductivity. The operational temperature limit for Nafion-based membranes is approximately 100 °C, which remains lower than the material's glass transition temperature of 110 °C and in case this is exceeded, the membrane exhibits breakdown of the ionic clusters and a rise in crystallinity. Unlike high temperatures, fuel cells employed in automotive applications must also endure repeated encounters with extremely low temperatures reaching -40 °C, which can result in ice formation and melting. Moreover, through freeze/thaw cycle tests, a decline in fuel cell performance and longevity was noted when examining the impact of the characteristics of the membrane [191, 193]. In an experiment conducted by Qiangu Yan et al. [194], the performance of the membrane was assessed across a temperature range spanning from -15 °C to 80 °C. The researchers observed the presence of cracks, pinholes, and detachment of the CL on both the membrane and GDL and they noticed that the fuel cell could function at below zero temperatures, specifically -15 °C and -5 °C, without the need for humidification and cleaning, as long as the

cathode temperature remained above -5 °C during operation. In addition, there is a volume expansion of the water when it freezes of 9%, which leads to uneven stresses and consequently to damage the fuel cell components. Because of the above, Cho et al. [195] after testing a Nafion 112 membrane in 385 freeze/thaw cycles at temperatures between -10-80 °C, found that the membrane was not destroyed but underwent molecular reorganization and aggregation in the hydrophilic regions, and thus a reduction of its durability [191].

### Parameters leading to chemical failure

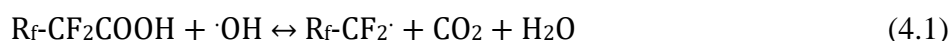
Chemical degradation in a PEM fuel cell is the result of chemical attack, leading to the breakdown of the membrane's structure and functionality. This attack is often initiated by active oxygen species, which cause the loss of ions and damage to the membrane. The primary mechanism of chemical degradation involves the rupture of perfluorocarbon side chains and backbone groups within the polymeric membrane. This degradation process leads to a reduction in proton conductivity and mechanical strength, ultimately resulting in a decrease in the power output of the fuel cell. Defects in the membrane, such as unsaturated C=C bonds or residual C-H bonds in the main chain, can act as vulnerable sites for chemical degradation over time. These sites are prone to chemical reactions that further deteriorate the membrane's integrity. Chemical degradation of the membrane occurs due to the formation of peroxy- and hydroperoxyl-radicals, which attack the backbone and side chains, leading to lower PEM conductivity [191,196]. This phenomenon is known as side chain unzipping. General Electric provides a comprehensive description of the widely recognized mechanisms for the usual generation of peroxy compounds in PEM, which involves the following five steps [197]:



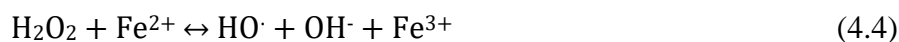
(III):  $HO_2^{\cdot} + H^{\cdot} \rightarrow H_2O_2$  (which can permeate into the vicinity of the deteriorated region at the front of the PEM)



X-ray Photoelectron Spectroscopy (XPS) analysis has shown that interactions between carbon, fluorine, and oxygen change during fuel cell operation. For example, hydroxy radicals can attack carboxylic end groups, resulting in the formation of different compounds. An example given by Curtin et al. [196] is the attack of hydroxyradicalson carboxylic end groups:



Chemically modified membranes developed by DuPont have demonstrated reduced fluorine release rates and improved durability by reducing the number of reactive end groups through alternative synthesis methods. Traditionally, it was believed that radicals in fuel cells are formed either at the cathode during the oxygen reduction reaction or from decomposition of  $\text{H}_2\text{O}_2$  at the anode. The presence of oxidizable metal ions, such as  $\text{Fe}^{2+}$ ,  $\text{H}_2\text{O}_2$ , and the polymer, has been used to analyze the resulting product. However, recent evidence suggests that radicals can also be generated through a reaction between molecular hydrogen and oxygen in the presence of Pt catalyst, without the intermediate formation of  $\text{H}_2\text{O}_2$ . This direct radical pathway is considered more significant in fuel cell degradation than  $\text{H}_2\text{O}_2$  pathway. Favorable conditions for degradation occur not only at the cathode and anode but also within the membrane itself when Pt particles deposit there due to electrode degradation [196]. Moreover, the presence of infectious ions, which are introduced by changes in water flow within the membrane can also drive in chemical degradation. Even a small percentage of infectious ions (5%) can lead to deterioration. The migration of  $\text{H}^+$  ions with foreign cations accelerates the dehydration of the membrane. When this process takes place near ion trace elements, such as  $\text{Fe}^{2+}$  and  $\text{Cu}^{2+}$  from corroded metal BPs, it catalyzes the formation of defects, resulting in membrane thinning and a reduction in PEM cell efficiency. This mechanism leads the membrane to dilution or even to the creation of holes and is described by the following equations [198]:



### 4.3.2 Catalyst Layer

In most state-of-the-art PEMFC designs the basic electrode structures are identical. As mentioned in chapter 3 the catalyst layer is a porous structure consisting of catalyst nanoparticles, which are usually platinum nanoparticles (Pt), which are scattered over the larger nanoparticles of the supporting material that are usually carbon nanoparticles and are saturated in ionomer thin films. Figure 4.10 illustrates once again the structure of a catalyst layer.

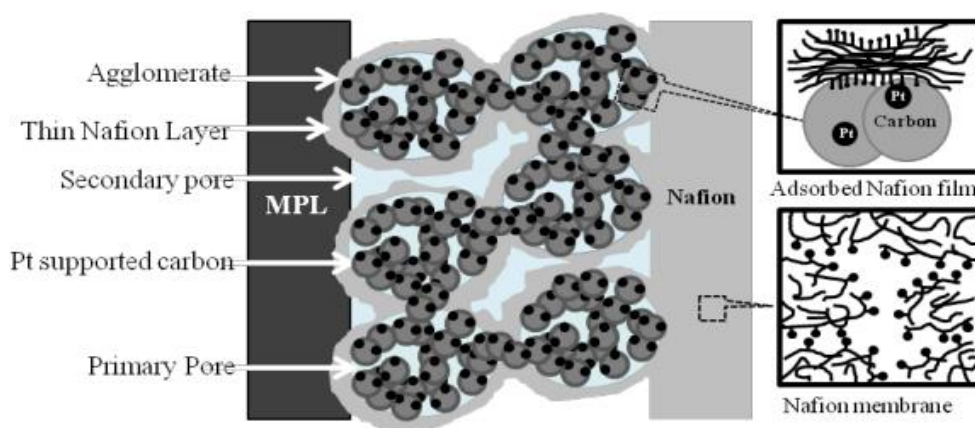
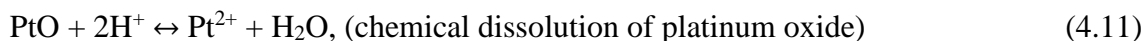


**Figure 4.9. Schematic representation of the structure of a catalyst layer [199].**

The electrode structures may be the same for both anode and cathode, but the degradation effects on the two electrodes differ. Therefore, in order to study and understand the degradation mechanisms of the catalyst layer, which have as a result the reduction of the performance and resistance of PEMFC, it would be worthy to analyze how these degradation mechanisms affect the anode catalyst layer and the cathode catalyst layer separately. Such degradation mechanisms of CL are the dissolution and deposition (agglomeration / sintering) of Pt nanoparticles, the dissolution of the ionomer in the catalyst layer, the corrosion of the supporting carbon and finally the contamination of the catalyst by CO. All the above degradation mechanisms will be analyzed in detail in this subsection and the parameters that activate or aggravate these degradation mechanisms will be presented [171].

The catalyst layer can be degraded due to dissolution and deposition (agglomeration / sintering) of Pt nanoparticles. The deposition (agglomeration / sintering) of Pt nanoparticles, also known as the “electrochemical Ostwald ripening” effect, occurs when small Pt particles dissolve in the acidic operating environment and then reposition on the surface of larger particles [200].

Initially, it has been observed that the dissolution of Pt nanoparticles is intense in intermediate potentials, and quite low or even negligible in low or high potentials. The oxidation and dissolution reactions of the Pt nanoparticles are presented below.



Experimental data have shown that the dissolution of platinum in the acidic operating environment under low potentials is very low. During exposure of platinum to an acidic environment and high potentials, PtO is formed, according to the reaction 4.10. The oxide layer effectively insulates platinum by delaying its dissolution (reaction 4.11). Therefore, in this case, the dissolution of platinum is quite low. However, the rate of dissolution of the uncovered platinum surface during its exposure to intermediate potentials in the acidic environment of the electrode is much more pronounced (reaction 4.9) [201-208].

Then, after the dissolution of the Pt particles, the phenomenon of “electrochemical Ostwald ripening” takes place. According to this phenomenon, Pt cations are extracted from the relatively smaller particles, to form larger Pt particles, through the electrolyte, due to a difference in chemical potential. At the same time, electrons are transferred to the larger Pt particles via the conductive support substrate. Thus, electrochemical Ostwald ripening continues to occur because it is unable to reach a quasi-equilibrium state (Figure 4.11a). This phenomenon can also occur when two Pt nanoparticles are in contact with each other and thus allow the transfer of electrons through their contact, while the transfer of Pt ions continues to occur through the electrolyte. The order of increase in the size of nanoparticles is of the order of nanometers (Figure 4.11b) [209].

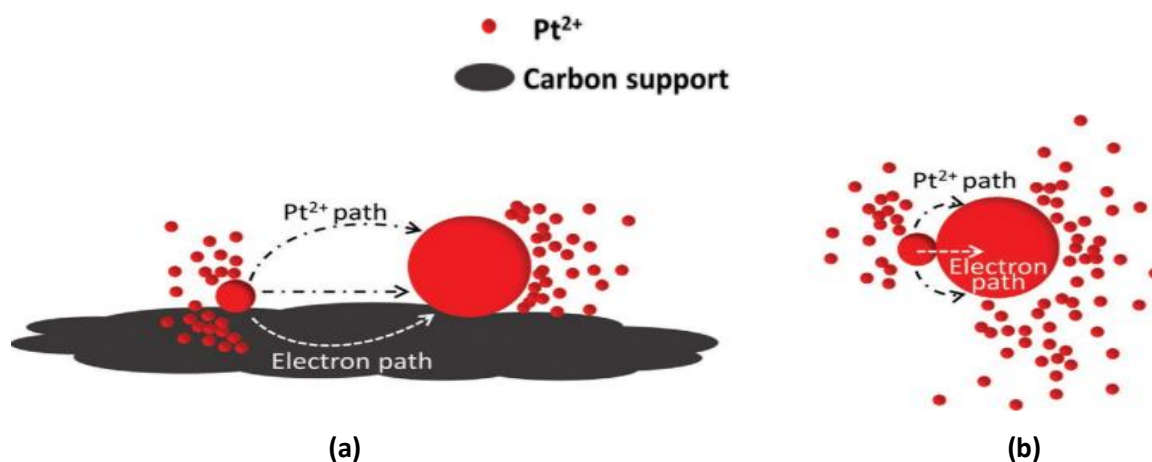


**Figure 4.10. Ostwald Ripening**

The degradation mechanism of dissolution and deposition of Pt nanoparticles causes a decrease in the electrochemical surface area (ECSA), and consequently a decrease in fuel cell efficiency. The stronger the particle growth, the smaller the ECSA and ultimately the fuel cell efficiency [168].

The parameters that trigger or aggravate the dissolution and deposition of Pt nanoparticles are various and are listed below, and many of them have been analyzed in the previous subsections. In section 4.2 of the chapter, we saw how different operating conditions can affect the performance and durability of PEMFCs. Some of these conditions affect the specific degradation mechanism leading to a decrease in the performance of the cell.

The cell potential cycling aggravates this mechanism, increasing the size of the Pt particles faster than operating with constant potential. As shown in Table 4.3, higher potentials accelerate the reduction of ECSA.

**Table 4.3. Influence of potential cycling on initial ECSA [210].**

# of potential cycles	% initial ECSA (0.1-0.75 V)	% initial ECSA (0.1-1.2 V)
300	96	60
900	90	23
1500	83	11

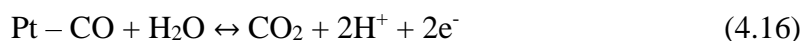
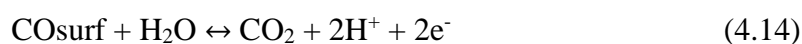
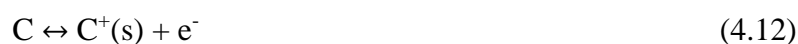
For example, the size of Pt particles after 1500 cycles from 0.1V to 1.2V, can be increased up to 8nm, with significant effects on ECSA reduction [168].

The operating temperature and relative humidity of the incoming reactants are parameters that aggravate this degradation mechanism. At higher temperatures the dissolution and deposition of particles is accelerated, thus degrading the catalyst. On the other hand, the lower the relative humidity (RH), the weaker the growth of the particles [200].

Finally, it is very important to note that the anode catalyst is not as strongly affected by this degradation mechanism as the cathode catalyst. It has been observed, through many long-term experiments, that the anode catalyst, regardless of the conditions under which the cell operates, remains unaffected by the “electrochemical Ostwald Ripening” effect.

The dissolution of the ionomer in the catalyst layer is another degradation mechanism of the catalyst layer, which occurs during long-term operation. This degradation mechanism causes a decrease in the ionic conductivity of the catalytic layer and a loss of contact of the catalyst particles. The dissolution of the ionomer is affected by the same parameters as the membrane. Finally, the degradation characterization of the ionomer is difficult [171].

Another very important degradation mechanism of the catalyst layer in PEMFCs is the corrosion of the catalyst support material, which, as we have mentioned several times in this paper, the catalyst support material is carbon. The mechanism for the carbon oxidation reaction appears to evolve through specific steps. Initially, some species of  $C^+(s)$  are formed (reaction 4.12), then rapid hydrolysis is made to the surface carbon oxides ( $CO_{surf}$ ) (reaction 4.13), to eventually evolve these carbon oxides to  $CO_2$  (reaction 4.14). It has been widely proven that the final step of  $CO_2$  evolution is accelerated in the presence of Pt (reactions 4.15 & 4.16) [209].



The corrosion of the supporting carbon results in the loss of Pt nanoparticles, which are scattered over the larger particles of the supporting carbon, or the deposition of Pt nanoparticles to form larger particles, leading to a reduction in ECSA, and in the extreme case of a collapse of the cell electrode. Also, this degradation mechanism can lead to a change in the pore structure of the electrode, with a consequent reduction in the hydrophobicity of CL and an increase in the transport resistance of the reactant gases. Moreover, the corrosion of supporting carbon leads to reduced electrical

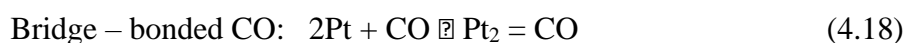
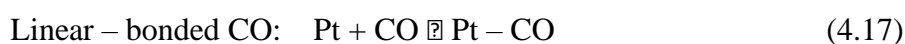
conductivity. In conclusion, PEMFC performance and durability are significantly affected by the loss of supportive carbon [201,209].

The rate of carbon corrosion in a PEMFC is affected by several parameters. General operating conditions in PEMFCs where low pH, low feed hydrogen concentrations and high operating potential exist, make carbon corrosion more severe. The main degradation parameters of the catalyst layer through corrosion of the supporting carbon are listed below [209].

Initially, the high-water content in the catalyst layer due to poor water management, helps to accelerate the rate of corrosion of the supporting carbon. In addition, as mentioned in subsection 4.2.2 when starting and shutting down a PEMFC the cathode potential may exceed 1.8V, which may negatively affect carbon corrosion. Another very important parameter, which triggers carbon corrosion and has been detailed in subsection 4.2.4 is hydrogen starvation. In the absence of hydrogen, the oxygen which exists at the anode reacts with carbon to form CO<sub>2</sub> [168,211].

Last, and perhaps one of the most important degradation mechanisms of the catalyst layer is CO poisoning [168]. This degradation mechanism has been presented quite in detail in subsection 4.2.3, as it is a degradation parameter due to impurities. Below will be presented in more detail the specific degradation mechanism of the catalyst layer.

The adsorption of CO to Pt is preferable to the adsorption of H to Pt due to the more negative Gibbs energy of the adsorption of CO to Pt than the corresponding Gibbs energy of the adsorption of H to Pt. CO can be adsorbed either in bare platinum positions, or in platinum positions already occupied by H, through two different types, linear – bonded CO (4.17) and bridge – bonded CO (4.18).



Adsorbed CO can be removed by oxidation [170].

Since PEMFCs are currently powered by a reformulated product containing CO, and given the barriers involved in storing hydrogen and the high cost of producing pure hydrogen, poisoning of PEMFC by CO is considered to be unavoidable. Currently, Pt is used in both electrodes, due to its high activity in HOR and ORR in acidic environments, but no solution has been found for its disadvantages due to its high cost and easy poisoning by CO. The combination of Pt with a second metal and new methods of electrocatalyst preparation with advanced morphologies and structures appear to enhance the tolerance to CO, while the use of a different supporting material from carbon seems to improve the stability of FC [170,212].

Table 4.4 presents the advantages and challenges of the most promising state-of-the-art electrocatalysts for CO tolerance.

**Table 4.4. Highly favorable electrocatalysts with advanced CO tolerance capabilities [170].**

Electrocatalyst	Advantages	Challenges
PtRuNi/C (composition gradient shell)	Following exposure to 10 ppm CO poisoning, an 11% decline in performance was observed, while complete stability was maintained throughout 100 hours of operation using a 10 ppm CO/H <sub>2</sub> feed	The synthesis method is intricate, and the CO tolerance under poisoning with CO concentrations exceeding 10 ppm has not been determined
Pt <sub>x</sub> AL-Pt <sub>69</sub> Co <sub>31</sub> /C	At 70 °C, the HOR activity retained 95% efficiency after exposure to 1000 ppm CO, while after enduring 1000 ppm CO poisoning and a durability test comprising 4000 cycles, the HOR activity retained 78%	The behavior of CO tolerance during H <sub>2</sub> -PEMFC operation is currently not known
PtRu@h-BN/C	After 30 ppm CO and 25% CO <sub>2</sub> poisoning, the potential loss was a mere 18 and 26 mV at 0.2 and 0.6 A cm <sup>-2</sup> , respectively. Also, the system exhibited exceptional stability both thermally and electrochemically	The synthesis method is intricate, and the stability of H <sub>2</sub> -PEMFC operation during CO poisoning for extended periods is currently uncertain
Pt/Ti <sub>x</sub> Mo <sub>1-x</sub> O <sub>2</sub> -C (x = 0.8-0.6)	CO oxidation occurs at potentials below 250 mV, and a 130 mV is observed at 1 A cm <sup>-2</sup> following exposure to 100 ppm CO poisoning	The HOR activity exhibits lower performance than Pt/C when CO is not present, due to reduced support conductivity. Also, the stability is compromised due to the leaching of unincorporated Mo
Pt/C MFP90°	After exposure to 100 ppm CO poisoning, there was only a 12% decrease in max power density	Elevated levels of PGM loading
Pt/C coated with DAcPy	Following 5 h poisoning with 100 ppm CO, the HOR activity retained 87% efficiency	Elevated levels of PGM loading alongside uncertain CO tolerance behavior during practical H <sub>2</sub> -PEMFC operation

It is important to highlight that the electrocatalysts mentioned in table 4.2 are the results of research conducted in the last decade and obviously there is a lot of room for improvement to address this degradation mechanism of the catalyst layer.

### 4.3.3 Gas Diffusion Media (GDM)

Chapter 3 mentioned that the gas diffusion media consists of two layers, the gas diffusion backing layer, or simply a gas diffusion layer, which is usually made of carbon fiber and consists of a macroporous substrate and the microporous layer, which contains carbon powder and a hydrophobic agent. The basic functions of gas diffusion media are the removal of liquid water from the catalyst layer to the flow field channels, the transfer of electrons without great resistances, the transfer of reactant gasses from the flow field channels to the corresponding catalyst layers and the appropriate hydration of the membrane. It is therefore obvious that the degradation of gas diffusion media exerts a notable influence on the performance and longevity of PEMFC [213].

The degradation of GDM is aggravated due to various parameters. Separating these parameters and studying the effects they cause in GDM helps to understand and address the endurance problems

that arise due to degradation of the specific component of the fuel cell [214]. The degradation of GDM is categorized into electrochemical, mechanical and thermal degradation [213].

### Electrochemical degradation

As with supportive carbon in the catalyst layer, gas diffusion media suffers from carbon corrosion. This degradation mechanism of GDM is caused by several parameters. Potential cycling, especially in high cell potentials, is a parameter that causes carbon loss due to corrosion. Chen et al. observed that, under simulated PEMFC conditions over a range of potentials between 1V and 1.4V, carbon is significantly reduced leading to dilution of GDL fibers to potentials above 1.2V. They also reported that ohmic resistances as well as gas transfer resistances increased significantly. The high temperatures as well as the low relative humidity (RHs) of the reactant gases are also parameters for accelerating carbon corrosion in the gas diffusion layer [213]. In addition, special operating conditions of the fuel cell, which have been analyzed in subsection 4.2, such as localized hydrogen starvation, start-up / shutdown are important parameters for worsening carbon corrosion of GDL [214].

### Mechanical degradation

Mechanical degradation involves mechanical and physical damages that can be caused by parameters such as compression force, freezing and thawing, and the flow of high-speed gas [200]. Compression force can reduce the performance of PEMFC, affecting the properties of the MPL / catalyst layer interface and the GDL / bipolar plates interface. Figure 4.12 shows the effects of increasing compression force [214].

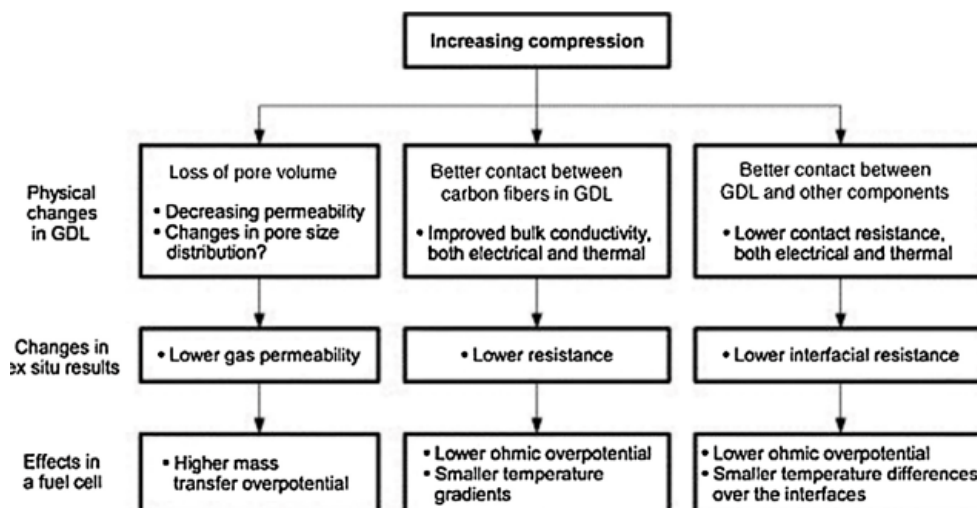


Figure 4.11. The consequences of higher compression on the GDM [215].

As shown in Figure 4.12, the increase in compression leads to a change in pore structure and a decrease in GDM permeability of the gas reactants. Therefore, mass transport resistance is increased. At the same time, however, increasing the compression of GDM can improve its electrical and thermal conductivity. Therefore, it reduces Ohmic Resistance [214]. In addition, the Bazylak

observed breakage of polytetrafluoroethylene (PTFE) coatings or detachment of PTFE from carbon fibers, via scanning electron microscope (SEM) images, when compressing GDM for five minutes at a pressure of 0.18, 0.36, 0.68, and 1.37 MPa [216]. This loss of PTFE hydrophobic leads to an increase in GDM porosity and a loss of GDM hydrophobic properties [217].

For automotive applications, PEMFC is exposed to subzero temperatures. The exposure of PEMFC to frost temperatures and the formation of ice inside the cell is a parameter of mechanical degradation of GDM. Experiments have shown that GDLs with increased rigidity can limit the mechanical stresses that the cell undergoes due to ice formation. Moreover, operation in freezing/thaw cycle may result in loss of PTFE and a decrease in hydrophobic properties of GDM [217].

Finally, despite the fact that the carbon black particles of the microporous layer and the carbon fibers of the gas diffusion layer are more stable than the carbon particles of the catalyst layer, the oxidation of carbon from the water that takes place in the GDM is significant. As a result, the gas transfer resistance increases and the performance of PEMFC decreases [218].

### **Thermal degradation**

The effect of temperature on GDL does not appear to be considered significantly in the literature. However, some observations have been made that high temperatures accelerate carbon corrosion. It is also believed that the manufacturing processes of MEA with hot press, and exposure of PEMFC to subzero temperatures may affect GDL and MPL negatively [218].

### **4.3.4 Bipolar Plates**

Bipolar plate (BP) degradation has significant adverse effects on the performance and durability of PEM fuel cells. The research carried out by Christoph Hartnig et al. [219] highlights the detrimental impact of BP degradation on cell performance, specifically the rise in cell resistance and overpotentials for oxygen reduction attributed to acid depletion from the CL, accompanied by a decrease in the ECSA. The research identifies three primary mechanisms of deterioration [175]: (i) the process of material dissolution in plates, leading to membrane poisoning and can result in contamination of the membrane, negatively affecting its performance, (ii) formation of a resistive surface layer resulting in high ohmic resistance. This resistance hinders the flow of current, reducing overall efficiency, (iii) and the high compressive pressure applied during the sealing of the fuel cell stack can induce mechanical stress on the BPs, leading to fractures and deformation. This compromises the structural integrity and performance of the fuel cell.

For carbon bipolar plate degradation, graphite is the most common material and has been used in a lot of studies. However, graphite BPs have limitations such as low mechanical properties, brittleness, high gas permeability, and high cost, which make them less suitable for long-term use. To overcome these limitations, as already mentioned, researchers have investigated the use of composite

materials, which offers improved mechanical strength, chemical stability, and flexibility. Under operating conditions in PEMFC, the corrosion of carbon in graphite and graphite composite BPs primarily involves the creation of surface oxide and the generation of CO<sub>2</sub> within an acidic environment. Although corrosion is generally not a major concern during regular operation, conditions like start-stop cycles or fuel starvation can exacerbate carbon corrosion [175,196].

On the other hand, metallic BPs offer better conductivity, impermeability, mechanical stability, and ease of machining flow field channels, which make them more suitable for reducing thickness and weight. However, metallic BPs are susceptible to corrosion in the aggressive operating environments such as high temperatures (60-80 °C), and low pH (2-4) and humidity, which leads to increase electrical resistance. Moreover, the metal cations formed during BP corrosion can contaminate the membrane and CLs, significantly impacting fuel cell capacity and durability [175,196, 198]. To mitigate corrosion, additional coating techniques are employed to create a thin protective and electronically conducting layer on the surface of metallic BPs [219]. The more recent researched coating materials for metal BPS are shown in the Table 4.5.

**Table 4.5. Coating materials for metallic BPs and their characteristics. [219].**

<b>Coating Materials</b>	<b>Characteristics</b>
Pure carbon	Corrosion resistance, Electrical conductivity, High residual stress
Doped carbon	Enhanced bonding properties in comparison to pure carbon
Transition-metal carbide (TMC)	Corrosion resistance, Electrical conductivity, High temperature treatment
Conductive polymer	Corrosion resistance, High ICR
Metal nitride	Corrosion resistance, High ICR
Noble metals	Corrosion resistance, High price

The selection of appropriate BP materials plays a crucial role in preventing degradation. While noble metals like platinum (Pt), niobium (Nb), and zirconium (Zr) exhibit excellent corrosion resistance, their high cost limits their widespread use. Aluminum (Al), titanium (Ti), nickel (Ni), and their alloys offer a reliable and cost-effective alternative due to good electrical conductivity, mechanical properties, and lower cost. However, the interface between the BP and GDL can experience interfacial contact resistance (ICR), which reduces fuel cell efficiency. Electrically resistant oxide films on the BP surface contribute to increased ICR and internal electrical resistance within the fuel cell. Corrosion of metallic BP materials also generates cations with multiple charges that can impact the durability of the catalyst and membrane [196,198].

To better understand BP degradation phenomena, researchers have developed approximate models, which consider factors such as BP surface, GDL structure, clamping pressure, carbon fiber deformation of GDL, and BP roughness stiffness to evaluate resistance at each point of contact and assess overall performance. However, the complete modeling of BP corrosion remains challenging, due to the complex

operating conditions of fuel cells, but there are existing corrosion models developed for other components, which can offer insights into BP corrosion by considering relevant parameters [160].

Moreover, to enhance fuel cell performance, it is crucial to consider geometric parameters such as channel length, number of channels, channels height-to-width ratio, rib width, channel depth, and flow direction. For example, the serpentine flow field configuration provides advantages such as improved reactant distribution, enhanced cooling, more uniform current distribution, and prevention of issues like flooding that are often encountered in parallel flow fields [176].

### **4.3.5 Sealing Materials (Gasket)**

The long-term reliability and durability of gaskets are crucial for ensuring overall fuel cell efficiency and durability. Any degradation or failure of gaskets can lead to leakage or mixing of reactants during operation, resulting in reduced fuel cell efficiency and potential safety hazards. Common degradation phenomena of sealing gaskets include the loss of elastic properties, loss of seal functionality, and leakage of seal components, which can contaminate the MEA. An analysis of gasket failure in a PEMFC stack revealed that increased stack temperature, pressure fluctuations, and thermal cycling were contributing factors, leading to gasket failure. Therefore, addressing degradation phenomena related to gaskets is essential to maintain their functionality and prevent component poisoning within the fuel cell system. The degradation phenomena associated with seals in fuel cell applications are generally not well-understood, and there is a limited amount of published research on seal degradation. In the study conducted by Jinzhu Tan et al. [163], the degradation of commercial silicone rubber in the PEMFC environment was investigated. Their findings indicated that chemical degradation plays a significant role in initiating changes in the surface chemistry of gaskets. This degradation process involves de-crosslinking and chain scission within the silicone rubber backbone. The presence of stress in the samples was observed to accelerate the degradation of silicone rubber. Another study showed that with increasing temperature, the degradation of silicone rubber became more pronounced, indicating molecular degradation. Moreover, in the presence of water, the oxygen content on the silicone surface increased, leading to the oxidation of side-chain groups. Over time, as the rubber was exposed to the fuel cell environment, the macromolecules underwent further degradation, resulting in reduced mechanical strength and deteriorated sealing performance of the PEMFC [176, 220].

## **4.4 Water Management**

Water management is a very important parameter for the long-term maintenance of power density and for the maintenance of high efficiency, stable operation, and humidity. Obviously, the performance and lifetime of PEMFC are affected by the accumulation of too much water inside the fuel cell. On the other hand, it is necessary to maintain proper moisture in the membrane, as the protons move in the hydrated parts of the ionomer through the dissolution of sulfonic acid bonds. It

is therefore obvious that the amount of water in the cell must be specific in order not to create problems. Water management is the process that controls the water balance. The water that is removed from the inside of the cell and the water that is transferred or formed inside the cell constitute the water balance. Figure 4.13 shows schematically all mechanisms of water transfer to and from the interior of PEMFC [221].

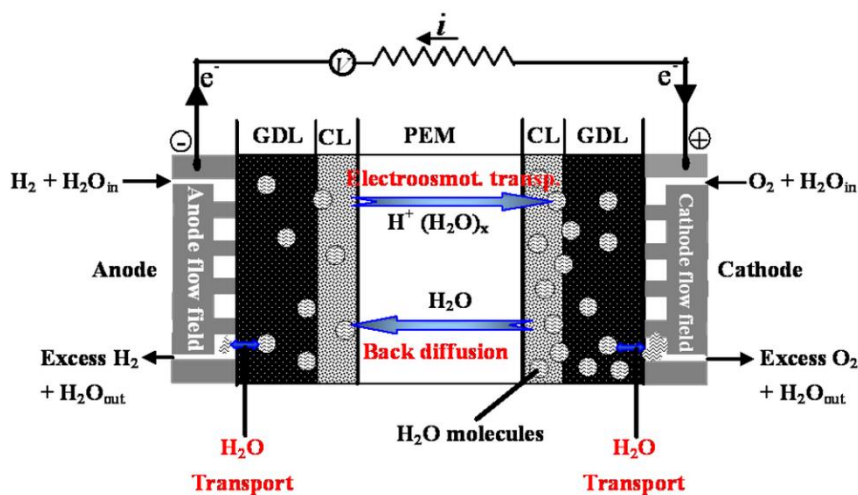


Figure 4.12. Water transport mechanisms inside of PEMFC [222].

As shown in Figure 4.13, water can either enter the fuel cell through humidified gases, or form inside it through the reduction reaction that occurs at the cathode. The removal of water from the interior part of the cell can be done by evaporation into the gas streams and with an outlet as liquid water along with the excess reactants. As shown in Figure 4.13 water transfer takes place between both electrodes, via the membrane. Protons, which migrate through membrane, are surrounded by a certain amount of water molecules. The transportation of protons from the anode side to the cathode is associated with the attraction of water molecules from the anode electrode to the cathode electrode. This water transfer mechanism is called electro-osmotic drag. Conversely, the water transfer mechanism from cathode to anode is called back diffusion. At high current densities the electro-osmotic drag overrides the back diffusion, while the back diffusion overrides the electro-osmotic drag at low current densities. Water management is done by various parts of the cell such as GDM and flow field channels and due to the many water transfer mechanisms, it is a complex process. Inappropriate water management can lead to either fuel cell flooding or dehydration of membrane. These situations have been observed to be devastating to both fuel cell performance and durability [222].

#### 4.4.1 Fuel Cell Flooding

Flooding is the phenomenon of water accumulation within PEMFC and is observed more frequently on the cathode electrode than on the anode electrode, due to the reduction reaction in which water is formed within PEMFC on the cathodic side of the membrane. The excess water blocks the pores of GDM and prevents access of hydrogen and especially oxygen to the catalyst layer. In other words, this phenomenon

increases the mass transfer resistance, leads to gas starvation, and reduces the rate of reactions, with a consequent decrease in cell performance. Flooding can also cause FC resilience issues. Corrosion of cell components such as catalyst layer, gas diffusion media and bipolar plate can be aggravated by the presence of excess water inside the fuel cell. Due to corrosion of bipolar plates, impurities are released inside the cell, which can contaminate the catalyst. Therefore, fuel cell flooding also leads to an increase in Ohmic resistance resulting in a decrease in FC performance [221].

## Cathode flooding

As already mentioned, cathode flooding is easier to observe in a PEMFC, mainly due to the reduction reaction that takes place on the cathodic side of membrane, on which water is formed. As we saw, in figure 4.13 water can enter the interior of the cathode electrode and through other water transfer mechanisms. Therefore, water entry can also be done through electro-osmotic drag, and through the over-humidified oxygen. On the other hand, the removal of water from the cathode electrode can be done through water back-diffusion to the anode, through evaporation and through capillary transfer of liquid water from the gas diffusion layer of the cathode. When the cathode electrode has a higher water content than the anode, the water back-diffusion to the anode occurs, which however has little influence on the cathode's water balance. Mostly only at low current densities manages to impose itself against electro-osmosis. At higher temperatures there is an acceleration of the water evaporation mechanism, while at higher air rates inside the cathode it becomes more active to transport liquid water outside the cell. Therefore, high temperatures, low current density, and high gas flow rate accelerate the removal of water from the FC [221]. Figure 4.14 below shows the influence of cathode flooding on PEMFC performance when operating below 51°C with a hydrogen and air flow rate of 2.0 A/cm<sup>2</sup> and 2.8 A/cm<sup>2</sup> respectively [223].

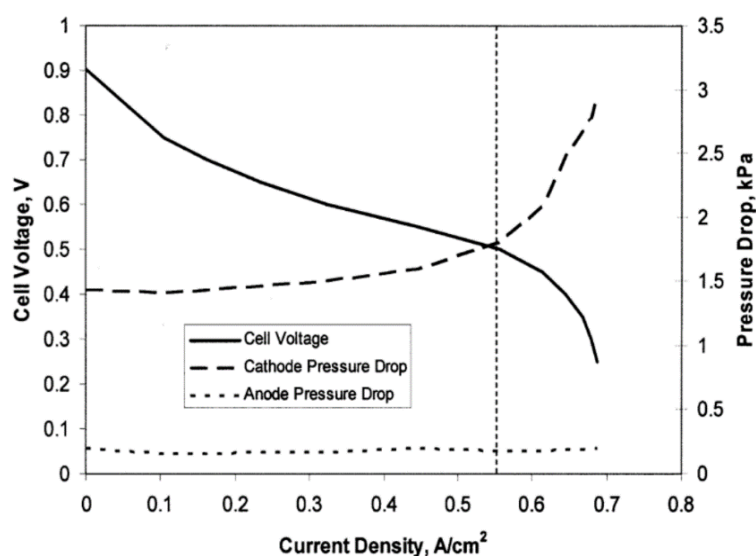


Figure 4.13. Effect of cathode flooding on PEMFC performance [223].

As shown in figure 4.14 the cathode flooding phenomenon causes by increasing current density, an increase in pressure drops with a consequent decrease in cell potential [222].

### **Anode flooding**

It takes much longer in order to observe the phenomenon of anode flooding. Under low power densities, as we have mentioned, the phenomenon of water back-diffusion to the anode prevails over electro-osmosis. In addition, at low operating temperatures of the cell, the evaporation of water is slowed down. Therefore, low operating temperatures and low current densities are worsening parameters of anode flooding. This phenomenon may occur much more rarely than cathode flooding, but it can cause disastrous consequences for FC. Fuel starvation and the corrosion of supporting carbon are consequences caused by anode flooding and can affect the performance and durability of PEMFC negatively [200].

### **Flow field channels flooding**

Flow field channels flooding has also been observed as a result of poor water management. The overflow of the flow channels can prevent the reactant gases from reaching the gas diffusion layers and then the catalyst layers (reactant starvation) by reducing the efficiency of the fuel cell. Even when multiple flow field channels are used, the flooding of a flow channel could create localized reactant starvation, with a consequent reduction in performance [200].

#### **4.4.2 Dehydration of Membrane**

As mentioned in subsection 4.3.2, membrane dehydration can significantly affect FC performance and resistance. This phenomenon is most often observed on the anodic side of the membrane. Poor water management can lead to dehydration of the membrane. Parameters such as the low relative humidity (RH) of the reactant gases, the high-power density, the high operating temperature, and the inability of the reduction reaction to compensate for the dewatering mechanisms, cause the membrane to become dehydrated. As mentioned earlier, during the operation of the cell under these conditions, the water evaporates very quickly, the electro-osmotic drag prevails over the water back-diffusion to the anode, and the flow of the reactant gases is quite dry, resulting in the elements of the anode being dehydrated. In addition, the pores of a dehydrated membrane shrink, resulting in lower rates of water back-diffusion to the anode.

As a result of the drying of the membrane, an increase in ionic resistance is caused since the conductivity of the protons of the membrane is directly related to its water content. Therefore, with the reduction of the water content of the membrane, the Ohmic losses increase, resulting in a significant reduction of the cell's potential, with a consequent decrease in power, which can however be regained by rewetting the membrane. However, operating the cell with a dehydrated membrane for a long time may lead to irreversible damage as described in subsection 4.3.2 [200,224].

## 4.5 Thermal Management

Since the operating temperature of PEMFC influences important parameters such as ionic conductivity and electrochemical activity and can play a regulatory role in water management, thermal management is a key parameter influencing the performance and durability of fuel cells. The operation of PEMFC at very low or very high temperatures can adversely affect it [200]. When PEMFC is exposed to frost temperatures, thermal management is especially important. In subsection 4.2.1 we saw that when a deactivated fuel cell is exposed for a long time to subzero temperatures, there are problems of durability. Components such as GDLs, membranes, and CLs are subject to mechanical stress during cooling/thaw cycles and as a result can be mechanically damaged. The resulting mechanical failure can cause an increase in thermal and electrical resistances, since the aforementioned layers will have detached due to ice formation [221]. In addition, Chan et al. showed that by lowering the operating temperature from 80°C to 30°C, the ionic resistance of a Nafion membrane can increase by up to 30%. Since the ionic resistance of the membrane is directly related to the performance of the cell the decrease in operating temperature causes a decrease in the performance of PEMFC [225]. On the other hand, at high operating temperatures it has been observed that PEMFCs have several advantages. Initially, the kinetics of reactions at high temperatures seem to be better. In addition, water management and cooling are improved, and waste heat can be recovered. An important advantage of the increase in operating temperature is the increase in the tolerance of PEMFC to CO. Increasing the tolerance to CO enables the cell to be supplied with low purity hydrogen, thus greatly reducing the operating costs of PEMFC. Despite the various advantages of PEMFC at operating temperatures above 100°C, its various components exhibit chemical instability and therefore their degradation is pronounced with consequent degradation of performance and strength [221]. Figure 4.15 presents a polarization diagram, comparing the performance of a high temperature PEMFC, operating at 200°C, and a low temperature PEMFC, operating at 80°C, and it appears that the performance is ultimately greater at lower operating temperatures [224].

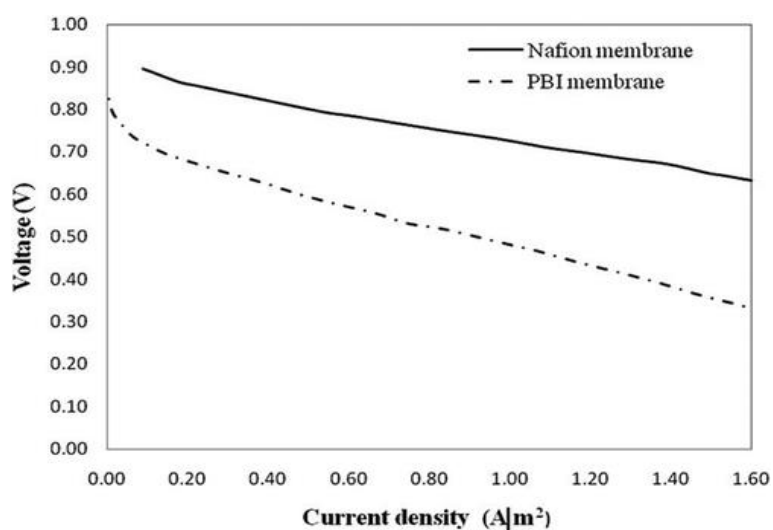


Figure 4.14. Polarization curve for HTPEMFC (PBI membrane) and for LTPEMFC (Nafion membrane) [224].

Therefore, according to what we have already mentioned, an optimum operating temperature range, in which the maximum output voltages are observed and the FC strength is not significantly degraded, is the temperatures between 60°C and 80°C for low temperature PEMFCs [224].

### 4.5.1 Cooling Methods

The redox reactions taking place on the anode and cathode electrodes are exothermic reactions. This means that during the production of electricity, heat is also produced as a by-product of these electrochemical reactions. In fact, it has been observed that more than half of the total chemical energy contained in hydrogen is converted into heat. Therefore, thermal management is necessary to maintain operating temperatures between 60°C and 80°C [224]. Reddy et al. reported that with the appropriate cooling method, the temperature variation may be less than 20°C [226]. Figure 4.16 below shows the available cooling methods divided into two categories, active cooling techniques and passive techniques.

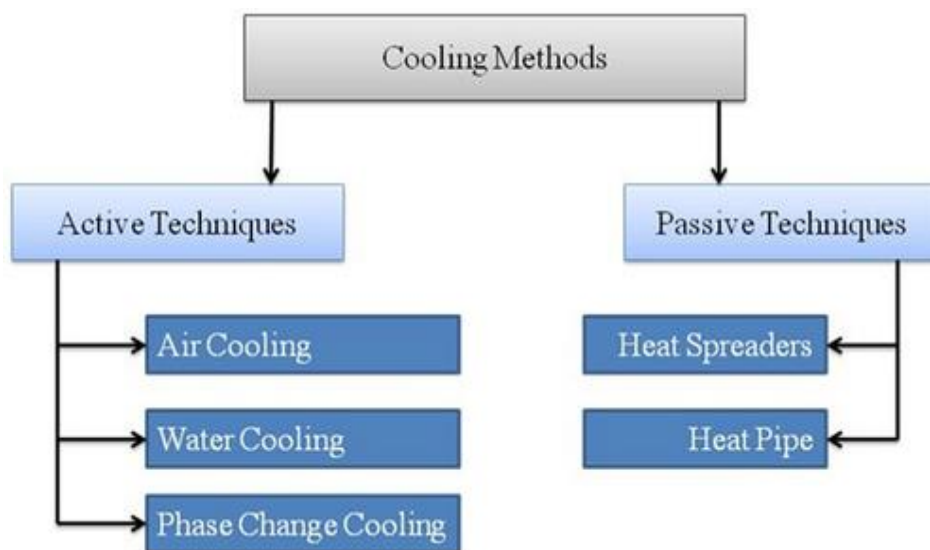


Figure 4.15. Cooling methods of PEMFC [224].

Active cooling techniques rely on devices that require input power to function. That is, it is necessary to consume electricity from an external source to cool PEMFC. On the other hand, devices in passive cooling techniques do not require electricity consumption for their operation. Finally, the choice of the appropriate cooling technique is made based on the size of the PEMFCs, the cost, the operating conditions, etc. in order to maintain the temperature in the optimal operating range [224].

## Chapter 5

### CONCLUSION

In today's world, the demand for energy is consistently increasing due to factors such as improved quality of life, rapid industrialization, and the growing global population. This heightened energy consumption has prompted the search for cleaner and more sustainable energy solutions, as the availability of traditional fossil fuels becomes increasingly limited, and their production contributes significantly to pollution and climate change. As a result, researchers have been exploring renewable energy sources that harness the power of sunlight, wind, and waves. However, the intermittent nature of these energy sources necessitates the development of efficient energy storage systems.

One particularly promising and sustainable option is the conversion of chemical energy into electricity using specialized devices such as batteries, capacitors, and fuel cells. These electrochemical devices offer advantages in terms of energy efficiency, environmental friendliness, and versatility. In this thesis, we focused on fuel cells and conducted an in-depth study of their working principles and the factors that can degrade their construction.

Fuel cells are devices that use hydrogen as a fuel to produce electricity through an electrochemical reaction. They offer several advantages, including high efficiency, zero-emission operation, and quiet operation. Hydrogen, the fuel used in fuel cells, can be generated through various methods, including hydrocarbon reforming and water electrolysis. These methods provide a sustainable and clean source of hydrogen, ensuring the overall environmental friendliness of fuel cell systems.

However, despite the numerous benefits offered by fuel cells, their commercialization faces challenges related to durability, cost, and infrastructure development. The long-term performance and durability of fuel cells are influenced by factors such as material degradation, operating conditions, water management, and thermal management. Understanding and addressing these factors are crucial for enhancing the reliability, lifespan, and cost-effectiveness of fuel cell systems. Material degradation is a significant concern in fuel cells, as the components of the cell, including the membrane, catalyst, and bipolar plates, can degrade over time due to chemical reactions, mechanical stress, and exposure to harsh operating conditions. Effective material selection and design strategies are essential to mitigate degradation and ensure long-term performance.

Optimizing operating conditions is another important aspect. Factors such as temperature, humidity, gas composition and startup/shutdown cycles must be carefully controlled to prevent accelerated degradation and ensure efficient operation. Temperature control is essential in fuel cell systems. Operating within the appropriate temperature range ensures efficient electrochemical reactions and

minimizes material degradation. Maintaining optimal temperature levels also promotes faster reaction kinetics and enhances overall energy conversion efficiency. Furthermore, temperature control helps to prevent thermal stresses that can lead to mechanical failure or degradation of cell components.

Humidity management is another critical aspect of fuel cell operation. The proper balance of humidity is essential for maintaining the hydration levels of the electrolyte and electrode materials within the cell. Excessive humidity can cause flooding, where the electrolyte becomes oversaturated with water, impeding reactant transport and reducing the cell's performance. On the other hand, insufficient humidity can result in membrane dehydration, leading to decreased proton conductivity and overall cell efficiency. Precise control of humidity levels, often achieved through the use of humidification and water management systems, is necessary for optimal fuel cell performance.

Controlling the gas composition is equally important. The proper supply and ratio of fuel and oxidant gases, such as hydrogen and oxygen or air, are critical for achieving efficient electrochemical reactions. Deviations from the optimal gas composition can lead to incomplete reactions, reduced cell voltage, and accelerated degradation of the catalyst and other cell components. Advanced gas delivery systems, gas sensors, and feedback control mechanisms are employed to ensure precise and continuous monitoring and adjustment of the gas composition within fuel cells.

Thermal management is crucial for maintaining temperature uniformity within the fuel cell stack and preventing thermal stresses that can damage the components. Effective heat dissipation and temperature control systems are necessary to ensure optimal performance and prevent premature failure.

Furthermore, the cost and infrastructure associated with fuel cells need to be addressed for widespread adoption. Research and development efforts are focused on reducing the production cost of fuel cell systems, improving their scalability, and establishing the necessary infrastructure for hydrogen production, storage, and distribution.

## References

- [1] P.A. Østergaard, N. Duic, Y. Noorollahi, H. Mikulcic, S. Kalogirou. Sustainable development using renewable energy technology, *Renewable Energy* 146, 2430-2437, 2020. Available: <https://doi.org/10.1016/j.renene.2019.08.094>.
- [2] International Energy Agency (IEA), 2016.
- [3] E. Richard, Sadik-Zada. Political Economy of Green Hydrogen Rollout: A Global Perspective *Sustainability* 13.23, 13464, 2021. Available: <https://doi.org/10.3390/su132313464>.
- [4] "What is hydrogen and how is it made?" *The World of Hydrogen*. Available: <https://www.theworldofhydrogen.com/gasunie/what-is-hydrogen/>.
- [5] C.M. Kalamaras and A.M. Efstathiou. Hydrogen Production Technologies: Current State and Future Developments, Conference Paper, 2013.
- [6] Βασικές έννοιες και αρχές της ηλεκτροχημείας. Α. Ηλεκτροχημική κυψέλη, 2018.
- [7] Electrochemical Cells, Chemistry LibreTexts, 2020. Available: <https://chem.libretexts.org/@go/page/41636>.
- [8] R. Seeber, C.Zanardi, and G. Inzelt. Links between electrochemical thermodynamics and kinetics, *ChemTexts*, 18, 1-16 2015. Available: <https://doi.org/10.1007/s40828-015-0018-9>.
- [9] V.S. Bagotsky. Fundamentals of Electrochemistry (Second Edition), The Electrochemical Society Series, 33-50, 2005.
- [10] R. Wu, P. Tsiakaras, P.K.Shen. Facile synthesis of bimetallic Pt-Pd symmetry-broken concave nanocubes and their enhanced activity toward oxygen reduction reaction, *Applied Catalysis B: Environmental*, 251, 49-56, 2019.
- [11] N. Chouhan and R.S. Liu. Electrochemical Technologies for Energy Storage and Conversion, 1-5, 2011.
- [12] K. Scott. An Introduction to microbial Fuel Cells, *Microbial Electrochemical and Fuel Cells: Fundamentals and Applications*, 4-9, 2015.
- [13] S. Li, Z.Q. Tian, Y. Liu, Z. Jang, S.W. Hasan, X. Chen, P. Tsiakaras. P.K. Shen. Hierarchically skeletal multi-layered Pt-Ni nanocrystals for highly efficient oxygen reduction and methanol oxidation reactions, *Chinese Journal of Catalysis*, 42.4, 648-657, 2021.
- [14] R. O' Hayre, S.W. Cha, W.G. Colella, F.B. Prinz. *Fuel Cells Fundamentals*, 1-3 2016.
- [15] Z. Chen, C. Hao, B. Yan, Q. Chen, H. Feng, X. Mao, J. Cen, Z.Q. Tian, P. Tsiakaras, P.K. Shen, ZIF-Mg(OH)<sub>2</sub> Dual Template Assisted Self-Confinement of Small PtCo NPs as Promising Oxygen Reduction Reaction in PEM Fuel Cell, *Advanced Energy Materials* 12.32, 2201600, 2022.
- [16] F. Barbir. Main Cell Components, Material Properties, and Processes, *PEM Fuel Cells: Theory and Practice*, 70-72, 2012.
- [17] R. O' Hayre, S.W. Cha, W.G. Colella, F.B. Prinz. *Fuel Cells Fundamentals*, 3-23 2016.
- [18] C. Molochas, P. Tsiakaras. Carbon Monoxide Tolerant Pt-Based Electrocatalysts for H<sub>2</sub>-PEMFC Applications: Current Progress and Challenges, *Catalysts* 11.9, 1127, 2021.
- [19] Y. Wang, C. He, A. Brouzgou, Y. Liang, R. Fu, D. Wu, P. Tsiakaras, S. Song. A facile soft-template synthesis of ordered mesoporous carbon/tungsten carbide composites with high surface area for methanol electrooxidation, *Journal of Power Sources*, 200, 8-13, 2012.
- [20] T. Najam, S.S.A. Shah, S. Ibraheem, X. Cai, E. Hussain, S. Suleman, M.S. Javed, P. Tsiakaras. Single-atom catalysis for zinc-air/O<sub>2</sub> batteries, water electrolyzers and fuel cells applications *Energy Storage Materials* 45, 504-540, 2022.

- [21] N. Chouhan and R. Liu. *Electrochemical Technologies for Energy Storage and Conversion*, 32-37, 2011.
- [22] M.C. Pera, D. Hissel, H. Gualous, C. Turpin. *Fuel Cells, Electrochemical Components*, 110-120, 2013.
- [23] D. Medvedev, V. Maragou, E. Pikalova, A. Demin, P. Tsiakaras. Novel composite solid state electrolytes on the base of BaCeO<sub>3</sub> and CeO<sub>2</sub> for intermediate temperature electrochemical devices, *Journal of Power Sources*, 221, 217-227, 2013.
- [24] J. Lyagaeva, D. Medvedev, A. Demin, P. Tsiakaras. Insights on thermal and transport features of BaCe<sub>0.8-x</sub>Zr<sub>x</sub>Y<sub>0.2</sub>O<sub>3-δ</sub> proton-conducting materials, *Journal of Power Sources*, 278, 436-444, 2015.
- [25] L. Carrette Dr., K. Andreas Friedrich Dr., U. Stimming Prof. Dr. *Fuel Cells: Principles, Types, Fuels, and Applications*, ChemPhysChem, 1.4, 162-193, 2000. Available: [https://doi.org/10.1002/1439-7641\(20001215\)1:4<162::AID-CPHC162>3.0.CO;2-Z](https://doi.org/10.1002/1439-7641(20001215)1:4<162::AID-CPHC162>3.0.CO;2-Z).
- [26] G.M. Andreadis, A.K. Podias, P. Tsiakaras. The effect of the parasitic current on the direct ethanol PEM fuel cell operation, *Journal of Power Sources*, 181,2, 214-227, 2008.
- [27] S. Song, V. Maragou, P. Tsiakaras. How far are direct alcohol fuel cells from our energy future? *J. Fuel Cell Sci. Technol.*, 4.2, 203-209, 2007.
- [28] F. Coutelieris, S. Douvartzides, P. Tsiakaras. The importance of the fuel choice on the efficiency of a solid oxide fuel cell system, *Journal of Power Sources*, 123.2, 200-205, 2003.
- [29] X. Li, Y. Huang, Z. Chen, S. Hu, J. Zhu, P. Tsiakaras, P.K. Shen. Novel PtNi nanoflowers regulated by a third element (Rh, Ru, Pd) as efficient multifunctional electrocatalysts for ORR, MOR, and HER, *Chemical Engineering Journal*, 454, 140131, 2023.
- [30] C. Molochas, P. Tsiakaras. Carbon Monoxide Tolerant Pt-Based Electrocatalysts for H<sub>2</sub>-PEMFC Applications: Current Progress and Challenges, *Catalysts* 11.9, 1127, 2021.
- [31] S.S. Shah, T. Najam, M.S Javed, M.M Rahman, P. Tsiakaras. Novel Mn-/Co-N x Moieties Captured in N-Doped Carbon Nanotubes for Enhanced Oxygen Reduction Activity and Stability in Acidic and Alkaline Media, *ACS Applied Materials & Interfaces*, 13.19, 23191-23200, 2021.
- [32] X. Li, Y. Liu, J. Zhu, P. Tsiakaras, P.K. Shen. Enhanced oxygen reduction and methanol oxidation reaction over self-assembled Pt-M (M= Co, Ni) nanoflowers, *Journal of Colloid and Interface Science*, 607, 1411-1423, 2022.
- [33] S.A. Grigoriev, V.I. Porembsky, V.N. Fateev. Pure hydrogen production by PEM electrolysis for hydrogen energy, *International Journal of Hydrogen Energy*, 31.2, 171-175, 2006. Available: <https://doi.org/10.1016/j.ijhydene.2005.04.038>.
- [34] L. Zhang, J. Lu, S. Yin, L. Luo, S. Jing, A. Brouzgou, J. Chen, P.K. Shen, P. Tsiakaras. One-pot synthesized boron-doped RhFe alloy with enhanced catalytic performance for hydrogen evolution reaction, *Applied Catalysis B: Environmental*, 230, 58-64, 2018.
- [35] M.C. Pera, D. Hissel, H. Gualous, C. Turpin. *Water Electrolyzers, Electrochemical Components*, 90-95, 2013.
- [36] M.M. Rashid, M.K. Al Mesfer, H. Naseem, M. Danish. Hydrogen Production by Water Electrolysis: A Review of Alkaline Water Electrolysis, PEM Water Electrolysis and High Temperature Water Electrolysis, *International Journal of Engineering and Advanced Technology (IJEAT)*, 4.3, 2015.
- [37] S.S. Shah, N.A. Khan, M. Imran, M. Rashid, M.K. Tufail, A. Rehman, P. Tsiakaras. Recent Advances in Transition Metal Tellurides (TMTs) and Phosphides (TMPs) for Hydrogen Evolution Electrocatalysis, *Membranes*, 13.1, 113, 2023.

- [38] Z. Xie, Z. Song, J. Zhao, Y. Li, X. Cai, D. Liu, J. Shen, P. Tsiakaras. CuZr Metal Glass Powder as Electrocatalysts for Hydrogen and Oxygen Evolution Reactions, *Catalysts*, 12.11, 1378, 2022.
- [39] W. Xie, J. Huang, L. Huang, S. Geng, S. Song, P. Tsiakaras. Y Wang Novel fluorine-doped cobalt molybdate nanosheets with enriched oxygen-vacancies for improved oxygen evolution reaction activity, *Applied Catalysis B: Environmental*, 303, 120871, 2022.
- [40] B. Zhang, J. Shan, W. Wang, P. Tsiakaras. Y. Li Oxygen Vacancy and Core–Shell Heterojunction Engineering of Anemone-Like CoP@ CoOOH Bifunctional Electrocatalyst for Efficient Overall Water Splitting, *Small*, 18.12, 2106012, 2022.
- [41] D. Liu, Z. Song, S. Cheng, Y. Wang, A. Saad, S. Deng, J. Shen, X. Huang, P. Tsiakaras. Mesoporous IrNiTa metal glass ribbon as a superior self-standing bifunctional catalyst for water electrolysis, *Chemical Engineering Journal*, 431, 134210, 2022.
- [42] A. Saad, Y. Gao, K.A. Owusu, W. Liu, Y. Wu, A. Ramiere, H. Guo, P. Tsiakaras. Ternary Mo<sub>2</sub>NiB<sub>2</sub> as a Superior Bifunctional Electrocatalyst for Overall Water Splitting, *Small*, 18.6, 2104303, 2022.
- [43] A. Saad, D. Liu, Y. Wu, Z. Song, Y. Li, N. Tayyaba, K. Zong, P. Tsiakaras, X. Cai. Ag nanoparticles modified crumpled borophene supported Co<sub>3</sub>O<sub>4</sub> catalyst showing superior oxygen evolution reaction (OER) performance, *Applied Catalysis B: Environmental*, 298, 120529, 2021.
- [44] J. Cen, E. Jiang, Y. Zhu, Z. Chen, P. Tsiakaras, P.K. Shen. Enhanced electrocatalytic overall water splitting over novel one-pot synthesized Ru–MoO<sub>3-x</sub> and Fe<sub>3</sub>O<sub>4</sub>–NiFe layered double hydroxides on Ni foam, *Renewable Energy*, 177, 1346-13, 2021.
- [45] A. Ursua, L.M. Gandia, P. Sanchis. Hydrogen Production from Water Electrolysis: Current Status and Future Trends, *Proceedings of the IEEE*, 100.2, 410-426, 2012.
- [46] J. Lu, Z. Tang, L. Luo, S. Yin, P.K. Shen, P. Tsiakaras, Worm-like S-doped RhNi alloys as highly efficient electrocatalysts for hydrogen evolution reaction, *Applied Catalysis B: Environmental*, 255, 117737, 2019.
- [47] S. Jing, D. Wang, S. Yin, J. Lu, P.K. Shen, P. Tsiakaras. P-doped CNTs encapsulated nickel hybrids with flower-like structure as efficient catalysts for hydrogen evolution reaction, *Electrochimica Acta*, 298, 142-149, 2019.
- [48] P. Xu, L. Qiu, L. Wei, Y. Liu, D. Yuan, Y. Wang, P. Tsiakaras. Efficient overall water splitting over Mn doped Ni<sub>2</sub>P microflowers grown on nickel foam, *Catalysis Today*, 355, 815-821, 2020.
- [49] C. Yu, J. Lu, L. Luo, F. Xu, P.K. Shen, P. Tsiakaras, S Yin, Bifunctional catalysts for overall water splitting: CoNi oxyhydroxide nanosheets electrodeposited on titanium sheets, *Electrochimica Acta*, 301, 449-45, 2019.
- [50] L. Yan, B. Zhang, J. Zhu, Y. Li, P. Tsiakaras, P.K. Shen. Electronic modulation of cobalt phosphide nanosheet arrays via copper doping for highly efficient neutral-pH overall water splitting, *Applied Catalysis B: Environmental*, 265, 118555, 2020.
- [51] B. Zhang, J. Shan, W. Wang, P. Tsiakaras, Y. Li. Oxygen Vacancy and Core–Shell Heterojunction Engineering of Anemone-Like CoP@ CoOOH Bifunctional Electrocatalyst for Efficient Overall Water Splitting, *Small*, 2106012, 2022.
- [52] W. Xie, J. Huang, L. Huang, S. Geng, S. Song, P. Tsiakaras. Y. Wang. Novel fluorine-doped cobalt molybdate nanosheets with enriched oxygen-vacancies for improved oxygen evolution reaction activity, *Applied Catalysis B: Environmental*, 303, 120871, 2022.
- [53] S. Jing, P. Ding, Y. Zhang, H. Liang, S. Yin, P. Tsiakaras. Lithium-sulfur battery cathodes made of porous biochar support CoFe@ NC metal nanoparticles derived from Prussian blue analogues, *Ionics*, 25.11, 5297-5304, 2019.

- [54] S. Jing, Y. Zhang, F. Chen, H. Liang, S. Yin, P. Tsiakaras. Novel and highly efficient cathodes for Li-O<sub>2</sub> batteries: 3D self-standing NiFe@ NC-functionalized N-doped carbon nanonet derived from Prussian blue analogues/biomass composites, *Applied Catalysis B: Environmental*, 245, 721-732, 2019.
- [55] H. Liang, Y. Zhang, F. Chen, S. Jing, S. Yin, P. Tsiakaras. A novel NiFe@ NC-functionalized N-doped carbon microtubule network derived from biomass as a highly efficient 3D free-standing cathode for Li-CO<sub>2</sub> batteries, *Applied Catalysis B: Environmental*, 244, 559-567, 2019.
- [56] H. Liang, F. Chen, M. Zhang, S. Jing, B. Shen, S. Yin, P. Tsiakaras. Highly performing free standing cathodic electrocatalysts for Li-O<sub>2</sub> batteries: CoNiO<sub>2</sub> nanoneedle arrays supported on N-doped carbon nanonet, *Applied Catalysis A: General*, 574, 114-121, 2019.
- [57] G. Zhang, Y. Shi, H. Wang, L. Jiang, X. Yu, S. Jing, S. Xing, P. Tsiakaras. A facile route to achieve ultrafine Fe<sub>2</sub>O<sub>3</sub> nanorods anchored on graphene oxide for application in lithium-ion battery, *Journal of Power Sources*, 416, 118-124, 2019.
- [58] H. Liang, Z. Gai, F. Chen, S. Jing, W. Kan, B. Zhao, S. Yin, P. Tsiakaras. Fe<sub>3</sub>C decorated wood-derived integral N-doped C cathode for rechargeable Li-O<sub>2</sub> batteries, *Applied Catalysis B: Environmental*, 324, 122203, 2023.
- [59] C. Witt. *Batteries 101* B&H eXplora, 2018.
- [60] A.R. Dehghani-Sani, E. Tharumalingam, M.B. Dusseault, R. Fraser. Study of energy storage systems and environmental challenges of batteries, *Renewable and Sustainable Energy Reviews*, 104, 192-208, 2019. Available: <https://doi.org/10.1016/j.rser.2019.01.023>.
- [61] R.M. Dell. Batteries: fifty years of materials development, *Solid State Ionics*, 134.1-2, 139-158, 2000. Available: [https://doi.org/10.1016/S0167-2738\(00\)00722-0](https://doi.org/10.1016/S0167-2738(00)00722-0).
- [62] J. Collins, G. Gourdin, D. Qu. Chapter 3.23 - Modern applications of Green Chemistry: Renewable Energy, *Green Chemistry*, 771-860, 2018.
- [63] R. Dell, David Anthony James Rand. *Understanding Batteries*, 53-67, 2001.
- [64] R. Dell, David Anthony James Rand. *Understanding Batteries*, 70-79, 2001.
- [65] R. Dell, David Anthony James Rand. *Understanding Batteries*, 100-105, 2001.
- [66] *A Guide to Sealed Lead Acid Battery Construction* Power Sonic, 2021.
- [67] R. Dell, David Anthony James Rand, *Understanding Batteries*, (2001) 126-141.
- [68] I. Buchmann. *Nickel Based Batteries*, Battery University, 2021.
- [69] R. Dell, David Anthony James Rand, *Understanding Batteries*, 143-158, 2001.
- [70] A. Bhatt, R. Withers, G. Wang. *Lithium-ion batteries*, Australian Academy of Science, 2016.
- [71] T. Najam, S.S. Shah, L. Peng, M.S. Javed, M. Imran, M.Q. Zhao, P. Tsiakaras. Synthesis and nano-engineering of MXenes for energy conversion and storage applications: Recent advances and perspectives, *Coordination Chemistry Reviews*, 454, 214339, 2022.
- [72] S.S. Shah, T. Najam, A. Brouzgou, P. Tsiakaras. Alkaline Oxygen Electrocatalysis for Fuel Cells and Metal-Air Batteries, *Encyclopedia of Electrochemistry*; Wiley-VCH Verlag GmbH & Co, 9, 1-28, 2017.
- [73] H. Liang, X. Gong, L. Jia, F. Chen, Z. Rao, S. Jing, P. Tsiakaras. Highly efficient Li-O<sub>2</sub> batteries based on self-standing NiFeP@ NC/BC cathode derived from biochar supported Prussian blue analogues, *Journal of Electroanalytical Chemistry*, 867, 114124, 2020.

- [74] D. Lyu, S. Yao, A. Ali, Z.Q. Tian, P. Tsiakaras, PK Shen. N, S Codoped Carbon Matrix-Encapsulated Co<sub>9</sub>S<sub>8</sub> Nanoparticles as a Highly Efficient and Durable Bifunctional Oxygen Redox Electrocatalyst for Rechargeable Zn–Air Batteries, *Advanced Energy Materials*, 2101249, 2021.
- [75] Y. Li, S.H. Talib, D. Liu, K. Zong, A. Saad, Z. Song, J. Zhao, W. Liu, F. Liu, Q. Ji, P. Tsiakaras. Improved oxygen evolution reaction performance in Co<sub>0.4</sub>Mn<sub>0.6</sub>O<sub>2</sub> nanosheets through Triple-doping (Cu, P, N) strategy and its application to Zn-air battery, *Applied Catalysis B: Environmental*, 320, 122023, 2023.
- [76] S. Jing, Z. Gai, M. Li, S. Tang, S. Ji, H. Liang, F. Chen, S. Yin, P. Tsiakaras. Enhanced electrochemical performance of a Li-O<sub>2</sub> battery using Co and N co-doped biochar cathode prepared in molten salt medium, *Electrochimica Acta*, 410, 140002, 2022.
- [77] A. Saad, Y. Gao, A. Ramiere, T. Chu, G. Yasin, Y. Wu, S. Ibraheem, M. Wang, P. Tsiakaras. Understanding the Surface Reconstruction on Ternary W<sub>x</sub>CoB<sub>x</sub> for Water Oxidation and Zinc–Air Battery Applications, *Small*, 18.17, 2201067, 2022.
- [78] H. Liang, L. Jia, F. Chen, S. Jing, P. Tsiakaras. A novel efficient electrocatalyst for oxygen reduction and oxygen evolution reaction in Li-O<sub>2</sub> batteries: Co/CoSe embedded N, Se co-doped carbon, *Applied Catalysis B: Environmental*, 317, 121698, 2022.
- [79] R. Drummond, C. Huang, P.S. Grant, S.R. Duncan. Overcoming diffusion limitations in supercapacitors using layered electrodes, *Journal of Power Sources* 433, 126579, 2019. Available: <https://doi.org/10.1016/j.jpowsour.2019.04.107>.
- [80] S. Zhang, N. Pan, S. Pan. Review of Supercapacitor Performance Evaluation, *Advanced Energy Materials Supercapacitor Performance Evaluation*, 5.6, 2014. Available: <https://doi.org/10.1002/aenm.201401401>.
- [81] A. González, E. Goikolea, J.A. Barrena, and R. Mysyk. Review on supercapacitors: Technologies and materials, *Renewable and Sustainable Energy Reviews*, 58, 1189-1206, 2016. Available: <https://doi.org/10.1016/j.rser.2015.12.249>.
- [82] B.K. Kim, S. Sy, A. Yu, J. Zhang. Electrochemical Supercapacitors for Energy Storage and Conversion, *Handbook of Clean Energy Systems*, 1-25, 2015. Available: <https://doi.org/10.1002/9781118991978.hces112>.
- [83] M. Yaseen, M.A. Khattak, M. Humayun, M. Usman, S.S. Shah, S. Bibi, B.S. Hasnain, S.M. Ahmad, A. Khan, N. Shah, A.A. Tahir, and H. Ullah. A Review of Supercapacitors: Materials Design, Modification, and Applications, *Energies*, 14.22, 7779, 2021. Available: <https://doi.org/10.3390/en14227779>.
- [84] M.S. Halper, J.C. Ellenbogen. Supercapacitors: A brief overview, The MITRE Corporation, McLean, Virginia, USA, 2006.
- [85] J. Libich, J. Máca, J. Vondrák, O. Čech, M. Sedlaříková. Supercapacitors: Properties and applications, *Journal of Energy Storage*, 17, 224-227, 2018. Available: <https://doi.org/10.1016/j.est.2018.03.012>.
- [86] Y. Yang, Y. Han, W. Jiang, Y. Zhang, Y. Xu, and A.M. Ahmed. Application of the Supercapacitor for Energy Storage in China: Role and Strategy, *Energies*, 12.1, 354, 2021. Available: <https://doi.org/10.3390/app12010354>.
- [87] P. Forouzandeh, V. Kumaravel, S.C. Pillai. Electrode Materials for Supercapacitors: A Review of Recent Advances, *Catalysts* 10.9, 969, 2020. Available: <https://doi.org/10.3390/catal10090969>.
- [88] L.A. Dunyushkina, A.A. Pankratov, V.P. Gorelov, A. Brouzgou, P. Tsiakaras. Deposition and Characterization of Y-doped CaZrO<sub>3</sub> Electrolyte Film on a Porous SrTi<sub>0.8</sub>Fe<sub>0.2</sub>O<sub>3-δ</sub> Substrate, *Electrochimica Acta*, 202, 39-46, 2016.

- [89] A. Kalyakin, G. Fadeyev, A. Demin, E. Gorbova, A. Brouzgou, A. Volkov, P. Tsiakaras. Application of Solid oxide proton-conducting electrolytes for amperometric analysis of hydrogen in H<sub>2</sub>+N<sub>2</sub>+H<sub>2</sub>O gas mixtures, *Electrochimica Acta*, 141, 120-125, 2014.
- [90] G. Fadeyev, A. Kalyakin, A. Demin, A. Volkov, A. Brouzgou, P. Tsiakaras. Electrodes for solid electrolyte sensors for the measurement of CO and H<sub>2</sub> content in air, *International Journal of Hydrogen Energy*, 38.30, 13484-13490, 2013.
- [91] G. Balkourani, T. Damartzis, A. Brouzgou, P. Tsiakaras. Cost effective synthesis of graphene nanomaterials for non-enzymatic electrochemical sensors for glucose: a comprehensive review, *Sensors*, 22.1, 355, 2022.
- [92] E. Gorbova, F. Tzorbatzoglou, C. Molochas, D. Chloros, A. Demin, P. Tsiakaras. Fundamentals and Principles of Solid-State Electrochemical Sensors for High Temperature Gas Detection, *Catalysts*, 12.1, 1, 2022.
- [93] A. Kalyakin, A. Demin, E. Gorbova, A. Volkov, P. Tsiakaras. Combined amperometric-potentiometric oxygen sensor, *Sensors and Actuators B: Chemical*, 313, 127999, 2020.
- [94] T. Aldhafeeri, M.K. Tran, R. Vrolyk, M. Pope, and M. Fowler. A Review of Methane Gas Detection Sensors: Recent Developments and Future Perspectives, *Inventions*, 5.3, 28, 2020. Available: <https://doi.org/10.3390/inventions5030028>.
- [95] U. Guth, W. Vonau and J. Zosel. Recent developments in electrochemical sensor application and technology—a review, *Measurement Science and Technology*, 20.4, 2009. Available: <https://doi.org/10.1088/0957-0233/20/4/042002>.
- [96] N.R. Stradiotto, H. Yamanaka, and M.V.B. Zanoni. Electrochemical Sensors: a powerful tool in analytical chemistry, *Journal of the Brazilian Chemical Society*, 14.2, 2003. Available: <https://doi.org/10.1590/S0103-50532003000200003>.
- [97] J.R. Stetter, W.R. Penrose, and S. Yao. Sensors, Chemical Sensors, Electrochemical Sensors, and ECS, *Journal of The Electrochemical Society*, 150.2, 11-16, 2013. Available: <https://doi.org/10.1149/1.1539051>.
- [98] A. Demin, E. Gorbova, A. Brouzgou, A. Volkov, P. Tsiakaras. Sensors based on solid oxide electrolytes, *Solid Oxide-Based Electrochemical Devices*, 167-215, 2020.
- [99] A. Kalyakin, A. Volkov, A. Demin, E. Gorbova, P. Tsiakaras. Determination of nitrous oxide concentration using a solid-electrolyte amperometric sensor, *Sensors and Actuators B: Chemical*, 297, 126750, 2019.
- [100] A. Volkov, E. Gorbova, A. Vylkov, D. Medvedev, A. Demin, P. Tsiakaras. Design and applications of potentiometric sensors based on proton-conducting ceramic materials. A brief review, *Sensors and Actuators B: Chemical*, 244, 1004-1015, 2017.
- [101] A. Kalyakin, A. Volkov, J. Lyagaeva, D. Medvedev, A. Demin, P. Tsiakaras. Combined amperometric and potentiometric hydrogen sensors based on BaCe<sub>0.7</sub>Zr<sub>0.1</sub>Y<sub>0.2</sub>O<sub>3-δ</sub> proton-conducting ceramic, *Sensors and Actuators B: Chemical*, 231, 175-182, 2016.
- [102] A. Kalyakin, J. Lyagaeva, D. Medvedev, A. Volkov, A. Demin, P. Tsiakaras. Characterization of proton-conducting electrolyte based on La<sub>0.9</sub>Sr<sub>0.1</sub>Y<sub>0.3</sub>O<sub>3-δ</sub> and its application in a hydrogen amperometric sensor, *Sensors and Actuators B: Chemical*, 225, 446-452, 2016.
- [103] G. Fadeyev, A. Kalyakin, E. Gorbova, A. Brouzgou, A. Demin, A. Volkov, P. Tsiakaras. A simple and low-cost amperometric sensor for measuring H<sub>2</sub>, CO, and CH<sub>4</sub>, *Sensors and Actuators B: Chemical*, 221, 879-883, 2015.

- [104] G. Fadeyev, A. Kalyakin, A. Demin, A. Volkov, A. Brouzgou, P. Tsiakaras. Electrodes for solid electrolyte sensors for the measurement of CO and H<sub>2</sub> content in air, *International Journal of Hydrogen energy*, 38.30, 13484-13490, 2013.
- [105] G. Balkourani, A. Brouzgou, M. Archonti, N. Papandrianos, S. Song, P. Tsiakaras. Emerging materials for the electrochemical detection of COVID-19, *Journal of Electroanalytical Chemistry*, 893, 115289, 2021.
- [106] A. Brouzgou, E. Gorbova, Y. Wang, S. Jing, A. Seretis, Z. Liang, P. Tsiakaras. Nitrogen-doped 3D hierarchical ordered mesoporous carbon supported palladium electrocatalyst for the simultaneous detection of ascorbic acid, dopamine, and glucose, *Ionics*, 25.12, 6061-6070, 2019.
- [107] E. Gorbova, G. Balkourani, C. Molochas, D. Sidiropoulos, A. Brouzgou, A.K. Demin, P. Tsiakaras. Brief Review on High-Temperature Electrochemical Hydrogen Sensors, *Catalysts*, 12.12, 1647, 2022.
- [108] A. Kalyakin, A.K. Demin, E. Gorbova, A. Volkov, P. Tsiakaras. Sensor Based on a Solid Oxide Electrolyte for Measuring the Water-Vapor and Hydrogen Content in Air, *Catalysts*, 12.12, 1558, 2022.
- [109] G. Balkourani, A. Brouzgou, C.L. Vecchio, A.S. Aricò, V. Baglio, P. Tsiakaras. Selective electro-oxidation of dopamine on Co or Fe supported onto N-doped ketjenblack, *Electrochimica Acta*, 409, 139943, 2022.
- [110] G. Balkourani, T. Damartzis, A. Brouzgou, P. Tsiakaras. Cost effective synthesis of graphene nanomaterials for non-enzymatic electrochemical sensors for glucose: a comprehensive review, *Sensors*, 22.1, 355, 2022.
- [111] E. Gorbova, F. Tzorbatzoglou, C. Molochas, D. Chloros, A. Demin, P. Tsiakaras, Fundamentals and principles of solid-state electrochemical sensors for high temperature gas detection, *Catalysts*, 12.1, 1, 2022.
- [112] G. Balkourani, A. Brouzgou, M. Archonti, N. Papandrianos, S. Song, P. Tsiakaras. Emerging materials for the electrochemical detection of COVID-19, *Journal of Electroanalytical Chemistry*, 893, 115289, 2021.
- [113] G. Balkourani, K. Molochas, A. Brouzgou, P. Tsiakaras. Me-NC (Me= Fe, Co) Electrocatalysts with EDTA-Derived N for Dopamine Electrochemical Detection, *ECS Meeting Abstracts*, 2079, 2021.
- [114] X. Yuan, D. Yuan, F. Zeng, W. Zou, F. Tzorbatzoglou, P. Tsiakaras, Y. Wang. Preparation of graphitic mesoporous carbon for the simultaneous detection of hydroquinone and catechol, *Applied Catalysis B: Environmental*, 129, 367-374, 2013.
- [115] M.L. Perry and T.F. Fuller. A Historical Perspective of Fuel Cell Technology in the 20th Century, *Journal of Electrochemical Society*, 149.7, 59-67, 2002. Available: <https://doi.org/10.1149/1.1488651>.
- [116] E.I. Ortiz-Rivera, A.L. Reyes-Hernandez, and R.A. Febo. Understanding the history of fuel cells, *IEEE Conference on the History of Electric Power*, 2007. Available: <https://doi.org/10.1109/HEP.2007.4510259>.
- [117] J.M. Andújar and F. Segura. Fuels cells: History and updating. A walk along two centuries, *Renewable and Sustainable Energy Reviews*, 13.9, 2309-2322, 2009. Available: <https://doi.org/10.1016/j.rser.2009.03.015>.
- [118] P. Sharma, O.P. Pandey. Chapter 1 - Proton exchange membrane fuel cells: fundamentals, advanced technologies, and practical applications, *PEM Fuel Cells Fundamentals, Advanced Technologies, and Practical Application*, 1-24, 2022. Available: <https://doi.org/10.1016/B978-0-12-823708-3.00006-7>.

- [119] F. Barbir. PEM Fuel Cells: Theory and Practice, 10-12, 2012.
- [120] F. Barbir. PEM Fuel Cells, Fuel Cell Technology Reaching Towards Commercialization, 27-51, 2010.
- [121] X. Yuan, H. Wang. PEM Fuel Cell Fundamentals, PEM Fuel Cell Electrocatalysts and Catalyst Layer: Fundamentals and Applications, 17-25, 2008.
- [122] P. Sharma, O.P. Pandey. Proton exchange membrane fuel cells: fundamentals, advanced technologies, and practical applications, PEM Fuel Cells Fundamentals, Advanced Technologies, and Practical Application, 25-35, 2022.
- [123] T. Taner. Proton Exchange Membrane Fuel Cell, 19-21, 2018.
- [124] F. Barbir. Main Cell Components, Material Properties, and Processes, PEM Fuel Cells: Theory and Practice, 73-75, 2012.
- [125] X. Yuan, H. Wang. PEM Fuel Cell Fundamentals, PEM Fuel Cell Electrocatalysts and Catalyst Layers: Fundamentals and Applications, 1-17, 2008.
- [126] G. Kaur. PEM Fuel Cells: Fundamentals, Advanced Technologies, and Practical Application, 91-104, 2022.
- [127] Y. Wang, D.F. Diaz, K.S. Chen, Z. Wang, X.C. Adroher. Materials, technological status, and fundamentals of PEM fuel cells – A review, *Materials Today*, 32, 178-203, 2020. Available: <https://doi.org/10.1016/j.mattod.2019.06.005>.
- [128] S. Ghosh. Nafion – Alchetron, The Free Social Encyclopedia, 2022.
- [129] T. Xiao, R. Wang, Z. Chang, Z. Fang, Z. Zhu, C. Xu. Electrolyte membranes for intermediate temperature proton exchange membrane fuel cell, *Progress in Natural Science: Materials International*, 30.6, 743-750, 2020. Available: <https://doi.org/10.1016/j.pnsc.2020.08.014>.
- [129] P. Choi, N.H. Jalani, and R. Datta. Thermodynamics and Proton Transport in Nafion II. Proton Diffusion Mechanisms and Conductivity, *Journal of The Electrochemical Society*, 2005.
- [130] Z. Qi, Proton exchange membrane fuel cells, CRC Press, 11-18, 2013.
- [131] F. Barbir, PEM fuel cells: theory and practice, 73-92, 2012.
- [132] Q. Yan, H. Toghiani, J. Wu. Investigation of water transport through membrane in a PEM fuel cell by water balance experiments, *Journal of Power Sources*, 158.1, 316-325, 2006. Available: <https://doi.org/10.1016/j.jpowsour.2005.09.013>.
- [133] J. Zhang, PhD. Proton Exchange Membrane Fuel Cells, 18-26, 2014.
- [134] F. Barbir. Main Cell Components, Material Properties, and Processes, PEM Fuel Cells: Theory and Practice, 92-97, 2012.
- [135] B Zhang, J Shan, W Wang, P Tsiakaras, Y Li. Oxygen Vacancy and Core–Shell Heterojunction Engineering of Anemone-Like CoP@ CoOOH Bifunctional Electrocatalyst for Efficient Overall Water Splitting, *Small*, 2106012, 2022.
- [136] G. Kaur. PEM Fuel Cells: Fundamentals, Advanced Technologies, and Practical Application, 91-104, 2022.
- [137] P.K. Shen. PEM Fuel Cell catalyst layers and MEAs, PEM Fuel Cell Electrocatalysts and Catalyst Layers: Fundamentals and Applications, 355-367, 2008.
- [138] P.K. Shen. PEM Fuel Cell catalyst layers and MEAs, PEM Fuel Cell Electrocatalysts and Catalyst Layers: Fundamentals and Applications, 369-374, 2008.
- [139] A. Albarbar, M. Alrweq. Proton Exchange Membrane Fuel Cells: Design, Modelling and Performance Assessment techniques, 13-18, 2018.

- [140] Y. Wang, D.F. Diaz, K.S. Chen, Z. Wang, X.C. Adroher. Materials, technological status, and fundamentals of PEM fuel cells – A review, *Materials Today*, 32, 178-203, 2020. Available: <https://doi.org/10.1016/j.mattod.2019.06.005>.
- [141] M.A. Goula, S.K. Kontou, P. Tsiakaras. Hydrogen production by ethanol steam reforming over a commercial Pd/ $\gamma$ -Al<sub>2</sub>O<sub>3</sub> catalyst, *Applied Catalysis B: Environmental*, 49.2, 135-144, 2004.
- [142] C. Yu, F. Xu, L. Luo, H.S. Abbo, S.J.J. Titinchi, P.K. Shen, P. Tsiakaras, S. Yin, Bimetallic Ni–Co phosphide nanosheets self-supported on nickel foam as high-performance electrocatalyst for hydrogen evolution reaction, *Electrochimica Acta*, 317, 191-198, 2019.
- [143] B. Long, H. Yang, M. Li, M.S. Balogun, W. Mai, G. Ouyang, Y. Tong, P. Tsiakaras, S. Song. Interface charges redistribution enhanced monolithic etched copper foam based Cu<sub>2</sub>O layer/TiO<sub>2</sub> nanodots heterojunction with high hydrogen evolution electrocatalytic activity. *Applied Catalysis B: Environmental*, 243, 365-372, 2019.
- [144] W.R. Daud, R.E. Rosli, E.H. Majlana, S.A. Hamid, R. Mohamed, T. Husaini. PEM fuel cell system control: A review, *Renewable Energy*, 113, 620-638, 2017. Available: <https://doi.org/10.1016/j.renene.2017.06.027>.
- [145] Y. Wang, D.F. Diaz, K.S. Chen, Z. Wang, X.C. Adroher. Materials, technological status, and fundamentals of PEM fuel cells – A review, *Materials Today* 32, 205-211, 2020.
- [146] F. Barbir. Main Cell Components, Material Properties, and Processes. *PEM Fuel Cells: Theory and Practice*, 90-92, 2012.
- [147] W.R. Daud, R.E. Rosli, E.H. Majlana, S.A. Hamid, R. Mohamed, T. Husaini. PEM fuel cell system control: A review, *Renewable Energy*, 113, 638-650, 2017.
- [148] K. Xiong, W. Wu, S. Wang, L. Zhang. Modeling, design, materials, and fabrication of bipolar plates for proton exchange membrane fuel cell: A review, *Applied Energy*, 301, 117443, 2021. Available: <https://doi.org/10.1016/j.apenergy.2021.117443>.
- [149] F. Barbir, *PEM fuel cells: theory and practice*, 104-112 2012.
- [150] F. Barbir, *PEM fuel cells: theory and practice* 13-16, 2012.
- [151] A. Hermann, T. Chaudhuri and P. Spagnol, *International Journal of Hydrogen Energy*, 30, 1297-1302, 2005. Available: <https://doi.org/10.1016/j.ijhydene.2005.04.016>.
- [152] R. Omrani, B Shabani. Review of gas diffusion layer for proton exchange membrane-based technologies with a focus on unitised regenerative fuel cells, *International Journal of Hydrogen Energy*, 44.7, 3834-3860, 2019. Available: <https://doi.org/10.1016/j.ijhydene.2018.12.120>.
- [153] Y.X. Song, C.Z. Zhang, C.Y. Ling, M. Han, R.Y. Yong, D. Sun, et al. Review on current research of materials, fabrication, and application for bipolar plate in proton exchange membrane fuel cell, *International Journal of Hydrogen Energy*, 45.54, 29832-29847, 2020. Available: <https://doi.org/10.1016/j.ijhydene.2019.07.231>.
- [154] D. Shi, L. Cai, C. Zhang, D. Chen, Z. Pan, Z. Kang, Y. Liu, J. Zhang. Fabrication methods, structure design and durability analysis of advanced sealing materials in proton exchange membrane fuel cells, *Chemical Engineering Journal*, 454.1, 139995, 2023. Available: <https://doi.org/10.1016/j.cej.2022.139995>.
- [155] Z. Zhang, Y. Shang and T. Zhang. An equivalent mechanical model investigating endplates deflection for PEM fuel cell stack, *Advances in Mechanical Engineering*, 13.7, 1-14, 2021. Available: <https://doi.org/10.1177/168781402111030039>.
- [156] B. Liu, M. Wei, W. Zhang, C. Wu. Effect of impact acceleration on clamping force design of fuel cell stack, *Journal of Power Sources*, 303, 118-125, 2016. Available: <https://doi.org/10.1016/j.jpowsour.2015.10.061>.

- [157] C.H. Chien, Y.L. Hu, T.H. Su, H.T. Liu, C.T. Wang, P.F. Yang, Y.X. Lu. Effects of bolt pre-loading variations on performance of GDL in a bolted PEMFC by 3-D FEM analysis, *Energy*, 113, 1174-1187, 2016. Available: <https://doi.org/10.1016/j.energy.2016.07.075>.
- [158] M.M. Hussain, J. Baschuk, X. Li, I. Dincer. Thermodynamic analysis of a PEM fuel cell power system, *International Journal of Thermal Sciences*, 44.9, 903-911, 2005. Available: <https://doi.org/10.1016/j.ijthermalsci.2005.02.009>.
- [159] V. Liso, S.S. Araya. Chapter 6 - Thermodynamics and operating conditions for proton exchange membrane fuel cells, *PEM Fuel Cells Fundamentals, Advanced Technologies, and Practical Application*, 123-136, 2022. Available: <https://doi.org/10.1016/B978-0-12-823708-3.00014-6>.
- [160] H. Tsuchiya, O. Kobayashi. Mass production cost of PEM fuel cell by learning curve, *International Journal of Hydrogen Energy*, 29.10, 985-990, 2004. Available: <https://doi.org/10.1016/j.ijhydene.2003.10.011>.
- [161] L. Xiong, A. Manthiram. High performance membrane-electrode assemblies with ultra-low Pt loading for proton exchange membrane fuel cells, *Electrochimica Acta*, 50.16-17, 3200-3204, 2005. Available: <https://doi.org/10.1016/j.electacta.2004.11.049>.
- [162] R. O'Hayre, S.J. Lee, S.W. Cha, F.B. Prinz. A sharp peak in the performance of sputtered platinum fuel cells at ultra-low platinum loading, *Journal Power of Sources*, 109.2, 483-493, 2002. Available: [https://doi.org/10.1016/S0378-7753\(02\)00238-0](https://doi.org/10.1016/S0378-7753(02)00238-0).
- [163] J. Zhang. *PEM fuel cell electrocatalysts and catalyst layers: fundamentals and applications*, Springer Science & Business Media, 2008.
- [164] Y. Wang, K.S. Chen, J. Mishler, S.C. Cho, X.C. Adroher. A review of polymer electrolyte membrane fuel cells: Technology, applications, and needs on fundamental research, *Applied Energy*, 88.4, 981-1007, 2011. Available: <https://doi.org/10.1016/j.apenergy.2010.09.030>.
- [165] S. Satyapal. U.S. Department of Energy Hydrogen Program: 2021 Annual Merit Review and Peer Evaluation Report, June 7-11, 2021. Available: <https://www.osti.gov/biblio/1863940>.
- [166] A. Albarbar, M. Alrweq. *Proton Exchange Membrane Fuel Cells: Design, Modelling and Performance Assessment Techniques*, 2017.
- [167] O.Z. Sharaf, M.F. Orhan. An overview of fuel cell technology: fundamentals and applications, *Renewable and Sustainable Energy Reviews*, 32, 810-853, 2014. Available: <https://doi.org/10.1016/j.rser.2014.01.012>.
- [168] W. Schmittinger, A. Vahidi. A review of the main parameters influencing long-term performance and durability of PEM fuel cells, *Journal of Power Sources*, 180.1, 1-14, 2008. Available: <https://doi.org/10.1016/j.jpowsour.2008.01.070>.
- [169] D. Chen, P. Pei, Y. Li, Peng Ren, Y. Meng, X. Song, Z. Wu. Proton exchange membrane fuel cell stack consistency: Evaluation methods, influencing factors, membrane electrode assembly parameters and improvement measures, *Energy Conversion and Management*, 261, 115651, 2022. Available: <https://doi.org/10.1016/j.enconman.2022.115651>.
- [170] C. Molochas and P. Tsiakaras. Carbon Monoxide Tolerant Pt-Based Electrocatalysts for H<sub>2</sub>-PEMFC Applications: Current Progress and Challenges, *Catalysts*, 11.9, 1127, 2021. Available: <https://doi.org/10.3390/catal11091127>.
- [171] M. Jourdan, H. Mounir, A. El Marjani. Compilation of factors affecting durability of Proton Exchange Membrane Fuel Cell (PEMFC), 2014 International Renewable and Sustainable Energy Conference (IRSEC), 14998472, 2014. Available: [10.1109/IRSEC.2014.7059906](https://doi.org/10.1109/IRSEC.2014.7059906).

- [172] L. Xia, C. Zhang, M. Hu, S. Jiang. Investigation of parameter effects on the performance of high-temperature PEM fuel cell, *International Journal of Hydrogen Energy*, 43.52, 23441-23449, 2018. Available: <https://doi.org/10.1016/j.ijhydene.2018.10.210>.
- [173] H. Askaripour. International journal of heat and mass transfer effect of operating conditions on the performance of a PEM fuel cell, *International Journal of Heat and Mass Transfer*, 144, 118705, 2019. Available: <https://doi.org/10.1016/j.ijheatmasstransfer.2019.118705>.
- [174] V. Hirpara, V. Patel, Y. Zhang, R. Anderson, N. Zhu, L. Zhang. Investigating the effect of operating temperature on dynamic behavior of droplets for proton exchange membrane fuel cells, *International Journal of Hydrogen Energy*, 45.27, 14145-14155, 2020. Available: <https://doi.org/10.1016/j.ijhydene.2020.03.128>.
- [175] H.L. Nguyen, J. Han, X.L. Nguyen, S. Yu, Y.M. Goo, and D.D. Le. Review of the Durability of Polymer Electrolyte Membrane Fuel Cell in Long-Term Operation: Main Influencing Parameters and Testing Protocols, *Energies*, 14.13, 4048, 2021. Available: <https://doi.org/10.3390/en14134048>.
- [176] R. Singh, A.S. Oberoi, T. Singh. Factors influencing the performance of PEM fuel cells: A review on performance parameters, water management, and cooling techniques, *International Journal of Energy Research*, 46.4, 3810-3842, 2021. Available: <https://doi.org/10.1002/er.7437>.
- [177] M. Amirinejad, S. Rowshanzamir, M.H. Eikani. Effects of operating parameters on performance of a proton exchange membrane fuel cell, *Journal of Power Sources*, 161.2, 872-875, 2006. Available: <https://doi.org/10.1016/j.jpowsour.2006.04.144>.
- [178] L. Wang, A. Husar, T. Zhou, H. Liu. A parametric study of PEM fuel cell performances, *International Journal of Hydrogen Energy*, 28.11, 1263-1272, 2003. Available: [https://doi.org/10.1016/S0360-3199\(02\)00284-7](https://doi.org/10.1016/S0360-3199(02)00284-7).
- [179] R. Borup, J. Meyers, B. Pivovar, Y.S Kim, R. Mukundan, N. Garland, D. Myers, M. Wilson, F. Garzon, D. Wood, et al. Scientific aspects of polymer electrolyte fuel cell durability and degradation, *Chemical Reviews*, 107.10, 3904-3951, 2007. Available: <https://doi.org/10.1021/cr050182l>.
- [180] P. Pei, H. Chen. Main factors affecting the lifetime of Proton Exchange Membrane fuel cells in vehicle applications: A review, *Applied Energy*, 125, 60-75, 2014. Available: <https://doi.org/10.1016/j.apenergy.2014.03.048>.
- [181] R. Lin, X. Cui, J. Shan, L. Técher, F. Xiong, Q. Zhang. Investigating the effect of start-up and shut-down cycles on the performance of the proton exchange membrane fuel cell by segmented cell technology, *International Journal Hydrogen Energy*, 40.43, 14952-14962, 2015. Available: <https://doi.org/10.1016/j.ijhydene.2015.09.042>.
- [182] S.Y. Ahn, S.J. Shin, H.Y. Ha, S.A. Hong, Y.C. Lee, T.W. Lim, I.H. Oh. Performance and lifetime analysis of the kW-class PEMFC stack, *Journal of Power Sources*, 106.1-2, 295-303, 2002. Available: [https://doi.org/10.1016/S0378-7753\(01\)01032-1](https://doi.org/10.1016/S0378-7753(01)01032-1).
- [183] J.J. Baschuk, X. Li. Carbon monoxide poisoning of proton exchange membrane fuel cells, *International Journal of Energy Research*, 25.8, 695-713, 2001. Available: <https://doi.org/10.1002/er.713>.
- [184] X. Cheng, Z. Shi, N. Glass, L. Zhang, J. Zhang, D. Song, Z.S Liu, H. Wang, J. Shen. A review of PEM hydrogen fuel cell contamination: Impacts, mechanisms, and mitigation, *Journal of Power Sources*, 165.2, 739-756, 2007. Available: <https://doi.org/10.1016/j.jpowsour.2006.12.012>.
- [185] F.A. Uribe, S. Gottesfeld, and T.A. Zawodzinski Jr. Effect of Ammonia as Potential Fuel Impurity on Proton Exchange Membrane Fuel Cell Performance, *Journal of Electrochemical Society*, 149.3, 293-296, 2002. Available: <https://doi.org/10.1149/1.1447221>.

- [186] A. Taniguchi, T. Akita, K. Yasuda, Y. Miyazaki. Analysis of electrocatalyst degradation in PEMFC caused by cell reversal during fuel starvation, *Journal of Power Sources*, 130.1-2, 42-49, 2004. Available: <https://doi.org/10.1016/j.jpowsour.2003.12.035>.
- [187] D. Qiu, L. Peng, X. Lai, M. Ni, W. Lehnert. Mechanical failure and mitigation strategies for the membrane in a proton exchange membrane fuel cell, *Renewable and Sustainable Energy Reviews*, 113, 109289, 2019. Available: <https://doi.org/10.1016/j.rser.2019.109289>.
- [188] S. Kundu, M.W. Fowler, L.C. Simon, S. Grot. Morphological features (defects) in fuel cell membrane electrode assemblies, *Journal of Power Sources*, 157.2, 650-656, 2006. Available: <https://doi.org/10.1016/j.jpowsour.2005.12.027>.
- [189] Y.H. Lai, D.A. Dillard. Mechanical durability characterization and modeling of ionomeric membranes, *Handbook of fuel cells*, 2010.
- [190] R.M. Khorasany, E. Kjeang, G. Wang, R. Rajapakse. Simulation of ionomer membrane fatigue under mechanical and hygrothermal loading conditions, *Journal Power Sources*, 279, 55-63, 2015. Available: <https://doi.org/10.1016/j.jpowsour.2014.12.133>.
- [191] T. Jahnke, G. Futter, A. Latz, T. Malkow, G. Papakonstantinou, G. Tsotridis et al. Performance and degradation of Proton Exchange Membrane Fuel Cells: State of the art in modeling from atomistic to system scale, *Journal of Power Sources*, 304, 207-233, 2016. Available: <https://doi.org/10.1016/j.jpowsour.2015.11.041>.
- [191] F.A. de Bruijn, V.A.T. Dam, G.J.M. Janssen. Review: Durability and Degradation Issues of PEM Fuel Cell Components, *Fuel Cells*, 8.1, 3-22, 2008. Available: <https://doi.org/10.1002/face.200700053>.
- [192] A. Kusoglu, A.M. Karlsson, M.H. Santare, S. Cleghorn, W.B. Johnson. Mechanical response of fuel cell membranes subjected to a hygro-thermal cycle, *Journal of Power Sources*, 161.2, 987-996, 2006. Available: <https://doi.org/10.1016/j.jpowsour.2006.05.020>.
- [193] H.F.M. Mohamed, Y. Kobayashi, C.S. Kuroda, A. Ohira. Impact of Heating on the Structure of Perfluorinated Polymer Electrolyte Membranes: A Positron Annihilation Study, *Macromolecular Chemistry and Physics*, 212.7, 708-714, 2011. Available: <https://doi.org/10.1002/macp.201000693>.
- [194] Q. Yan, H. Toghiani, Y.W. Lee, K. Liang, H. Causey. Effect of sub-freezing temperatures on a PEM fuel cell performance, startup and fuel cell components, *Journal of Power Sources*, 160.2, 1242-1250, 2006. Available: <https://doi.org/10.1016/j.jpowsour.2006.02.075>.
- [195] E. Cho, J.J. Ko, H.Y. Ha, S.A. Hong. Effects of water removal on the performance degradation of PEMFCs repetitively brought to < 0 °C, *Journal of The Electrochemical Society*, 151.5, A661, 2004. Available: <https://doi.org/10.1149/1.1683580>.
- [196] A.B. LaConti, M. Hamdan, R.C. McDonald. Mechanisms of membrane degradation. 'Handbook of fuel cells' (2010): 1700–1712. Available: <https://doi.org/10.1002/9780470974001.f303055>.
- [197] C. Hartnig, T.J. Schmidt. On a new degradation mode for high-temperature polymer electrolyte fuel cells: How bipolar plate degradation affects cell performance, *Electrochimica Acta*, 56.11, 4237-4242, 2011. Available: <https://doi.org/10.1016/j.electacta.2011.01.088>.
- [198] J. Zhao, X. Li. A review of polymer electrolyte membrane fuel cell durability for vehicular applications: Degradation modes and experimental techniques, *Energy Conversion and Management*, 199, 112022, 2019. Available: <https://doi.org/10.1016/j.enconman.2019.112022>.
- [199] K. Kang, S. Park, A. Jo, K. Lee, H. Ju. Development of ultralight and thin bipolar plates using epoxy-carbon fiber preregs and graphite composites, *International Journal of Hydrogen, Energy*, 42.3, 1691-1697, 2017. Available: <https://doi.org/10.1016/j.ijhydene.2016.05.027>.

- [200] H.L. Nguyen, J. Han, X.L. Nguyen, S. Yu, Y.M Goo and D.D Le. Review of the Durability of Polymer Electrolyte Membrane Fuel Cell in Long-Term Operation: Main Influencing Parameters and Testing Protocols, *Hydrogen Energy*, 14.13, 4048, 2021. Available: <https://doi.org/10.3390/en14134048>.
- [201] X. Yu, S. Ye. Recent advances in activity and durability enhancement of Pt/C catalytic cathode in PEMFC: Part II: Degradation mechanism and durability enhancement of carbon supported platinum catalyst, *Journal of Power Sources*, 172.1, 145-154, 2007. Available: <https://doi.org/10.1016/j.jpowsour.2007.07.048>.
- [202] C Molochas, P Tsiakaras. Carbon Monoxide Tolerant Pt-Based Electrocatalysts for H<sub>2</sub>-PEMFC Applications: Current Progress and Challenges, *Catalysts*, 11.9, 1127, 2021.
- [203] K. Wang, H. Chen, X. Zhang, Y. Tong, S. Song, P. Tsiakaras. Y Wang, Iron oxide@ graphitic carbon core-shell nanoparticles embedded in ordered mesoporous N-doped carbon matrix as an efficient cathode catalyst for PEMFC, *Applied Catalysis B: Environmental* 264, 118468, 2020.
- [204] C.G. Vayenas, S. Bebelis, I.V. Yentekakis, P. Tsiakaras. Non-faradaic electrochemical modification of catalytic activity reversible promotion of platinum metals catalysts. *Platinum Metals Rev*, 34.3, 122, 1990.
- [205] P. Tsiakaras, C. Athanasiou, G. Marnellos, M. Stoukides, J.E. ten Elshof. Methane activation on a La<sub>0.6</sub>Sr<sub>0.4</sub>Co<sub>0.8</sub>Fe<sub>0.2</sub>O<sub>3</sub> perovskite: Catalytic and electrocatalytic results *Applied catalysis A: General*, 169.2, 249-261, 1998.
- [206] P. Tsiakaras, C.G. Vayenas. Oxidative coupling of CH<sub>4</sub> on Ag catalyst-electrodes deposited on ZrO<sub>2</sub> (8 mol% Y<sub>2</sub>O<sub>3</sub>), *Journal of Catalysis*, 144.1, 333-347, 1993.
- [207] K. Wang, Y. Wang, Z. Liang, Y. Liang, D. Wu, S. Song, P. Tsiakaras. Ordered mesoporous tungsten carbide/carbon composites promoted Pt catalyst with high activity and stability for methanol electrooxidation, *Applied Catalysis B: Environmental*, 147, 518-525, 2014.
- [208] E. Gorbova, V. Maragou, D. Medvedev, A. Demin, P. Tsiakaras. Influence of sintering additives of transition metals on the properties of gadolinium-doped barium cerate, *Solid State Ionics*, 179, 21-26, 887-890, 2008.
- [209] J. Zhang, Y. Yuan, L. Gao, G. Zeng, M. Li, and H. Huang. Stabilizing Pt-Based Electrocatalysts for Oxygen Reduction Reaction: Fundamental Understanding and Design Strategies, *Advanced materials*, 33.20, 2006494, 2021. Available: <https://doi.org/10.1002/adma.202006494>.
- [210] A. Brouzgou, A. Seretis, S.Song, P.K. Shen, P. Tsiakaras. CO tolerance and durability study of PtMe (Me = ¼ Ir or Pd) electrocatalysts for H<sub>2</sub>-PEMFC application, *International Journal of Hydrogen Energy*, 46.26, 13865-13877, 2021. Available: <https://doi.org/10.1016/j.ijhydene.2020.07.224>.
- [211] A. Brouzgou, A. Seretis, S. Song, P.K. Shen, P. Tsiakaras, CO tolerance and durability study of PtMe (Me= Ir or Pd) electrocatalysts for H<sub>2</sub>-PEMFC application, *International Journal of Hydrogen Energy* 46 (26), 13865-13877, (2021) .
- [212] R.L. Borup, J.R. Davey, F.H. Garzon, D.L. Wood, M.A. Inbody, *Journal Power of Sources*, 163, 76-81, 2006.
- [213] M.M. Mench, E.C. Kumbur, T.N. Veziroglu. Polymer Electrolyte Fuel cell degradation, 237-243, 2012.
- [214] J. Park, H. Oh, T. Ha, Y. Il Lee, K. Min. A review of the gas diffusion layer in proton exchange membrane fuel cells: Durability and degradation, *Applied energy*, 155.1, 866-880, 2015. Available: <https://doi.org/10.1016/j.apenergy.2015.06.068>.

- [215] M. Sun, Y. Lee, Y. Song, H. Wu, G. Wang, H. Zhang, M. Chen, Q. Fu, X. Bao. CO-tolerant PtRu@h-BN/C core-shell electrocatalysts for proton exchange membrane fuel cells, *Appl. Surf. Sci.*, 450, 244–250, 2018.
- [216] W. Schmittinger, A. Vahidi. A review of the main parameters influencing long-term performance and durability of PEM fuel cells. “*Journal of Power Sources*” 180.1 (2008): 1-14. Available: <https://doi.org/10.1016/j.jpowsour.2008.01.070>.
- [217] P.S. Selsky, H. Schmies, A. Latz, T. Jahnke. Lattice Boltzmann simulation of liquid water transport in gas diffusion layers of proton exchange membrane fuel cells: Impact of gas diffusion layer and microporous layer degradation on effective transport properties, *Journal of Power Sources*, 556.1, 232415, 2023. Available: <https://doi.org/10.1016/j.jpowsour.2022.232415>.
- [218] M.M. Mench, E.C. Kumbur, T.N. Veziroglu. Polymer Electrolyte Fuel cell degradation, 237-243, 2012.
- [219] H. Pourrahmani, M. Siavashi, A. Yavarinasab, M. Matian, N. Chitgar, L. Wang, and J. Van herle. A Review on the Long-Term Performance of Proton Exchange Membrane Fuel Cells: From Degradation Modeling to the Effects of Bipolar Plates, Sealings, and Contaminants, *Energies*, 15.14, 5081, 2022. Available: <https://doi.org/10.3390/en15145081>.
- [220] G. Li, J. Tan, J. Gong. Degradation of the elastomeric gasket material in a simulated and four accelerated proton exchange membrane fuel cell environments, *Journal of Power Sources*, 205, 244-251, 2012. Available: <https://doi.org/10.1016/j.jpowsour.2011.06.092>.
- [221] W. Schmittinger, A. Vahidi. A review of the main parameters influencing long-term performance and durability of PEM fuel cells, *Journal of Power Sources*, 180.1, 1-14, 2008. Available: <https://doi.org/10.1016/j.jpowsour.2008.01.070>.
- [222] Mengbo Ji and Zidong Wei. A Review of Water Management in Polymer Electrolyte Membrane Fuel Cells, *Energies*, 2.4, 1057-1106, 2009. Available: <https://doi.org/10.3390/en20401057>.
- [223] He, W.S.; Lin, G.Y.; Nguyen, T.V. Diagnostic tool to detect electrode flooding in proton-exchange-membrane fuel cells. *AIChE J*, 2003, 49, 3221-3228.
- [224] Rupinder Singh, Amandeep Singh Oberoi, Talwinder Singh. Factors influencing the performance of PEM fuel cells: A review on performance parameters, water management, and cooling techniques, *International Journal of Energy Research*, 46.4, 3810-3842, 2022. Available: <https://doi.org/10.1002/er.7437>.
- [225] C.H. Lee, H.B. Park, Y.M. Lee, R.D. Lee. Importance of Proton Conductivity Measurement in Polymer Electrolyte Membrane for Fuel Cell Application. *Industrial. Engineering Chemistry Research*, 44.20, 7617-7626, 2005.
- [226] E.H. Reddy, S. Jayanti. Thermal management strategies for a 1 kWe stack of a high temperature proton exchange membrane fuel cell, *Applied Thermal Engineering*, 48, 465-475, 2012.